

CONTEXT MATTERS FOR BLACK BEARS: EVALUATING SPATIALLY EXPLICIT
DENSITY ESTIMATORS AND TRADE-OFFS IN RESOURCE SELECTION

By

Jennifer B. Smith

A THESIS

Submitted to
Michigan State University
in partial fulfillment of the requirements
for the degree of

Fisheries and Wildlife – Master of Science

2018

ABSTRACT

CONTEXT MATTERS FOR BLACK BEARS: EVALUATING SPATIALLY EXPLICIT DENSITY ESTIMATORS AND TRADE-OFFS IN RESOURCE SELECTION

By

Jennifer B. Smith

Widespread urbanization, habitat fragmentation, and climate change drive significant, multi-scale variation in wildlife populations and their habitat use. As a result, effective management of wildlife require fine-scale quantification of population density and resource selection, particularly for wide-ranging species. In this thesis I address these needs for the American black bear (*Ursus americanus*) in the Lower Peninsula of Michigan, USA. In my first chapter, I evaluated factors affecting spatially explicit density estimates from repurposed black bear hair snare data. I fit these data to a spatial capture-recapture model and simulated outcomes under a suite of parameter scenarios. Results indicated that while this method produced cost-effective bear density estimates, the accuracy of the estimates depended on scenario parameters. In my second chapter, I quantified functional relationships in black bear use of agriculture. I estimated a resource selection function from GPS telemetry data of 12 black bears. Both male and female bears were less likely to use agriculture as it increased in the landscape, and when they were located close to developed land covers. The odds of male bears using agriculture declined with increasing bear density. Comparatively, the odds of females using agriculture increased in areas of higher density. These relationships reflect the influence of environmental context on the trade-offs involved in black bears using agricultural habitat.

ACKNOWLEDGEMENTS

Completion of this research would not have been possible without the support, dedication, and kindness I received from many people. First and foremost, I thank my parents, Steve and Tracy, and my sister, Alex. Their unconditional love, compassion, support, and unwavering belief in me is the foundation of my life. I couldn't have done this without you and I love you more than I can express.

I thank my major advisor, Dr. David Williams, for guiding me through this process with patience, humor, confidence, and encouragement. I thank him for pushing me to reach my potential, for exposing me to the satisfaction of and enjoyment in tackling quantitative puzzles, and for calmly weathering my moments of doubt. Many thanks to committee members Dr. Gary Roloff and Dr. Scott Winterstein for insightful conversations about landscape ecology, biological relevance, and their thought-provoking questions that improved the rigor of this project.

This research would not have been possible without the Michigan Department of Natural Resources. Their efforts collected all the data involved in this thesis and their collaboration allowed me to pursue my research objectives. I owe many thanks to Dr. Dwayne Etter and Mike Wegan, who consistently supported, educated, and encouraged me. Thank you for making this fun, for fueling my curiosity, for giving me opportunities every wildlife biologist dreams of, and for never doubting my ability.

I thank Dr. Bill Porter and Dr. Rose Stewart for much needed support, perspective, critique, and mentoring. I thank Josh for always listening to and grounding me, and for your steady confidence, reassurance, and love. Finally, I thank my fellow lab members in the Quantitative Wildlife Center for your incredibly helpful feedback, thoughtful discussions,

brainstorming sessions, and friendship. Special thanks to Dr. Bryan Stevens for all of the ‘light bulb’ conversations and your genuine, selfless, investment in my intellectual growth. I am remarkably fortunate to have worked with so many intelligent, amiable, passionate, and dedicated individuals.

This work was generously funded by the Boone and Crockett Endowment, the Safari Club International Michigan Involvement Committee, the Michigan Department of Natural Resources, the Fisheries and Wildlife Department at Michigan State University, the Hal and Jean Glassen Foundation, and by the U.S. Fish and Wildlife Service through the Pittman-Robertson Wildlife Restoration Act Grant MI W-155-R. Thank you.

TABLE OF CONTENTS

LIST OF TABLES	vi
LIST OF FIGURES	vii
INTRODUCTION	1
LITERATURE CITED	5
CHAPTER 1: PERFORMANCE OF A SPATIAL CAPTURE-RECAPTURE MODEL FOR REPURPOSED BLACK BEAR HAIR SNARE DATA	8
Introduction.....	8
Methods.....	10
<i>Data</i>	10
<i>Simulations</i>	10
Results.....	12
Discussion.....	14
Management implications.....	18
APPENDICES	19
APPENDIX I: Tables.....	20
APPENDIX II: Figures	25
LITERATURE CITED	72
CHAPTER 2: CONTEXT MATTERS: VARIATION IN BLACK BEAR USE OF AGRICULTURAL LANDSCAPES.....	75
Introduction.....	75
Methods.....	77
<i>Study area</i>	77
<i>Black bear location data</i>	78
<i>Availability</i>	79
<i>Covariates</i>	79
<i>Autocorrelation</i>	81
<i>Modeling framework</i>	81
Results.....	83
Discussion.....	85
Management implications.....	88
APPENDICES	89
APPENDIX I: Tables.....	90
APPENDIX II: Figures	96
LITERATURE CITED	105

LIST OF TABLES

Table 1.1. Percentage of iterations with maximization or failure to calculate variance errors, median percent relative bias (%RB), median absolute deviation of the relative bias (MAD RB), median relative standard error (RSE), and median absolute deviation of the RSE (MAD RSE) of the density estimate for simulated scenarios of spatial capture-recapture models that experienced > 20% failed iterations (n=10)	23
Table 1.2. Percentage of iterations with maximization or failure to calculate variance errors, median percent relative bias (%RB), median absolute deviation of the relative bias (MAD RB), median relative standard error (RSE), and median absolute deviation of the RSE (MAD RSE) of the density estimator for 71 simulated scenarios of spatial capture-recapture models. Rows with “---” represent scenarios that were removed from further analysis because > 20% of replicates were unsuccessful	24
Table 2.1. Variables used to develop a resource selection function for black bears from 2011 – 2015 in the Lower Peninsula of Michigan	95
Table 2.2. Fixed-effects structure of candidate logistic regression models of female and male black bear resource selection from 2011 – 2015 in the Lower Peninsula, Michigan that are ≤ 10 Δ AIC of the top model. Amount of support (Akaike’s information criterion (AIC and Δ AIC) and model weight (w_i) are shown for each model	97
Table 2.3. Summary of the generalized linear logistic regression model for predicting use of agriculture in 12 bear-years of female black bear data from 2011 – 2015 in Lower Peninsula, Michigan	98
Table 2.4. Summary of the generalized linear mixed effect logistic regression model for predicting use of agriculture in 9 bear-years of male black bear data from 2011 – 2015 in Lower Peninsula, Michigan	99

LIST OF FIGURES

Figure 1.1. Locations of hair snare traps in the northern Lower Peninsula of Michigan in 2009. Shaded polygons represent the three bear management units in this region28

Figure 1.2a. Distribution of relative standard error of the density estimate for simulated scenarios of spatial capture-recapture models. Scenarios are grouped by combinations of g_0 , σ , and density and are aggregated across number of sampling occasions. Only scenarios that did not encounter maximization or variance calculation warnings in $> 80\%$ of iterations are represented ($n=71$). Grey “X” symbols are placeholders for the missing groups of scenarios, which were removed from further analysis because $> 20\%$ of iterations failed. The red, dashed, line is $RSE = 0$29

Figure 1.2b. Distribution of relative standard error of the density estimate for simulated scenarios of spatial capture-recapture models. Scenarios are grouped by combinations of g_0 , σ , and number of sampling occasions and are aggregated across density values. Only scenarios that did not encounter maximization or variance calculation warnings in $> 80\%$ of iterations are represented ($n=71$). Grey “X” symbols are placeholders for the missing groups of scenarios, which were removed from further analysis because $> 20\%$ of iterations failed. The red, dashed, line is $RSE = 0$30

Figure 1.3a. Distribution of relative bias of the density estimate for simulated scenarios of spatial capture-recapture models. Scenarios are grouped by combinations of g_0 , σ , and density and are aggregated across number of sampling occasions. Only scenarios that did not encounter maximization or variance calculation warnings in $> 80\%$ of iterations are represented ($n=71$). Grey “X” symbols are placeholders for the missing groups of scenarios, which were removed from further analysis because $> 20\%$ of iterations failed. The red, dashed, line is $RSE = 0$31

Figure 1.3b. Distribution of relative bias of the density estimate for simulated scenarios of spatial capture-recapture models. Scenarios are grouped by combinations of g_0 , σ , and number of sampling occasions and are aggregated across density values. Only scenarios that did not encounter maximization or variance calculation warnings in $> 80\%$ of iterations are represented ($n=71$). Grey “X” symbols are placeholders for the missing groups of scenarios, which were removed from further analysis because $> 20\%$ of iterations failed. The red, dashed, line is $RSE = 0$32

Figure 1.4. Distribution of relative bias (left boxplot) and relative standard error (right boxplot) in the density estimate for a simulated scenario of a spatial capture-recapture model ($D = 10$ bears/100 km², $\sigma = 2$ km, $g_0 = 0.005$, and sampling occurred over 3 weeks)33

Figure 1.5. Distribution of relative bias (left boxplot) and relative standard error (right boxplot) in the density estimate for a simulated scenario of a spatial capture-recapture model ($D = 50$ bears/100 km², $\sigma = 2$ km, $g_0 = 0.005$, and sampling occurred over 3 weeks)33

Figure 1.6. Distribution of relative bias (left boxplot) and relative standard error (right boxplot) in the density estimate for a simulated scenario of a spatial capture-recapture model ($D = 100$ bears/100 km ² , $\sigma = 2$ km, $g_0 = 0.005$, and sampling occurred over 3 weeks)	34
Figure 1.7. Distribution of relative bias (left boxplot) and relative standard error (right boxplot) in the density estimate for a simulated scenario of a spatial capture-recapture model ($D = 10$ bears/100 km ² , $\sigma = 5$ km, $g_0 = 0.005$, and sampling occurred over 3 weeks)	34
Figure 1.8. Distribution of relative bias (left boxplot) and relative standard error (right boxplot) in the density estimate for a simulated scenario of a spatial capture-recapture model ($D = 50$ bears/100 km ² , $\sigma = 5$ km, $g_0 = 0.005$, and sampling occurred over 3 weeks)	35
Figure 1.9. Distribution of relative bias (left boxplot) and relative standard error (right boxplot) in the density estimate for a simulated scenario of a spatial capture-recapture model ($D = 100$ bears/100 km ² , $\sigma = 5$ km, $g_0 = 0.005$, and sampling occurred over 3 weeks)	35
Figure 1.10. Distribution of relative bias (left boxplot) and relative standard error (right boxplot) in the density estimate for a simulated scenario of a spatial capture-recapture model ($D = 10$ bears/100 km ² , $\sigma = 12$ km, $g_0 = 0.005$, and sampling occurred over 3 weeks)	36
Figure 1.11. Distribution of relative bias (left boxplot) and relative standard error (right boxplot) in the density estimate for a simulated scenario of a spatial capture-recapture model ($D = 50$ bears/100 km ² , $\sigma = 12$ km, $g_0 = 0.005$, and sampling occurred over 3 weeks)	36
Figure 1.12. Distribution of relative bias (left boxplot) and relative standard error (right boxplot) in the density estimate for a simulated scenario of a spatial capture-recapture model ($D = 100$ bears/100 km ² , $\sigma = 12$ km, $g_0 = 0.005$, and sampling occurred over 3 weeks)	37
Figure 1.13. Distribution of relative bias (left boxplot) and relative standard error (right boxplot) in the density estimate for a simulated scenario of a spatial capture-recapture model ($D = 10$ bears/100 km ² , $\sigma = 2$ km, $g_0 = 0.02$, and sampling occurred over 3 weeks)	37
Figure 1.14. Distribution of relative bias (left boxplot) and relative standard error (right boxplot) in the density estimate for a simulated scenario of a spatial capture-recapture model ($D = 50$ bears/100 km ² , $\sigma = 2$ km, $g_0 = 0.02$, and sampling occurred over 3 weeks)	38
Figure 1.15. Distribution of relative bias (left boxplot) and relative standard error (right boxplot) in the density estimate for a simulated scenario of a spatial capture-recapture model ($D = 100$ bears/100 km ² , $\sigma = 2$ km, $g_0 = 0.02$, and sampling occurred over 3 weeks)	38
Figure 1.16. Distribution of relative bias (left boxplot) and relative standard error (right boxplot) in the density estimate for a simulated scenario of a spatial capture-recapture model ($D = 10$ bears/100 km ² , $\sigma = 5$ km, $g_0 = 0.02$, and sampling occurred over 3 weeks)	39

Figure 1.17. Distribution of relative bias (left boxplot) and relative standard error (right boxplot) in the density estimate for a simulated scenario of a spatial capture-recapture model ($D = 50$ bears/100 km², $\sigma = 5$ km, $g_0 = 0.02$, and sampling occurred over 3 weeks)39

Figure 1.18. Distribution of relative bias (left boxplot) and relative standard error (right boxplot) in the density estimate for a simulated scenario of a spatial capture-recapture model ($D = 100$ bears/100 km², $\sigma = 5$ km, $g_0 = 0.02$, and sampling occurred over 3 weeks)40

Figure 1.19. Distribution of relative bias (left boxplot) and relative standard error (right boxplot) in the density estimate for a simulated scenario of a spatial capture-recapture model ($D = 10$ bears/100 km², $\sigma = 12$ km, $g_0 = 0.02$, and sampling occurred over 3 weeks)40

Figure 1.20. Distribution of relative bias (left boxplot) and relative standard error (right boxplot) in the density estimate for a simulated scenario of a spatial capture-recapture model ($D = 50$ bears/100 km², $\sigma = 12$ km, $g_0 = 0.02$, and sampling occurred over 3 weeks)41

Figure 1.21. Distribution of relative bias (left boxplot) and relative standard error (right boxplot) in the density estimate for a simulated scenario of a spatial capture-recapture model ($D = 100$ bears/100 km², $\sigma = 12$ km, $g_0 = 0.02$, and sampling occurred over 3 weeks)41

Figure 1.22. Distribution of relative bias (left boxplot) and relative standard error (right boxplot) in the density estimate for a simulated scenario of a spatial capture-recapture model ($D = 10$ bears/100 km², $\sigma = 2$ km, $g_0 = 0.2$, and sampling occurred over 3 weeks)42

Figure 1.23. Distribution of relative bias (left boxplot) and relative standard error (right boxplot) in the density estimate for a simulated scenario of a spatial capture-recapture model ($D = 50$ bears/100 km², $\sigma = 2$ km, $g_0 = 0.2$, and sampling occurred over 3 weeks)42

Figure 1.24. Distribution of relative bias (left boxplot) and relative standard error (right boxplot) in the density estimate for a simulated scenario of a spatial capture-recapture model ($D = 100$ bears/100 km², $\sigma = 2$ km, $g_0 = 0.2$, and sampling occurred over 3 weeks)43

Figure 1.25. Distribution of relative bias (left boxplot) and relative standard error (right boxplot) in the density estimate for a simulated scenario of a spatial capture-recapture model ($D = 10$ bears/100 km², $\sigma = 5$ km, $g_0 = 0.2$, and sampling occurred over 3 weeks)43

Figure 1.26. Distribution of relative bias (left boxplot) and relative standard error (right boxplot) in the density estimate for a simulated scenario of a spatial capture-recapture model ($D = 50$ bears/100 km², $\sigma = 5$ km, $g_0 = 0.2$, and sampling occurred over 3 weeks)44

Figure 1.27. Distribution of relative bias (left boxplot) and relative standard error (right boxplot) in the density estimate for a simulated scenario of a spatial capture-recapture model ($D = 100$ bears/100 km², $\sigma = 5$ km, $g_0 = 0.2$, and sampling occurred over 3 weeks)44

Figure 1.28. Distribution of relative bias (left boxplot) and relative standard error (right boxplot) in the density estimate for a simulated scenario of a spatial capture-recapture model ($D = 10$ bears/100 km ² , $\sigma = 12$ km, $g_0 = 0.2$, and sampling occurred over 3 weeks)	45
Figure 1.29. Distribution of relative bias (left boxplot) and relative standard error (right boxplot) in the density estimate for a simulated scenario of a spatial capture-recapture model ($D = 50$ bears/100 km ² , $\sigma = 12$ km, $g_0 = 0.2$, and sampling occurred over 3 weeks)	45
Figure 1.30. Distribution of relative bias (left boxplot) and relative standard error (right boxplot) in the density estimate for a simulated scenario of a spatial capture-recapture model ($D = 100$ bears/100 km ² , $\sigma = 12$ km, $g_0 = 0.2$, and sampling occurred over 3 weeks)	46
Figure 1.31. Distribution of relative bias (left boxplot) and relative standard error (right boxplot) in the density estimate for a simulated scenario of a spatial capture-recapture model ($D = 10$ bears/100 km ² , $\sigma = 2$ km, $g_0 = 0.005$, and sampling occurred over 5 weeks)	46
Figure 1.32. Distribution of relative bias (left boxplot) and relative standard error (right boxplot) in the density estimate for a simulated scenario of a spatial capture-recapture model ($D = 50$ bears/100 km ² , $\sigma = 2$ km, $g_0 = 0.005$, and sampling occurred over 5 weeks)	47
1.33. Distribution of relative bias (left boxplot) and relative standard error (right boxplot) in the density estimate for a simulated scenario of a spatial capture-recapture model ($D = 100$ bears/100 km ² , $\sigma = 2$ km, $g_0 = 0.005$, and sampling occurred over 5 weeks)	47
Figure 1.34. Distribution of relative bias (left boxplot) and relative standard error (right boxplot) in the density estimate for a simulated scenario of a spatial capture-recapture model ($D = 10$ bears/100 km ² , $\sigma = 5$ km, $g_0 = 0.005$, and sampling occurred over 5 weeks)	48
Figure 1.35. Distribution of relative bias (left boxplot) and relative standard error (right boxplot) in the density estimate for a simulated scenario of a spatial capture-recapture model ($D = 50$ bears/100 km ² , $\sigma = 5$ km, $g_0 = 0.005$, and sampling occurred over 5 weeks)	48
Figure 1.36. Distribution of relative bias (left boxplot) and relative standard error (right boxplot) in the density estimate for a simulated scenario of a spatial capture-recapture model ($D = 100$ bears/100 km ² , $\sigma = 5$ km, $g_0 = 0.005$, and sampling occurred over 5 weeks)	49
Figure 1.37. Distribution of relative bias (left boxplot) and relative standard error (right boxplot) in the density estimate for a simulated scenario of a spatial capture-recapture model ($D = 10$ bears/100 km ² , $\sigma = 12$ km, $g_0 = 0.005$, and sampling occurred over 5 weeks)	49
Figure 1.38. Distribution of relative bias (left boxplot) and relative standard error (right boxplot) in the density estimate for a simulated scenario of a spatial capture-recapture model ($D = 50$ bears/100 km ² , $\sigma = 12$ km, $g_0 = 0.005$, and sampling occurred over 5 weeks)	50

Figure 1.39. Distribution of relative bias (left boxplot) and relative standard error (right boxplot) in the density estimate for a simulated scenario of a spatial capture-recapture model ($D = 100$ bears/100 km², $\sigma = 12$ km, $g_0 = 0.005$, and sampling occurred over 5 weeks)50

Figure 1.40. Distribution of relative bias (left boxplot) and relative standard error (right boxplot) in the density estimate for a simulated scenario of a spatial capture-recapture model ($D = 10$ bears/100 km², $\sigma = 2$ km, $g_0 = 0.02$, and sampling occurred over 5 weeks)51

Figure 1.41. Distribution of relative bias (left boxplot) and relative standard error (right boxplot) in the density estimate for a simulated scenario of a spatial capture-recapture model ($D = 50$ bears/100 km², $\sigma = 2$ km, $g_0 = 0.02$, and sampling occurred over 5 weeks)51

Figure 1.42. Distribution of relative bias (left boxplot) and relative standard error (right boxplot) in the density estimate for a simulated scenario of a spatial capture-recapture model ($D = 100$ bears/100 km², $\sigma = 2$ km, $g_0 = 0.02$, and sampling occurred over 5 weeks)52

Figure 1.43. Distribution of relative bias (left boxplot) and relative standard error (right boxplot) in the density estimate for a simulated scenario of a spatial capture-recapture model ($D = 10$ bears/100 km², $\sigma = 5$ km, $g_0 = 0.02$, and sampling occurred over 5 weeks)52

Figure 1.44. Distribution of relative bias (left boxplot) and relative standard error (right boxplot) in the density estimate for a simulated scenario of a spatial capture-recapture model ($D = 50$ bears/100 km², $\sigma = 5$ km, $g_0 = 0.02$, and sampling occurred over 5 weeks)53

Figure 1.45. Distribution of relative bias (left boxplot) and relative standard error (right boxplot) in the density estimate for a simulated scenario of a spatial capture-recapture model ($D = 100$ bears/100 km², $\sigma = 5$ km, $g_0 = 0.02$, and sampling occurred over 5 weeks)53

Figure 1.46. Distribution of relative bias (left boxplot) and relative standard error (right boxplot) in the density estimate for a simulated scenario of a spatial capture-recapture model ($D = 10$ bears/100 km², $\sigma = 12$ km, $g_0 = 0.02$, and sampling occurred over 5 weeks)54

Figure 1.47. Distribution of relative bias (left boxplot) and relative standard error (right boxplot) in the density estimate for a simulated scenario of a spatial capture-recapture model ($D = 50$ bears/100 km², $\sigma = 12$ km, $g_0 = 0.02$, and sampling occurred over 5 weeks)54

Figure 1.48. Distribution of relative bias (left boxplot) and relative standard error (right boxplot) in the density estimate for a simulated scenario of a spatial capture-recapture model ($D = 100$ bears/100 km², $\sigma = 12$ km, $g_0 = 0.02$, and sampling occurred over 5 weeks)55

Figure 1.49. Distribution of relative bias (left boxplot) and relative standard error (right boxplot) in the density estimate for a simulated scenario of a spatial capture-recapture model ($D = 10$ bears/100 km², $\sigma = 2$ km, $g_0 = 0.2$, and sampling occurred over 5 weeks)55

Figure 1.50. Distribution of relative bias (left boxplot) and relative standard error (right boxplot) in the density estimate for a simulated scenario of a spatial capture-recapture model ($D = 50$ bears/100 km², $\sigma = 2$ km, $g_0 = 0.2$, and sampling occurred over 5 weeks)56

Figure 1.51. Distribution of relative bias (left boxplot) and relative standard error (right boxplot) in the density estimate for a simulated scenario of a spatial capture-recapture model ($D = 100$ bears/100 km², $\sigma = 2$ km, $g_0 = 0.2$, and sampling occurred over 5 weeks)56

Figure 1.52. Distribution of relative bias (left boxplot) and relative standard error (right boxplot) in the density estimate for a simulated scenario of a spatial capture-recapture model ($D = 10$ bears/100 km², $\sigma = 5$ km, $g_0 = 0.2$, and sampling occurred over 5 weeks)57

Figure 1.53. Distribution of relative bias (left boxplot) and relative standard error (right boxplot) in the density estimate for a simulated scenario of a spatial capture-recapture model ($D = 50$ bears/100 km², $\sigma = 5$ km, $g_0 = 0.2$, and sampling occurred over 5 weeks)57

Figure 1.54. Distribution of relative bias (left boxplot) and relative standard error (right boxplot) in the density estimate for a simulated scenario of a spatial capture-recapture model ($D = 100$ bears/100 km², $\sigma = 5$ km, $g_0 = 0.2$, and sampling occurred over 5 weeks)58

Figure 1.55. Distribution of relative bias (left boxplot) and relative standard error (right boxplot) in the density estimate for a simulated scenario of a spatial capture-recapture model ($D = 10$ bears/100 km², $\sigma = 12$ km, $g_0 = 0.2$, and sampling occurred over 5 weeks)58

Figure 1.56. Distribution of relative bias (left boxplot) and relative standard error (right boxplot) in the density estimate for a simulated scenario of a spatial capture-recapture model ($D = 50$ bears/100 km², $\sigma = 12$ km, $g_0 = 0.2$, and sampling occurred over 5 weeks)59

Figure 1.57. Distribution of relative bias (left boxplot) and relative standard error (right boxplot) in the density estimate for a simulated scenario of a spatial capture-recapture model ($D = 100$ bears/100 km², $\sigma = 12$ km, $g_0 = 0.2$, and sampling occurred over 5 weeks)59

Figure 1.58. Distribution of relative bias (left boxplot) and relative standard error (right boxplot) in the density estimate for a simulated scenario of a spatial capture-recapture model ($D = 10$ bears/100 km², $\sigma = 2$ km, $g_0 = 0.005$, and sampling occurred over 7 weeks)60

Figure 1.59. Distribution of relative bias (left boxplot) and relative standard error (right boxplot) in the density estimate for a simulated scenario of a spatial capture-recapture model ($D = 50$ bears/100 km², $\sigma = 2$ km, $g_0 = 0.005$, and sampling occurred over 7 weeks)60

Figure 1.60. Distribution of relative bias (left boxplot) and relative standard error (right boxplot) in the density estimate for a simulated scenario of a spatial capture-recapture model ($D = 100$ bears/100 km², $\sigma = 2$ km, $g_0 = 0.005$, and sampling occurred over 7 weeks)61

Figure 1.61. Distribution of relative bias (left boxplot) and relative standard error (right boxplot) in the density estimate for a simulated scenario of a spatial capture-recapture model ($D = 10$ bears/100 km², $\sigma = 5$ km, $g_0 = 0.005$, and sampling occurred over 7 weeks)61

Figure 1.62. Distribution of relative bias (left boxplot) and relative standard error (right boxplot) in the density estimate for a simulated scenario of a spatial capture-recapture model ($D = 50$ bears/100 km², $\sigma = 5$ km, $g_0 = 0.005$, and sampling occurred over 7 weeks)62

Figure 1.63. Distribution of relative bias (left boxplot) and relative standard error (right boxplot) in the density estimate for a simulated scenario of a spatial capture-recapture model ($D = 100$ bears/100 km², $\sigma = 5$ km, $g_0 = 0.005$, and sampling occurred over 7 weeks)62

Figure 1.64. Distribution of relative bias (left boxplot) and relative standard error (right boxplot) in the density estimate for a simulated scenario of a spatial capture-recapture model ($D = 10$ bears/100 km², $\sigma = 12$ km, $g_0 = 0.005$, and sampling occurred over 7 weeks)63

Figure 1.65. Distribution of relative bias (left boxplot) and relative standard error (right boxplot) in the density estimate for a simulated scenario of a spatial capture-recapture model ($D = 50$ bears/100 km², $\sigma = 12$ km, $g_0 = 0.005$, and sampling occurred over 7 weeks)63

Figure 1.66. Distribution of relative bias (left boxplot) and relative standard error (right boxplot) in the density estimate for a simulated scenario of a spatial capture-recapture model ($D = 100$ bears/100 km², $\sigma = 12$ km, $g_0 = 0.005$, and sampling occurred over 7 weeks)64

Figure 1.67. Distribution of relative bias (left boxplot) and relative standard error (right boxplot) in the density estimate for a simulated scenario of a spatial capture-recapture model ($D = 10$ bears/100 km², $\sigma = 2$ km, $g_0 = 0.02$, and sampling occurred over 7 weeks)64

Figure 1.68. Distribution of relative bias (left boxplot) and relative standard error (right boxplot) in the density estimate for a simulated scenario of a spatial capture-recapture model ($D = 50$ bears/100 km², $\sigma = 2$ km, $g_0 = 0.02$, and sampling occurred over 7 weeks)65

Figure 1.69. Distribution of relative bias (left boxplot) and relative standard error (right boxplot) in the density estimate for a simulated scenario of a spatial capture-recapture model ($D = 100$ bears/100 km², $\sigma = 2$ km, $g_0 = 0.02$, and sampling occurred over 7 weeks)65

Figure 1.70. Distribution of relative bias (left boxplot) and relative standard error (right boxplot) in the density estimate for a simulated scenario of a spatial capture-recapture model ($D = 10$ bears/100 km², $\sigma = 5$ km, $g_0 = 0.02$, and sampling occurred over 7 weeks)66

Figure 1.71. Distribution of relative bias (left boxplot) and relative standard error (right boxplot) in the density estimate for a simulated scenario of a spatial capture-recapture model ($D = 50$ bears/100 km², $\sigma = 5$ km, $g_0 = 0.02$, and sampling occurred over 7 weeks)66

Figure 1.72. Distribution of relative bias (left boxplot) and relative standard error (right boxplot) in the density estimate for a simulated scenario of a spatial capture-recapture model ($D = 100$ bears/100 km², $\sigma = 5$ km, $g_0 = 0.02$, and sampling occurred over 7 weeks)67

Figure 1.73. Distribution of relative bias (left boxplot) and relative standard error (right boxplot) in the density estimate for a simulated scenario of a spatial capture-recapture model ($D = 10$ bears/100 km², $\sigma = 12$ km, $g_0 = 0.02$, and sampling occurred over 7 weeks)67

Figure 1.74. Distribution of relative bias (left boxplot) and relative standard error (right boxplot) in the density estimate for a simulated scenario of a spatial capture-recapture model ($D = 50$ bears/100 km², $\sigma = 12$ km, $g_0 = 0.02$, and sampling occurred over 7 weeks)68

Figure 1.75. Distribution of relative bias (left boxplot) and relative standard error (right boxplot) in the density estimate for a simulated scenario of a spatial capture-recapture model ($D = 100$ bears/100 km², $\sigma = 12$ km, $g_0 = 0.02$, and sampling occurred over 7 weeks)68

Figure 1.76. Distribution of relative bias (left boxplot) and relative standard error (right boxplot) in the density estimate for a simulated scenario of a spatial capture-recapture model ($D = 10$ bears/100 km², $\sigma = 2$ km, $g_0 = 0.2$, and sampling occurred over 7 weeks)69

Figure 1.77. Distribution of relative bias (left boxplot) and relative standard error (right boxplot) in the density estimate for a simulated scenario of a spatial capture-recapture model ($D = 50$ bears/100 km², $\sigma = 2$ km, $g_0 = 0.2$, and sampling occurred over 7 weeks)69

Figure 1.78. Distribution of relative bias (left boxplot) and relative standard error (right boxplot) in the density estimate for a simulated scenario of a spatial capture-recapture model ($D = 100$ bears/100 km², $\sigma = 2$ km, $g_0 = 0.2$, and sampling occurred over 7 weeks)70

Figure 1.79. Distribution of relative bias (left boxplot) and relative standard error (right boxplot) in the density estimate for a simulated scenario of a spatial capture-recapture model ($D = 10$ bears/100 km², $\sigma = 5$ km, $g_0 = 0.2$, and sampling occurred over 7 weeks)70

Figure 1.80. Distribution of relative bias (left boxplot) and relative standard error (right boxplot) in the density estimate for a simulated scenario of a spatial capture-recapture model ($D = 50$ bears/100 km², $\sigma = 5$ km, $g_0 = 0.2$, and sampling occurred over 7 weeks)71

Figure 1.81. Distribution of relative bias (left boxplot) and relative standard error (right boxplot) in the density estimate for a simulated scenario of a spatial capture-recapture model ($D = 100$ bears/100 km², $\sigma = 5$ km, $g_0 = 0.2$, and sampling occurred over 7 weeks)71

Figure 1.82. Distribution of relative bias (left boxplot) and relative standard error (right boxplot) in the density estimate for a simulated scenario of a spatial capture-recapture model ($D = 10$ bears/100 km², $\sigma = 12$ km, $g_0 = 0.2$, and sampling occurred over 7 weeks)72

Figure 1.83. Distribution of relative bias (left boxplot) and relative standard error (right boxplot) in the density estimate for a simulated scenario of a spatial capture-recapture model ($D = 50$ bears/100 km ² , $\sigma = 12$ km, $g_0 = 0.2$, and sampling occurred over 7 weeks)	72
Figure 1.84. Distribution of relative bias (left boxplot) and relative standard error (right boxplot) in the density estimate for a simulated scenario of a spatial capture-recapture model ($D = 100$ bears/100 km ² , $\sigma = 12$ km, $g_0 = 0.2$, and sampling occurred over 7 weeks)	73
Figure 2.1. Map of the study area (inset) and land covers in which black bear GPS locations occurred in the northern Lower Peninsula of Michigan from 2011 – 2015. Land cover types were reclassified from the 2011 National Land Cover Database	101
Figure 2.2. Functional response in use of agriculture for female (top) and male (bottom) black bears as bear density varied in the Lower Peninsula of Michigan from 2011 – 2015. The colored ribbons represent the 95% confidence interval around the estimated response (solid black line) for females (orange) and males (blue). The red dashed line indicates odds ratio=1, which is interpreted as having no effect on use.....	102
Figure 2.3. Functional response in use of agriculture for female (top) and male (bottom) black bears as the percent agriculture varied within the average sex-specific home range radius (5 km radius for females and 12 km radius for males). GPS locations were collected in the Lower Peninsula of Michigan from 2011 – 2015. The colored ribbons represent the 95% confidence interval around the estimated response (solid black line) for females (orange) and males (blue). The red dashed line indicates odds ratio=1, which is interpreted as having no effect on use	103
Figure 2.4. Functional response in use of agriculture for female (top) and male (bottom) black bears as distance to high-intensity (top) or low-intensity (bottom) human development varied in the Lower Peninsula of Michigan from 2011 – 2015. The colored ribbons represent the 95% confidence interval around the estimated response (solid black line) for females (orange) and males (blue). The red dashed line indicates odds ratio=1, which is interpreted as having no effect on use	104
Figure 2.5. Spline correlograms of spatial correlation, with 95% bootstrap confidence intervals, of the residuals from a logistic regression model of female black bear location data and all explanatory variables	105
Figure 2.6. Spline correlograms of temporal correlation, with 95% bootstrap confidence intervals of the residuals, from a logistic regression model of female black bear location data and all explanatory variables	106
Figure 2.7. Spline correlograms of spatial correlation, with 95% bootstrap confidence intervals, of the residuals from a logistic regression model of male black bear location data and all explanatory variables	107

Figure 2.8. Spline correlograms of temporal correlation, with 95% bootstrap confidence intervals of the residuals, from a logistic regression model of male black bear location data and all explanatory variables108

INTRODUCTION

In the 21st century, management of wildlife populations requires a difficult balance of pursuing fundamental knowledge, such as accurate estimation of population size and distribution of species across landscapes, while simultaneously adapting to an era in which spatiotemporal ecological processes are increasingly stochastic (Corlett 2015). Climate change is altering basic ecological patterns, including species distributions (reviewed in Walther et al. 2002), while rates of urbanization and land conversion continue to increase and fragment habitat on both broad and fine-scales (Wilcove et al. 1998). The resultant patchwork of habitat fragments affects population dynamics, behavioral processes, and patterns of movement (reviewed in Fischer and Lindenmayer 2007). Highly heterogeneous landscapes drive variation in local densities, complicating species' movement and resource selection, and challenge wildlife managers to predict how species will respond across a broad range of ecological conditions. Furthermore, habitat loss increases the overlap in space use between humans and wildlife, which often results in increased conflicts (Baruch-Mordo et al. 2008). Because of these challenges, spatially explicit estimations of population size and fine-scale quantification of species' behavior are especially informative for management and conservation.

In addition to rapid biotic changes, this century has seen rapid advances in quantitative and statistical tools. For instance, in the last 10 years spatial capture-recapture (SCR) models were developed (Borchers and Efford 2008, Royle and Young 2008) and statistical methods for quantifying functional relationships have diversified (Hebblewhite and Merrill 2008, Godvik et al. 2009, Matthiopoulos et al. 2011). SCR models incorporate the spatial information of a capture-mark-recapture dataset to estimate density of animal populations. Functional relationships quantify how probability of using a resource changes as a function of its availability

(Mysterud and Ims 1998). Both advancements provide tools to evaluate variation in population size and species' behavior at finer-scales than traditional methods. Such information is particularly useful for management of widespread, generalist species.

American black bears (*Ursus americanus*) are one of the best-known generalist species in North America. Though typically associated with forests, black bears have a demonstrated ability to exist and even thrive in human-dominated landscapes. This flexibility, coupled with the impacts of shrinking contiguous forested habitat, contributes to the increasing frequency and magnitude of black bear-human conflicts (Beckman et al. 2004). Management of this species, though crucial, is complicated. Bears play an important ecological role as a widespread omnivore, especially in regions of the eastern United States where they may be the only large mammalian predator (Noss et al. 1996). Black bears are relatively tolerant of anthropogenic influences and are of interest to diverse public groups. Black bears are prominent in the history, culture, and beliefs of many First Nations in North America. Black bears are popular both as a game species and for wildlife-viewing. Yet the public may consider encounters with bears a threat, a nuisance, or a treasured experience. Because of these diverse interests, management is often defined by social desires for this species. Managing black bears in Michigan is a prime example of this complexity.

The black bear population in Michigan has been increasing since the 1990s (Michigan Department of Natural Resources 2009). Bears have been managed by the state as a game species since 1925. Hunting regulations permit baiting, the use of archery and firearms, and the use of dogs, which have made bears a popular game species within Michigan's hunting community. Black bears are primarily distributed in the Upper Peninsula and northern Lower Peninsula of Michigan. This landscape is highly heterogeneous: the northern half of the Lower

Peninsula is dominated by forested landscapes that transition to urban- and agriculture-dominated landscapes in the southern half. As a result, local black bear densities vary greatly; bear densities are highest in the northern region and begin to decline as the landscape transitions from forest to agriculture. Due to this variation, managers were interested in estimating population density in a spatially explicit manner. Although still uncommon, occurrences of bears have increased in the southern Lower Peninsula during the past 5 years. This trend highlighted the need to understand how bears use resources when local densities and landscape composition are highly variable.

In Chapter 1, I evaluated the performance of a spatially explicit density estimator for black bears in the northern Lower Peninsula of Michigan. I simulated capture-mark-recapture data (CMR) from an existing array of hair-snare traps and fit the data to a spatial capture-recapture model. The hair-snare array was originally designed to provide an estimate of bear abundance for a large region (i.e., the northern Lower Peninsula); producing spatially explicit population estimates represented a repurposing of the data. To identify limitations to repurposing these data, I simulated data collection under 81 different scenarios and assessed variation in accuracy and precision of the density estimate. Density estimates were not robust across scenarios. Approximately 40% of simulated scenarios produced stable and reasonably accurate density estimates. Accuracy of the estimates were affected by all 4 simulated scenario characteristics. My results indicated it was essential to have supplemental information identifying the conditions under which the data were collected in order to repurpose CMR data from a trap array designed for non-spatial data analysis.

In Chapter 2, I explored black bear use of agriculture along the southern edge of their distribution. In the Lower Peninsula of Michigan this area is the transitional zone from a forest-

dominated to an agriculture-dominated landscape. I used GPS telemetry data from 12 radio collared black bears (n = 6 females, 6 males) to quantify how bear selection for agriculture was affected by a suite of covariates. Covariates included bear density, proportion of agriculture within the surrounding landscape, distance to developed land (e.g., roads, impervious surfaces), and distance to water. Use of agriculture was density-dependent for both male and female bears, but the direction of the relationship was sex-specific. Female bears were more likely to use agriculture in higher bear density areas, whereas males were less likely to use agriculture when bear densities were higher. In both sexes, use of agriculture varied as a function of distance to developments, and amount of agriculture in the surrounding landscape. These findings demonstrated the trade-offs involved in bear use of agriculture, the influence of environmental context on patterns of black bear resource selection, and suggested male and female bears perceived this context and the trade-offs it created differently.

Each of these chapters is written for independent publication with coauthors. Therefore, text invokes the plural “we” instead of singular “I”.

LITERATURE CITED

LITERATURE CITED

- Baruch-Mordo, S., S. W. Breck, K. R. Wilson, and D. M. Theobald. 2008. Spatiotemporal distribution of black bear–human conflicts in Colorado, USA. *Journal of Wildlife Management* 72:1853–1862.
- Beckmann, J. P., C. W. Lackey, and J. Berger. 2004. Evaluation of deterrent techniques and dogs to alter behavior of ‘nuisance’ black bears. *Wildlife Society Bulletin* 32:1141–1146.
- Borchers, D. L., and M. G. Efford. 2008. Spatially explicit maximum likelihood methods for capture-recapture studies. *Biometrics* 64:377–85.
- Corlett, R. T. 2015. The Anthropocene concept in ecology and conservation. *Trends in Ecology & Evolution* 30:36–41.
- Fischer, J., and D. B. Lindenmayer. 2007. Landscape modification and habitat fragmentation: a synthesis. *Global Ecology and Biogeography* 16:265–280.
- Godvik, I. M. R., L. E. Loe, J. O. Vik, V. Veiberg, R. Langvatn, and A. Mysterud. 2009. Temporal scales, trade-offs, and functional responses in red deer habitat selection. *Ecology* 90:699–710.
- Hebblewhite, M., and E. Merrill. 2008. Modelling wildlife–human relationships for social species with mixed-effects resource selection models. *Journal of Applied Ecology* 45:834–844.
- Matthiopoulos, J., M. Hebblewhite, G. Aarts, and J. Fieberg. 2011. Generalized functional responses for species distributions. *Ecology* 92:583–589.
- Michigan Department of Natural Resources. 2009. Michigan black bear management plan. Michigan Department of Natural Resources Wildlife Division, Lansing, Michigan, USA.
- Mysterud, A., and R. A. Ims. 1998. Functional responses in habitat use: availability influences relative use in trade-off situations. *Ecology* 79:1435–1441.
- Noss, R. F., H. B. Quigley, M. G. Hornocker, T. Merrill, and P. C. Paquet. 1996. Conservation biology and carnivore conservation in the Rocky Mountains. *Conservation Biology* 10:949–963.
- Royle, J. A., and K. V. Young. 2008. A hierarchical model for spatial capture-recapture data. *Ecology* 89:2281–2289.

Walther, G-R., E. Post, P. Convey, A. Menzel, C. Parmesan, T. J. C. Beebee, J-M. Fromentin, O. H-G., and F. Bairlein. 2002. Ecological responses to recent climate change. *Nature* 416:389–395.

Wilcove, D. S., D. Rothstein, J. Dubow, A. Phillips, and E. Losos. 1998. Quantifying threats to imperiled species in the United States. *BioScience* 48:607–615.

CHAPTER 1: PERFORMANCE OF A SPATIAL CAPTURE-RECAPTURE MODEL FOR REPURPOSED BLACK BEAR HAIR SNARE DATA

Introduction

Accurate estimates of the size and distribution of animal populations are fundamental to effective management of wildlife. Capture-mark-recapture (CMR) studies and models have been used extensively to produce these estimates. However, non-spatial CMR models do not directly quantify the effective sampling area (Sun et al. 2014), requiring them to estimate density post hoc. In the past decade, spatial capture-recapture (SCR) models were developed that produce spatially explicit density estimates (Borchers and Efford 2008, Royle and Gardner 2011). These new methods incorporate the spatial information inherent to a CMR dataset (e.g., location of traps and of detections) to estimate not only density, but also the parameters constituting the spatial detection process. Unlike non-spatial capture-recapture models, SCR models define detection probability as a function of two parameters: g_0 , which reflects the probability of detecting an individual at a trap, and sigma (σ), a spatial scale parameter defining how detection changes as a function of the distance between an individual and a trap. Estimating both g_0 and σ enables SCR models to estimate the locations of activity centers of detected animals. These characteristics allow SCR models to account for unequal exposure of individuals to traps, to quantify the effective sampling area, and therefore, the density of the studied population (Borchers and Efford 2008, Gardner et al. 2009, Royle and Gardner 2011).

The rapid advancement of computer-processing abilities and quantitative methods in ecology and related fields has resulted in proliferation of widely available, free, and user-friendly computer programs to conduct innovative statistical modeling. These tools offer opportunities not only to improve our ability to manage and conserve wildlife but to maximize the amount of information garnered from existing datasets. However, when existing data are repurposed for use

in new analytical methods, it is crucial to understand the limitations and assumptions involved. Wildlife biologists have been collecting CMR datasets to estimate abundance for decades. These abundance estimates are often converted post hoc to density estimates because the latter is independent from observational scale (Howe et al. 2013). Thus, directly estimating density in a spatially explicit manner from existing CMR data is appealing. The development of SCR models made this retrospective repurposing possible. However, the sampling design used to collect existing CMR data was likely not customized for SCR models, which could limit effective parameter estimation.

Although SCR models are flexible to diverse sampling designs (Efford and Fewster 2013), the spatial configuration and spacing of traps directly influence the accuracy and precision of parameter estimates in SCR models (Sollman et al. 2012, Sun et al. 2014, Wilton et al. 2014). In any CMR study, the spatial arrangement of the trap array should reflect the movement ecology of the studied species (Pollock et al. 1990). SCR models rely on sufficient individual detections, non-spatial recaptures, and recaptures at multiple traps (i.e., spatial recaptures) to identify the location of activity centers and, by extension, accurately estimate model parameters (Sun et al. 2014). If trap spacing is larger than the typical movements of individuals, it is unlikely the trapping array will collect the recaptures necessary for accurate parameter estimation. Thus, it is useful to consider the conditions (i.e., what true values of g_0 , σ , and density) under which SCR models based on existing CMR data may produce reliable estimates of density.

Here we evaluated estimating black bear (*Ursus americanus*) density using existing hair snare data gathered from a trapping array that was not intended to inform an SCR model. The hair snare array was originally designed to collect data for a non-spatial CMR model, which estimated bear abundance over the northern Lower Peninsula (NLP) of Michigan, while abiding

within logistical and financial restrictions. Trap spacing was variable in the array and the distribution of traps was not uniform over the landscape. Our objective was to identify the conditions under which an SCR model of repurposed data reliably estimated density and to describe how estimator performance changed across the plausible parameter space. We used simulations to evaluate performance of density estimates from an SCR model across a suite of conditions reflecting plausible parameter and sampling efforts. Previous studies have described how estimation performance changes with different configurations and spacing of traps; our study describes how performance relates to differences in parameter combinations (population and sampling characteristics) for a fixed trapping array.

Methods

Data

In 2003, biologists from the Michigan Department of Natural Resources deployed barbed-wire hair snares to estimate black bear abundance in the northern Lower Peninsula (NLP) of Michigan. Over 200 snares were distributed across 36,848 km² (see Dreher et al. 2007 for data collection procedures). The spatial arrangement of the snare array was irregular but spatially clustered (Fig 1.1). Capture data for 2003, 2005, 2009, and 2013 were each analyzed using non-spatial capture-recapture models. Across these 4 years, the number of snares differed slightly but existing locations were reused. In 2003 and 2005, 239 snares were deployed; in 2009 and 2013, 257 snares were deployed. This analysis evaluated model performance based on the snare arrangement from 2009.

Simulations

We designed 81 different scenarios that varied the values of SCR model parameters and the number of sampling occasions. The parameter space consisted of 3 values (a low, medium, and

high level) of density (D ; 10, 50, and 100 bears per 100 km²), sigma (σ ; 2, 5, and 12 km), detection probability at the trap (g_0 ; 0.005, 0.02, and 0.2), and number of sampling occasions (k ; 3, 5, and 7 weeks). The simulated values of D , σ , and g_0 encompassed the realistic value of each parameter for the NLP black bear population, as well as extreme lower and upper limits around that value. This range allowed us to quantify model performance broadly. Simulated sampling occasions represent the current protocol (5 weeks), as well as shortened and extended sampling options. These values allowed us to explore optimal sampling effort. Each scenario was simulated for 100 iterations, thereby generating 100 detection histories for each set of parameters and sampling frequencies.

We conducted simulations in program R (R version 3.2.2, www.r-project.org, accessed 01 Aug 2015) and used packages `secr` (version 3.1.0, <http://CRAN.R-project.org/package=secr>) and `secrdesign` (version 2.5.2, <http://CRAN.R-project.org/package=secrdesign>), which employ a maximum likelihood approach for parameter estimation. Simulated activity centers of individual bears were randomly distributed over the landscape according to a homogenous Poisson point process. Our spatial extent was defined by the boundaries of three Michigan Department of Natural Resources bear management units in the NLP (Fig 1.1). We assumed the population to be closed because the study area is bounded by Lake Michigan, Lake Huron, and heavy agriculture and urban land covers to the south. We assumed temporal closure because researchers sampled the population after bears emerged from hibernation, and sampling ended before hunting season began. We simulated a maximum number of 7 sampling weeks to maintain this assumption of temporal closure.

Model performance was assessed by multiple metrics: we determined how many replicates of a scenario encountered maximization errors or failure to calculate variances, we

calculated median relative standard error (RSE) of density estimates as an indicator of precision ($\frac{SE\ of\ estimate}{estimate}$), median relative bias (RB) of density estimates as an indicator of accuracy ($\frac{estimate-truth}{truth}$), and variability in RB and RSE across simulation replicates (measured as median absolute deviation, MAD) as indicators of stability of estimates.

Results

In 60 of the 81 simulated scenarios, at least 1 of the 100 replicates in each scenario encountered a likelihood maximization error and/or failure to calculate variance, indicating model parameters were inestimable. Scenarios with low detectability (i.e., $g_0 = 0.005$ and $\sigma = 2$ km) were prone to high rates of failing to estimate parameters (27 – 81% of replicates) (Table 1.1). 10 of these 60 scenarios that encountered failed replicates had such high failure rates ($\geq 20\%$) that we considered estimates unstable and removed them from further analysis (Table 1.1). Scenarios with 100% successful replicates ($n = 21$) consisted of diverse combinations of parameter values. However, 18 of these 21 scenarios were simulated with high detection probability at the trap, $g_0 = 0.2$ (Table 1.2)

Precision of density estimates and variation in the amount of error fluctuated across scenarios. However, estimates from most scenarios (54 out of 71) were reasonably precise ($\leq 20\%$ median RSE, Pollock et al. 1990) (Table 1.2). Median RSE and the median absolute deviation of the RSE declined with any increase in the value of g_0 , σ , density, or the number of sampling occasions (Figs 1.2a, 1.2b). The 17 scenarios with poor precision (median RSE $> 20\%$) were simulated with low or moderate values of g_0 (0.005 or 0.02), and σ was typically (15 out of 17 scenarios) simulated as a low to medium distance (2 or 5 km) (Figs 1.2a, 1.2b). All three values of density and number of sampling occasions were equally represented in scenarios that imprecisely estimated density.

Compared to their lower detection probability counterparts, scenarios simulated with a higher g_0 or larger σ generally reduced median RSE and MAD of RSE in the density estimate by a larger margin than did increasing density or number of weeks sampled. For example, in a scenario with $\sigma = 5$ km, $D = 50$ bears/100 km² and sampled for 5 weeks, the precision of density estimates improved as the probability of detecting an animal at the trap increased; when g_0 was simulated low ($g_0 = 0.005$), median RSE was 0.320, which reduced by 97% to a median RSE of 0.011 when $g_0 = 0.2$. In comparison, median RSE reduced by 33% as the number of sampling occasions increased from 3 to 7 weeks within a scenario of $g_0 = 0.2$, $\sigma = 5$ km, $D = 50$ bears/100 km² (Table 1.2). However, relative to their lower value counterpart scenarios, scenarios simulated with higher densities and sampled for longer periods of times did still estimate density with higher precision. For instance, the most precise density estimate was specific to a high-density scenario; median RSE = 0.005 when detection at the trap was high ($g_0 = 0.2$), sigma was large ($\sigma = 12$ km) and density was high ($D = 100$ bears/100 km²), regardless of number of weeks sampled.

Within the 71 retained scenarios, median relative bias in the density estimate ranged from 1–21% (Table 1.2). Median absolute deviation of RB ranged from 0.005 to 0.724. Unlike other metrics of performance, median relative bias in the estimation procedure was not consistently associated with the values of scenario parameters. Higher detection probability at a trap, larger σ , denser populations, and increasing sampling occasions reduced the MAD of relative bias, but not necessarily the median relative bias. Higher simulated density and g_0 values reduced median bias in 50% of scenarios (Fig 1.3a), while increasing σ or the number of sampling occasions produced a less biased density estimate in ~ 30% of scenario comparisons (Fig 1.3b). Because median bias of the density estimate was not as predictable as other metrics of performance, less than half of

all simulated scenarios ($n = 35$) produced relatively accurate and precise estimates (defined as $RB < 15\%$, $RSE < 0.2$, MAD of both RB and $RSE < 0.05$, and 90% of iterations were successful). These 35 scenarios included low, medium, and high simulated values of all 4 scenario parameters (D , g_0 , σ , and number of sampling occasions).

Discussion

Our findings demonstrated the importance of using simulations as a tool to evaluate limitations of confronting data collected for other purposes with new analytical techniques. Previous studies (Sollman et al. 2012, Sun et al. 2014, Wilton et al. 2014) used simulations to design trap layouts that were robust to heterogeneity in SCR model parameters, whereas we used simulations to quantify the performance of these models with the data from a single, existing, trap array under a variety of scenarios. We demonstrated that it is possible to obtain accurate and precise density estimates from a SCR model based on our repurposed data, but these results were not robust across our simulated parameter space. Of concern is how to proceed when an existing trap design is not robust, and simultaneously optimizing bias and precision is difficult and complicated by the interdependence of SCR model parameters. These challenges emphasize the need to assess usefulness of applying new methodology to existing data. Furthermore, our findings indicate additional sources of data are necessary to address these limitations.

Density estimates were not robust across scenarios and within scenario estimates were unstable across random realizations of the capture histories (i.e., among replicates of the same scenario). Certain patterns of improvement were obvious, but performance was conditional on all 4 characteristics of a scenario: population density (D), detection probability at the trap (g_0), the distance from the trap at which detection declines (σ), and the number of sampling occasions (k). This resulted in highly sensitive model performance across the parameter space. This limitation

was the true challenge of repurposing the hair snare data; reliable estimates only occurred when data are collected under specific conditions. Thus, although numerous scenarios produced defensible density estimates, the acceptable conditions for repurposing were rigid and did not allow for generalization.

For example, scenarios that minimized bias were not the same scenarios that optimized precision. This is reasonable considering bias and error measure different aspects of the estimation procedure, but it is also concerning because it can result in high confidence in estimates that are poor representations of truth and vice versa. Most scenarios estimated density with relatively low bias ($\pm 15\%$ median RB). If bias was consistent across simulated scenarios, then correction factors could be incorporated to account for this bias in density estimates, but this was generally not the case. Moreover, individual estimates from replicates were sensitive to random realizations of the detection history. Replicates of a single scenario estimated density with as little as 0.005% or as much as 190% difference between the point estimate and truth, yet median relative bias of the estimation procedure was 1.3% (Appendix II Fig 1.42). This is alarming because it indicates instability in the estimation procedure, even when median bias is negligible.

The parameters σ and g_0 influenced the estimation of density most strongly because they jointly define the detection process. The g_0 parameter is the intercept of the half-normal detection function. Therefore, it scales the magnitude of the probability of detecting an animal when its activity center is located at the trap (Reppucci et al. 2011). Detection probability declines as the distance between a trap and an individual's activity center increases, and σ defines the rate of this decline. A larger σ value slows the rate of decline in detection probability as distance from the trap increases; thus, detection remains higher over longer distances (Royle et al. 2014). The fact

that both parameters govern the detection process means the values of both parameters must be relatively high for accurate parameter estimation.

Due to the observed variable model performance, confidence in SCR density estimates generated from repurposed data is only possible with additional information about the studied population. Specifically, we require information to identify where the population and sampling design exists relative to the simulated parameter space. Sigma can be estimated from the movement ecology of the study species; the 95% home range radius = $\sigma * \text{sqrt}(5.99)$ (Reppucci et al. 2011, Sollmann et al. 2011). We can use VHF or GPS telemetry data to estimate home ranges, and therefore, σ . Population estimates from harvest or trail-camera data can approximate density (Rooseberry and Woolf 1991, Karanth and Nichols 1998) and the number of sampling weeks is predetermined.

For instance, in the NLP of Michigan, 15 black bears were outfitted with GPS radio collars during 2011 – 2015. We used these location data to calculate the average 95% home range radius of male and female bears. Radii were calculated from kernel density estimation determined by a least-squares cross validation smoothing bandwidth. The average 95% home range radius was 5 km for female bears, and 12 km for male bears (Smith 2018, Chapter 2). These distances convert to $\sigma = 2$ and 4.9 km respectively; average σ of all bears was ~ 3.25 km. In 2009, non-spatial CMR models estimated bear abundance as 1,500 bears over 36,848 km². Therefore, we can estimate a minimum black bear density of ~ 4 bear/100 km². The non-spatial CMR study estimated detection at the trap = 0.02 – 0.14 (Dreher et al. 2007). This supplemental information indicated CMR data collection from the hair snare trapping array in 2009 in the NLP occurred in a scenario with low density, moderate σ , moderate g_0 , and was sampled for 5 weeks. According to our simulations, density estimation under this scenario is consistently moderately

precise (median RSE < 0.2 and MAD of RSE = 0.02) with low median relative bias (5%). However, estimates were not stable among replicates (MAD of RB = 0.23). This instability cautions against its use for this trap layout and bear population. Although the central tendency of the estimation procedure has low bias, the method may fail due to a random difference in the realization of the capture history. When this is the case, an alternative for estimating density from this repurposed data is to directly integrate supplemental information about the population into the SCR model.

One of the major advantages of SCR models is the ability to incorporate multiple kinds of data into parameter estimation. In addition to capture-recapture data, SCR models can combine telemetry, spatial harvest, occupancy, or mark-resight data to improve estimation of parameters (Sollman et al. 2013, Chandler and Clark 2014). However, this pooling of data does not change the scenario in which data collection occurred, and our simulations do not provide inference about the performance of SCR models informed by multiple sources of data.

The simulated distribution of the bear population was based on a uniform Poisson process. This distribution assumes a uniform density of bears across the state space, which is not realistic (Brown 1984). Furthermore, hair snares in the 2009 array were distributed to reflect this recognized heterogeneity (Dreher et al. 2007). Future analyses should assess the implications of this mismatch by comparing simulated model performance from multiple distributions. Alternatively, future efforts could use a buffer around each hair snare to define the state space of the simulation. This may reduce the spatial mismatch between snare and bear locations, though it still would not reflect heterogeneous distribution of bears.

The existing hair snare trap array is irregularly distributed, which created variable trap spacing. However, on average traps were spaced 6 km apart. Trap spacing is recommended to be

$< 2\sigma$ (Sollman et al. 2012). If traps are farther apart than this recommendation, they may not collect adequate data for effective SCR parameter estimation (Sun et al. 2014). According to our home range estimates, the average σ of this population was ~ 3.25 km. Therefore, average trap spacing of this array only slightly exceeded the recommendation ($2*3.25$ km = 6.5 km), suggesting the spacing should allow for effective estimation when $\sigma > 3$ km. We might expect scenarios that simulated $\sigma = 2$ km to perform moderately well; however, in our simulations, nearly all scenarios that accurately and precisely estimated density required a minimum sigma of 5 km. Thus, our simulations suggest the guideline of spacing traps $< 2\sigma$ is a strict maximum. Alternatively, the variable trap spacing in this array resulted in an uneven generation of spatial data across the study area. The recommendation may not apply under these conditions. This emphasizes the importance of consistent trap spacing and discourages using an average distance to estimate if trap spacing is reflective of animal movement for non-uniform trap layouts.

Management implications

Repurposing an existing CMR hair snare dataset for SCR models is discouraged without knowledge of the population parameters and sampling design. This information is necessary to determine the conditions under which data collection occurred relative to the parameter space simulated in this analysis. For future sampling efforts in the NLP of Michigan, if, on average, the 95% home range radius of individuals is > 4 km, managers can implement sampling modifications that will produce reasonably accurate density estimates. Accuracy can be improved by sampling snares for 7 weeks and by improving detection probability at the trap. The latter can be increased by baiting traps, and by collecting camera footage of bear behavior at snares to determine if modifications to the snare design are necessary to address behaviors.

APPENDICES

APPENDIX I:

Tables

Table 1.1. Percentage of iterations with maximization or failure to calculate variance errors, median percent relative bias (%RB), median absolute deviation of the relative bias (MAD RB), median relative standard error (RSE), and median absolute deviation of the RSE (MAD RSE) of the density estimate for simulated scenarios of spatial capture-recapture models that experienced > 20% failed iterations (n=10).

Scenario				Metric				
D	g ₀	σ	k	% failed iterations	%RB	MAD RB	RSE	MAD RSE
10	0.005	2	3	81	2.92E+07	434000	1.42	1.48
			5	78	-79.24	0.16	1.32	0.25
			7	70	-70.16	0.14	1.34	0.19
50	0.02	2	3	47	-37.77	0.26	1.35	0.14
			5	36	-1.73	0.74	1.32	0.3
			7	27	-23.58	0.46	0.95	0.46
100	0.005	2	3	58	-59.19	0.22	1.34	0.17
			5	28	-18.24	0.48	0.88	0.43

Table 1.2. Percentage of iterations with maximization or failure to calculate variance errors, median percent relative bias (%RB), median absolute deviation of the relative bias (MAD RB), median relative standard error (RSE), and median absolute deviation of the RSE (MAD RSE) of the density estimator for 71 simulated scenarios of spatial capture-recapture models. Rows with “---” represent scenarios that were removed from further analysis because > 20% of replicates were unsuccessful.

Scenario				Metric					
D	g_0	σ	k	%. failed iterations	%RB	MAD RB	RSE	MAD RSE	
10	0.005	2	3	---	---	---	---	---	
			5	---	---	---	---	---	
			7	---	---	---	---	---	
		5	3	---	---	---	---	---	---
			5	9	8.30	0.724	0.808	0.325	
			7	5	21.01	0.571	0.537	0.149	
		12	3	1	12.85	0.312	0.238	0.028	
			5	0	8.00	0.151	0.140	0.012	
			7	0	6.13	0.100	0.097	0.006	
	0.02	2	3	---	---	---	---	---	
			5	11	-8.95	0.544	0.829	0.275	
			7	2	-7.10	0.561	0.575	0.142	
		5	3	3	4.83	0.357	0.298	0.056	
			5	3	4.91	0.228	0.171	0.018	
			7	1	3.82	0.148	0.122	0.010	
		12	3	1	7.47	0.058	0.059	0.002	
			5	5	6.85	0.038	0.037	0.001	
			7	2	7.87	0.032	0.029	0.001	
0.2	2	3	0	-2.72	0.160	0.144	0.011		
		5	0	-4.99	0.099	0.091	0.004		
		7	0	-5.31	0.085	0.070	0.003		
	5	3	1	3.21	0.032	0.033	0.000		
		5	0	3.14	0.030	0.025	0.000		
		7	1	3.35	0.022	0.022	0.000		

Table 1.2. (cont'd)

		12	3	16	10.83	0.016	0.016	0.000
			5	0	12.23	0.017	0.015	0.000
			7	0	13.35	0.014	0.015	0.000
50	0.005	2	3	---	---	---	---	---
			5	---	---	---	---	---
			7	---	---	---	---	---
		5	3	9	8.67	0.528	0.554	0.145
			5	2	11.78	0.439	0.319	0.054
			7	2	4.74	0.255	0.224	0.030
		12	3	0	6.18	0.106	0.102	0.006
			5	3	5.91	0.071	0.061	0.003
			7	1	6.91	0.041	0.044	0.001
	0.02	2	3	9	4.43	0.603	0.658	0.257
			5	1	1.02	0.363	0.376	0.074
			7	2	-2.68	0.240	0.270	0.038
		5	3	1	5.37	0.116	0.130	0.007
			5	3	3.49	0.078	0.077	0.003
			7	0	4.29	0.058	0.055	0.001
		12	3	4	6.99	0.029	0.026	0.000
			5	6	7.29	0.019	0.016	0.000
			7	7	7.26	0.015	0.013	0.000
	0.2	2	3	0	-4.07	0.062	0.065	0.003
			5	0	-5.11	0.047	0.041	0.001
			7	1	-6.14	0.029	0.032	0.001
		5	3	5	2.71	0.014	0.015	0.000
			5	4	2.92	0.011	0.011	0.000
			7	3	3.00	0.009	0.010	0.000
		12	3	14	10.69	0.007	0.007	0.000
			5	0	12.01	0.007	0.007	0.000
			7	0	13.34	0.008	0.007	0.000
100	0.005	2	3	---	---	---	---	---
			5	---	---	---	---	---
					-			
			7	14	10.46	0.499	0.684	0.223
		5	3	4	10.72	0.399	0.387	0.082
			5	8	5.99	0.211	0.220	0.025
			7	1	3.40	0.186	0.154	0.015

Table 1.2. (cont'd)

	12	3	1	6.46	0.075	0.073	0.003
		5	7	7.16	0.052	0.043	0.001
		7	1	6.93	0.032	0.031	0.001
0.02	2	3	4	4.11	0.454	0.475	0.085
		5	1	1.30	0.262	0.266	0.032
		7	0	-3.34	0.188	0.191	0.018
	5	3	4	4.63	0.090	0.091	0.004
		5	1	3.21	0.047	0.054	0.002
		7	0	3.38	0.032	0.039	0.001
	12	3	2	6.46	0.020	0.018	0.000
		5	8	7.39	0.012	0.012	0.000
		7	3	7.57	0.009	0.009	0.000
0.2	2	3	0	-4.96	0.046	0.046	0.001
		5	0	-5.53	0.030	0.029	0.001
		7	0	-6.13	0.019	0.022	0.000
	5	3	9	3.05	0.010	0.011	0.000
		5	9	3.16	0.008	0.008	0.000
		7	2	3.31	0.007	0.007	0.000
	12	3	13	10.75	0.006	0.005	0.000
		5	0	12.14	0.006	0.005	0.000
		7	0	13.33	0.006	0.005	0.000

APPENDIX II:

Figures

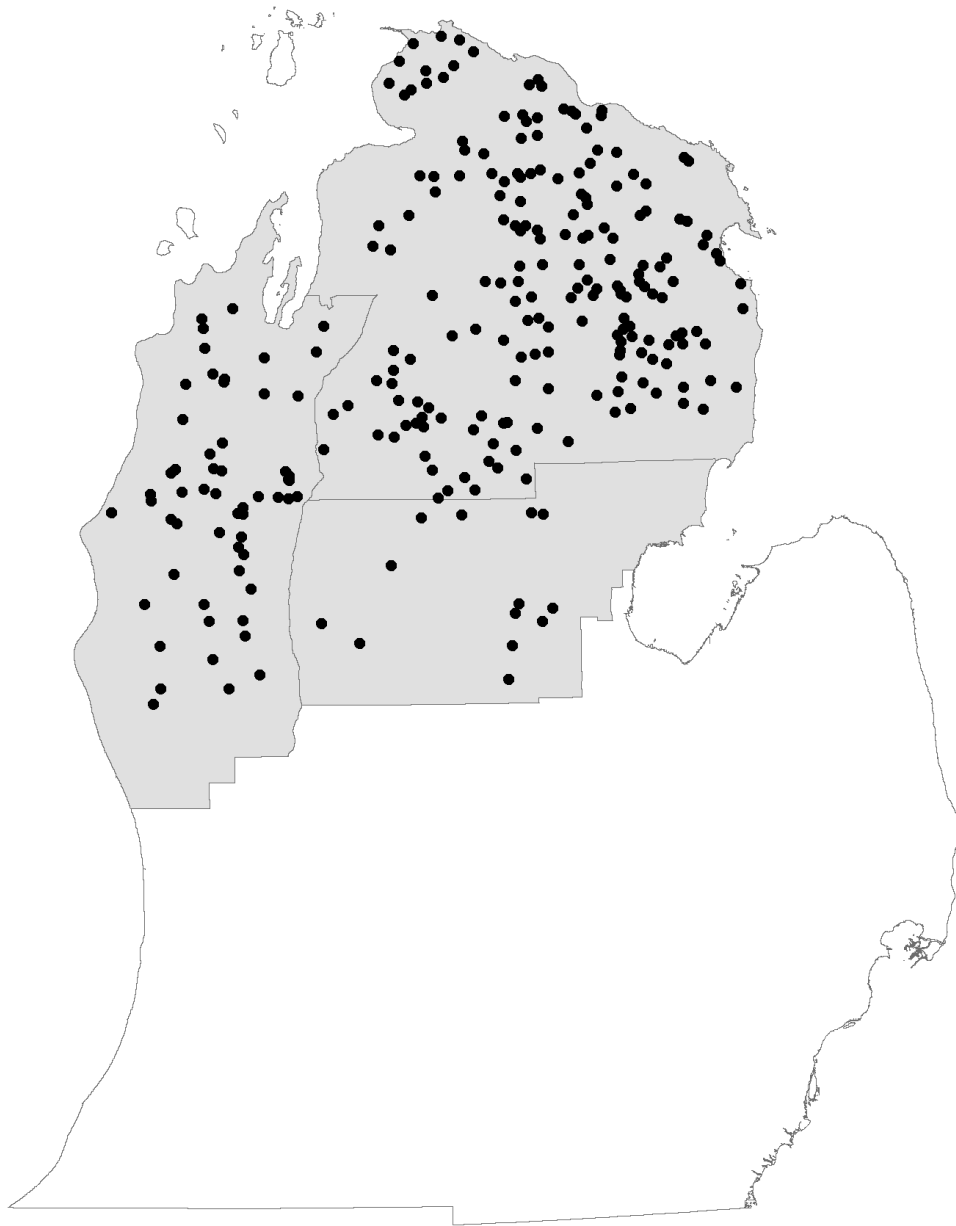


Figure 1.1. Locations of hair snare traps in the northern Lower Peninsula of Michigan in 2009. Shaded polygons represent the three bear management units in this region.

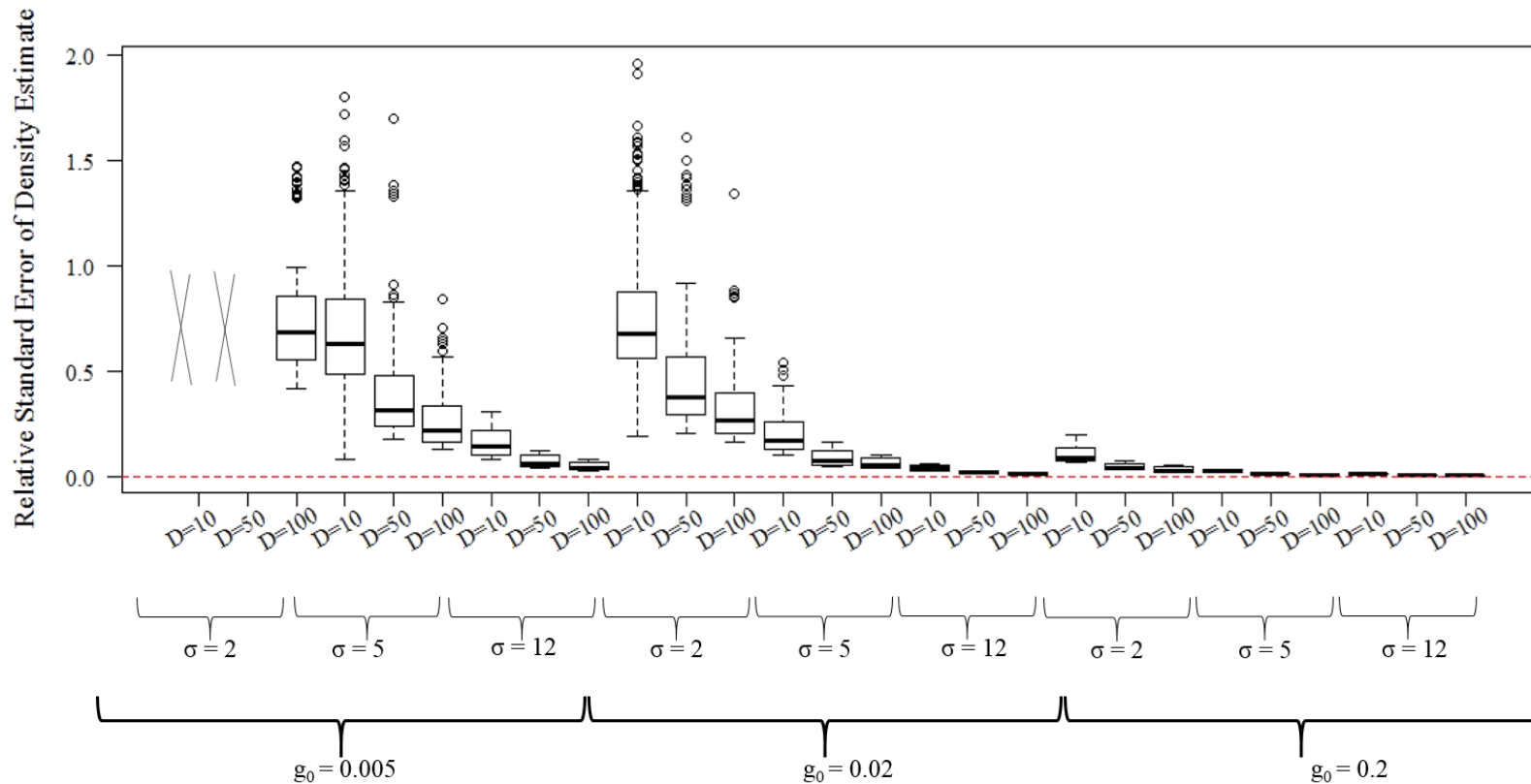


Figure 1.2a. Distribution of relative standard error of the density estimate for simulated scenarios of spatial capture-recapture models. Scenarios are grouped by combinations of g_0 , σ , and density and are aggregated across number of sampling occasions. Only scenarios that did not encounter maximization or variance calculation warnings in $> 80\%$ of iterations are represented ($n=71$). Grey “X” symbols are placeholders for the missing groups of scenarios, which were removed from further analysis because $> 20\%$ of iterations failed. The red, dashed, line is $RSE = 0$.

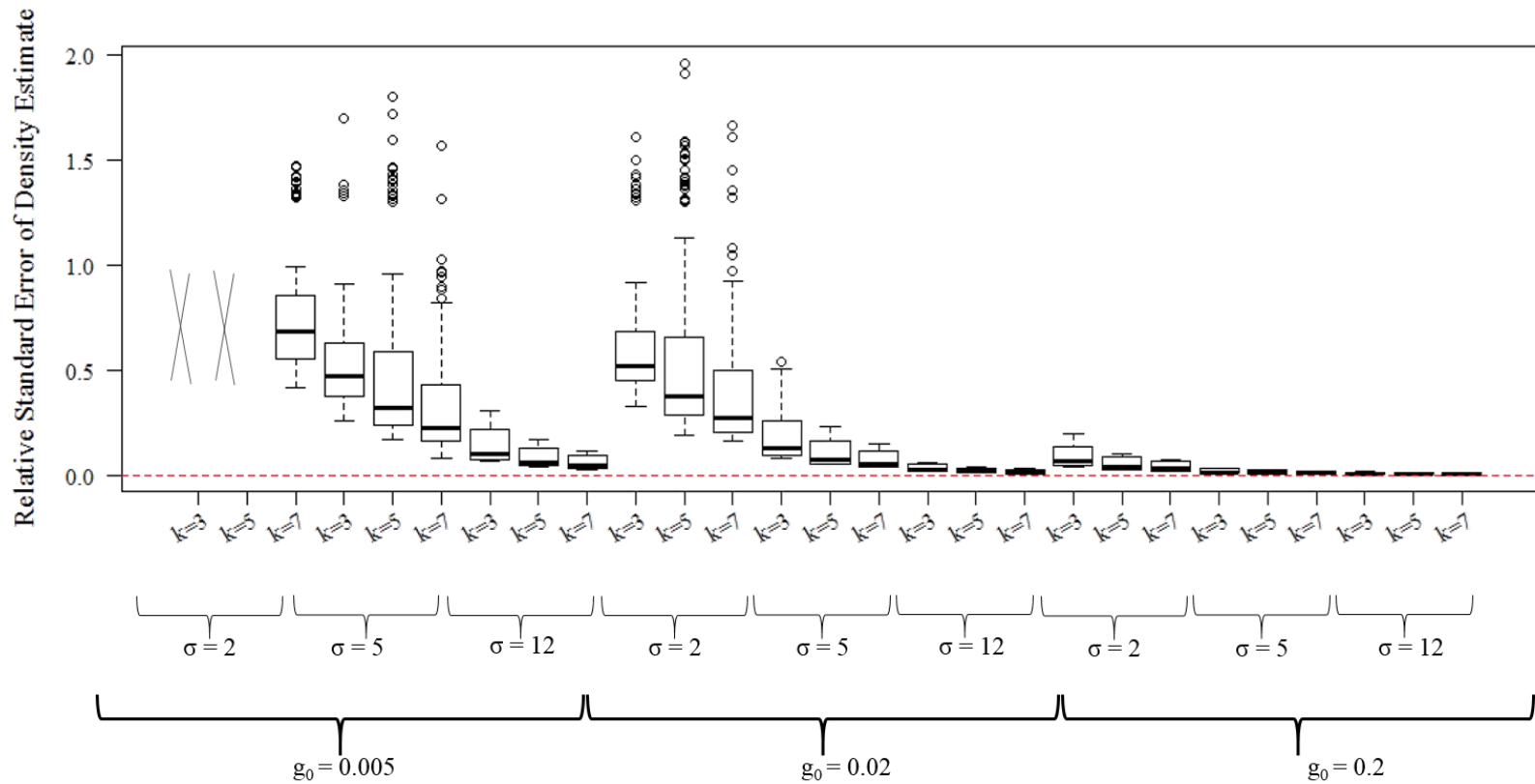


Figure 1.2b. Distribution of relative standard error of the density estimate for simulated scenarios of spatial capture-recapture models. Scenarios are grouped by combinations of g_0 , σ , and number of sampling occasions and are aggregated across density values. Only scenarios that did not encounter maximization or variance calculation warnings in $> 80\%$ of iterations are represented ($n=71$). Grey “X” symbols are placeholders for the missing groups of scenarios, which were removed from further analysis because $> 20\%$ of iterations failed. The red, dashed, line is $RSE = 0$.

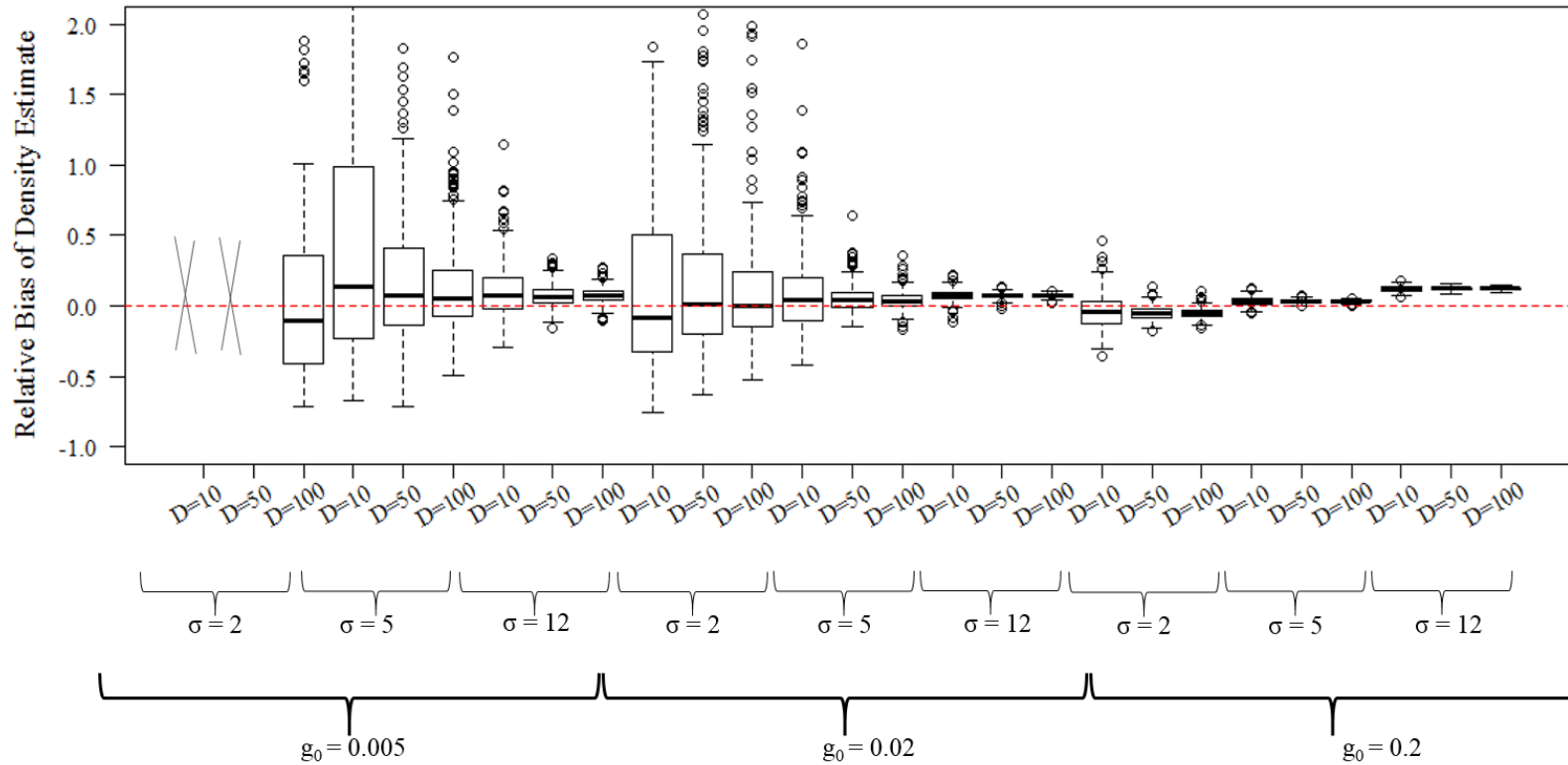


Figure 1.3a. Distribution of relative bias of the density estimate for simulated scenarios of spatial capture-recapture models. Scenarios are grouped by combinations of g_0 , σ , and density and are aggregated across number of sampling occasions. Only scenarios that did not encounter maximization or variance calculation warnings in $> 80\%$ of iterations are represented ($n=71$). Grey “X” symbols are placeholders for the missing groups of scenarios, which were removed from further analysis because $> 20\%$ of iterations failed. The red, dashed, line is RSE = 0.

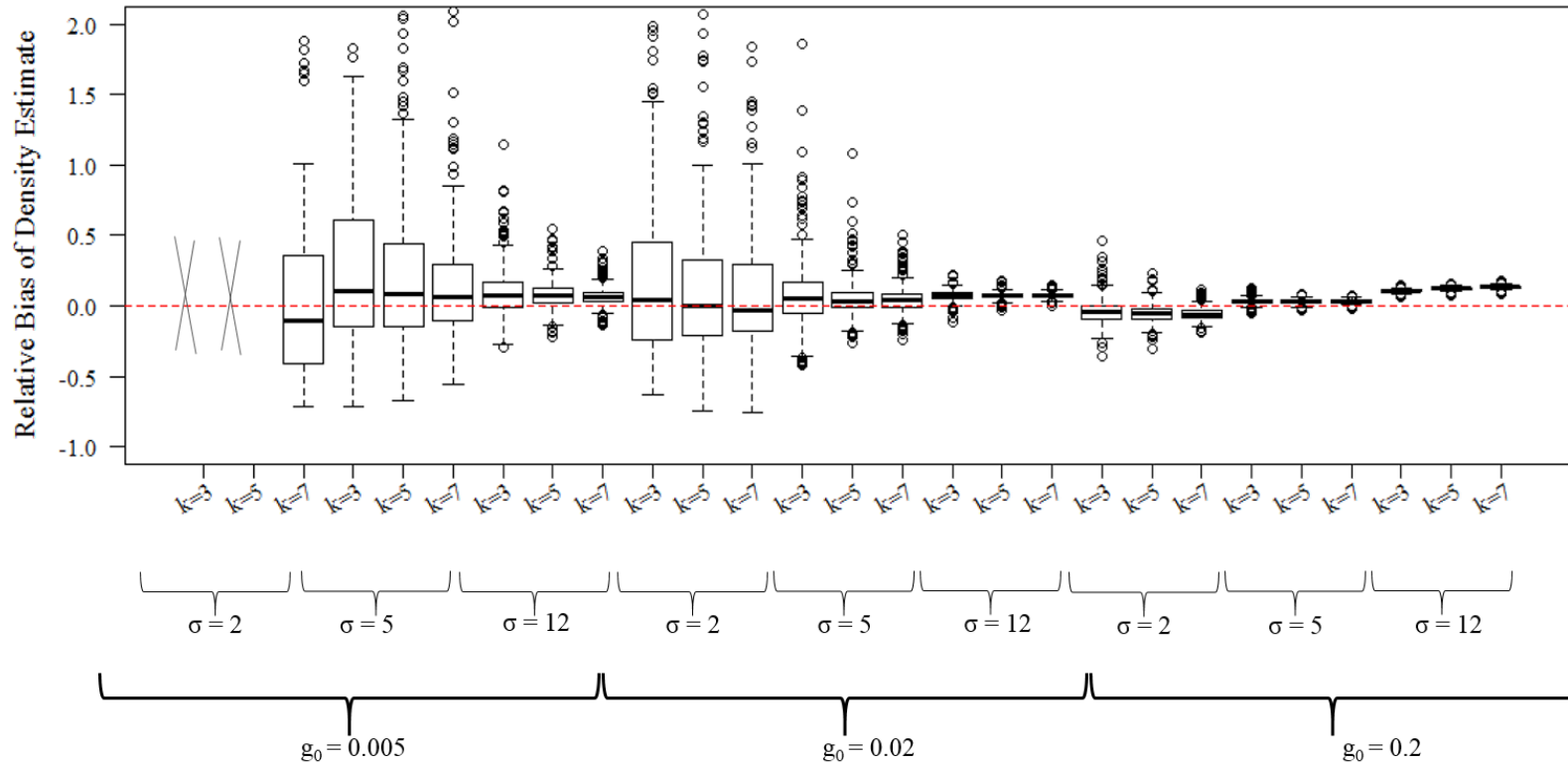


Figure 1.3b. Distribution of relative bias of the density estimate for simulated scenarios of spatial capture-recapture models. Scenarios are grouped by combinations of g_0 , σ , and number of sampling occasions and are aggregated across density values. Only scenarios that did not encounter maximization or variance calculation warnings in $> 80\%$ of iterations are represented ($n=71$). Grey “X” symbols are placeholders for the missing groups of scenarios, which were removed from further analysis because $> 20\%$ of iterations failed. The red, dashed, line is $RSE = 0$.

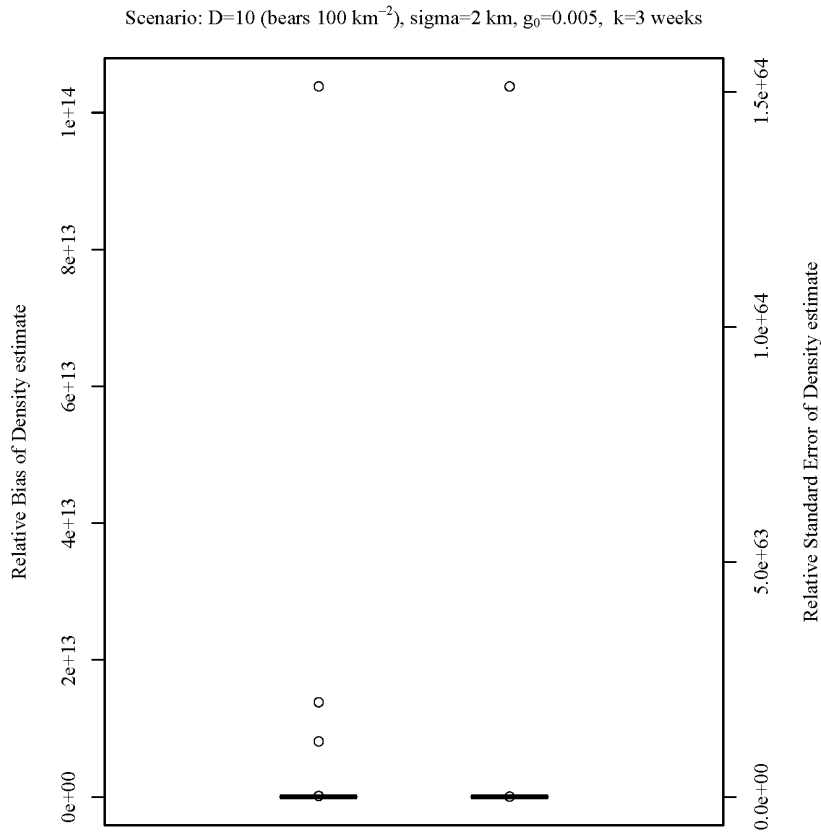


Figure 1.4. Distribution of relative bias (left boxplot) and relative standard error (right boxplot) in the density estimate for a simulated scenario of a spatial capture-recapture model ($D = 10$ bears/ 100 km^2 , $\sigma = 2 \text{ km}$, $g_0 = 0.005$, and sampling occurred over 3 weeks).

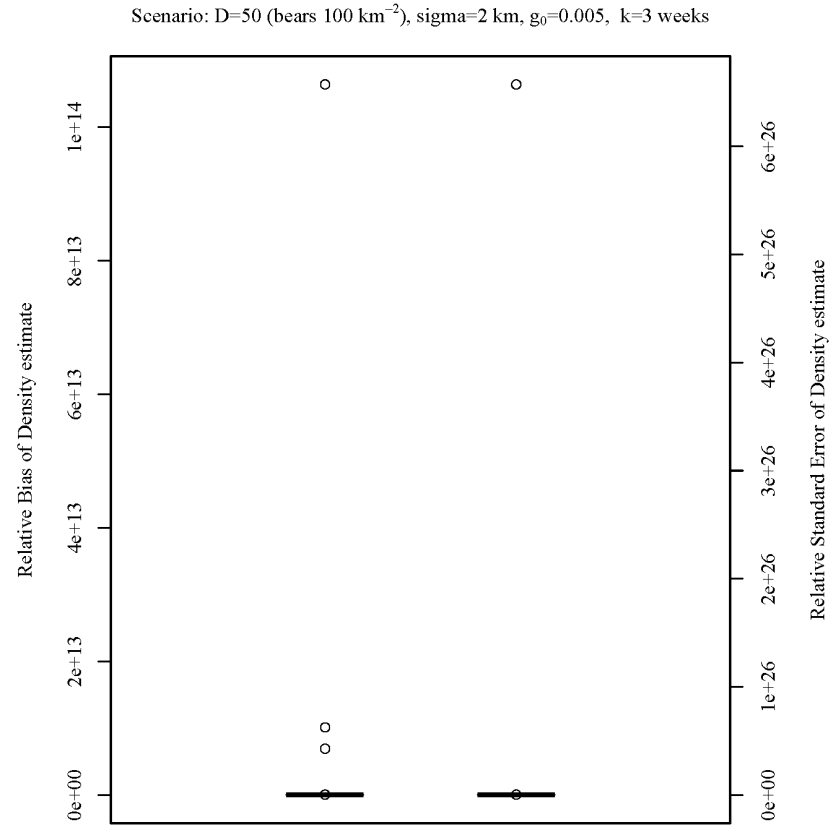


Figure 1.5. Distribution of relative bias (left boxplot) and relative standard error (right boxplot) in the density estimate for a simulated scenario of a spatial capture-recapture model ($D = 50$ bears/ 100 km^2 , $\sigma = 2 \text{ km}$, $g_0 = 0.005$, and sampling occurred over 3 weeks).

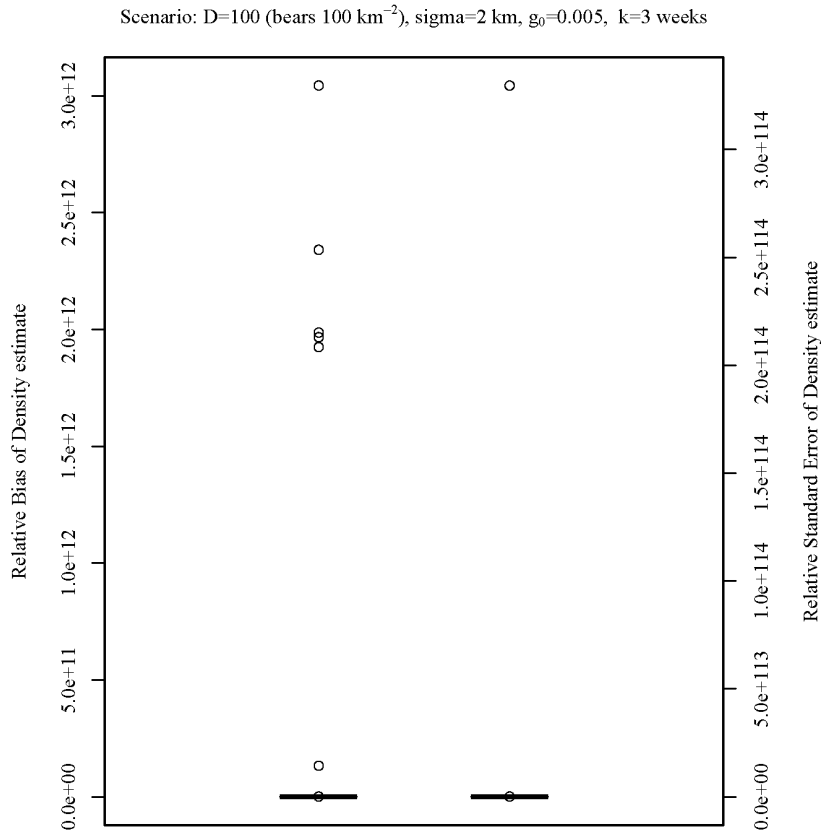


Figure 1.6. Distribution of relative bias (left boxplot) and relative standard error (right boxplot) in the density estimate for a simulated scenario of a spatial capture-recapture model ($D = 100$ bears/ 100 km^2 , $\sigma = 2 \text{ km}$, $g_0 = 0.005$, and sampling occurred over 3 weeks).

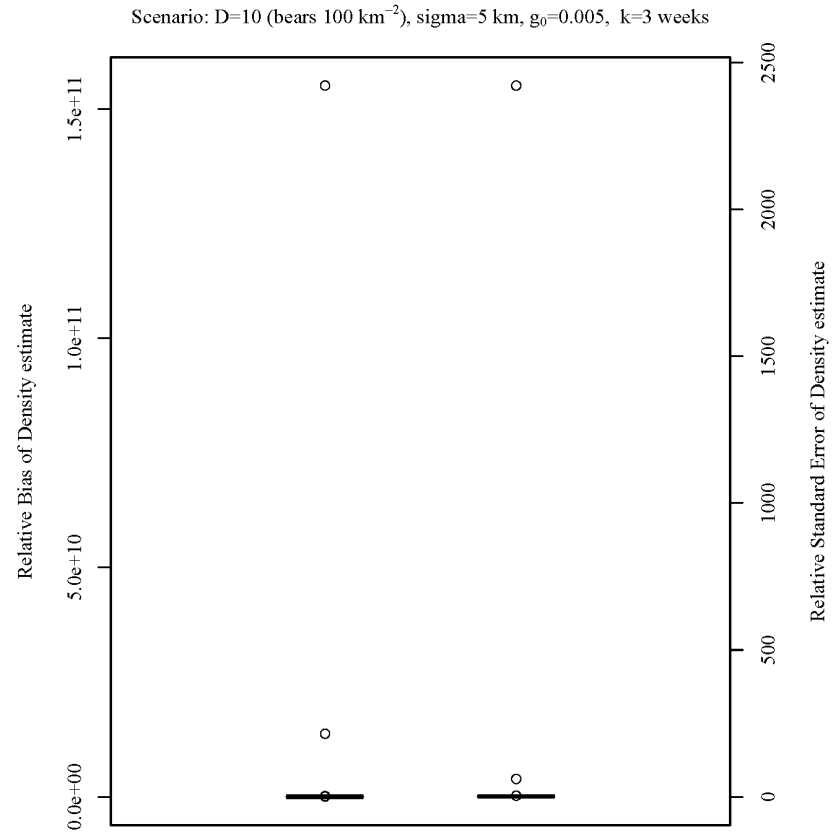


Figure 1.7. Distribution of relative bias (left boxplot) and relative standard error (right boxplot) in the density estimate for a simulated scenario of a spatial capture-recapture model ($D = 10$ bears/ 100 km^2 , $\sigma = 5 \text{ km}$, $g_0 = 0.005$, and sampling occurred over 3 weeks).

Scenario: $D=50$ (bears 100 km^{-2}), $\sigma=5 \text{ km}$, $g_0=0.005$, $k=3$ weeks

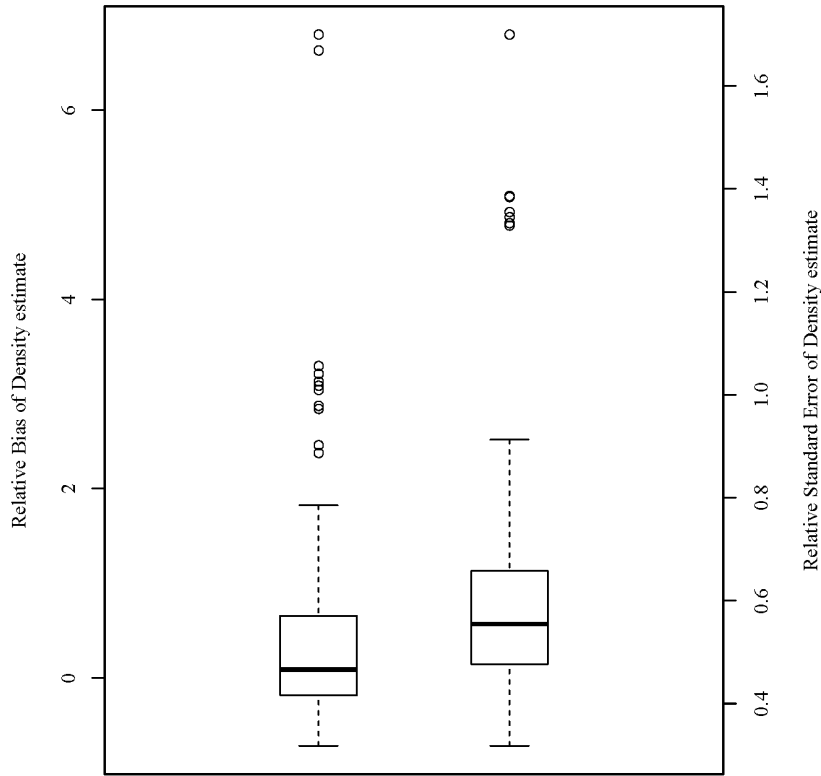


Figure 1.8. Distribution of relative bias (left boxplot) and relative standard error (right boxplot) in the density estimate for a simulated scenario of a spatial capture-recapture model ($D = 50$ bears/ 100 km^2 , $\sigma = 5 \text{ km}$, $g_0 = 0.005$, and sampling occurred over 3 weeks).

Scenario: $D=100$ (bears 100 km^{-2}), $\sigma=5 \text{ km}$, $g_0=0.005$, $k=3$ weeks

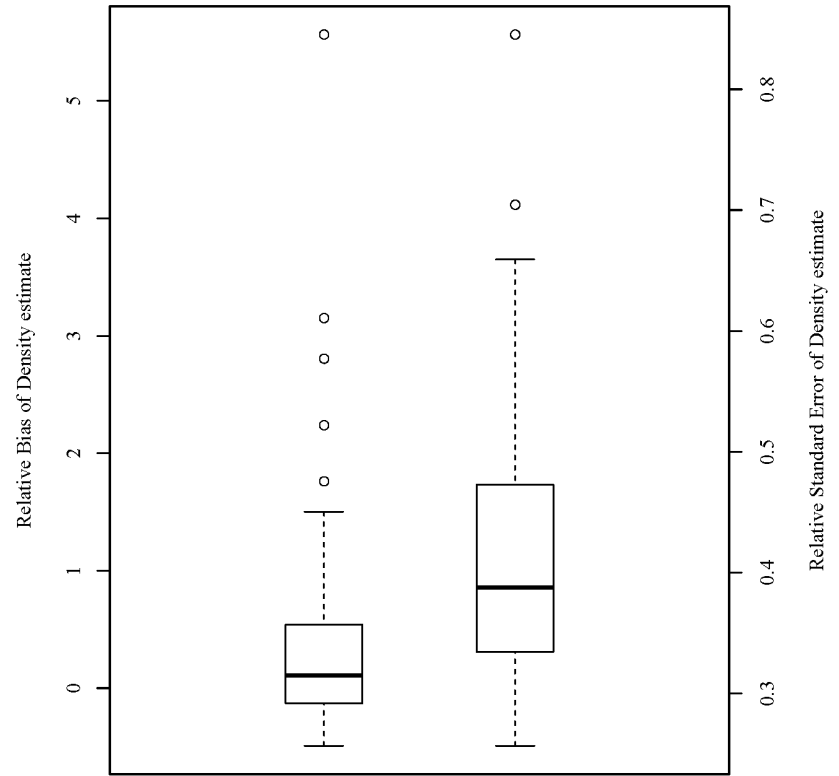


Figure 1.9. Distribution of relative bias (left boxplot) and relative standard error (right boxplot) in the density estimate for a simulated scenario of a spatial capture-recapture model ($D = 100$ bears/ 100 km^2 , $\sigma = 5 \text{ km}$, $g_0 = 0.005$, and sampling occurred over 3 weeks).

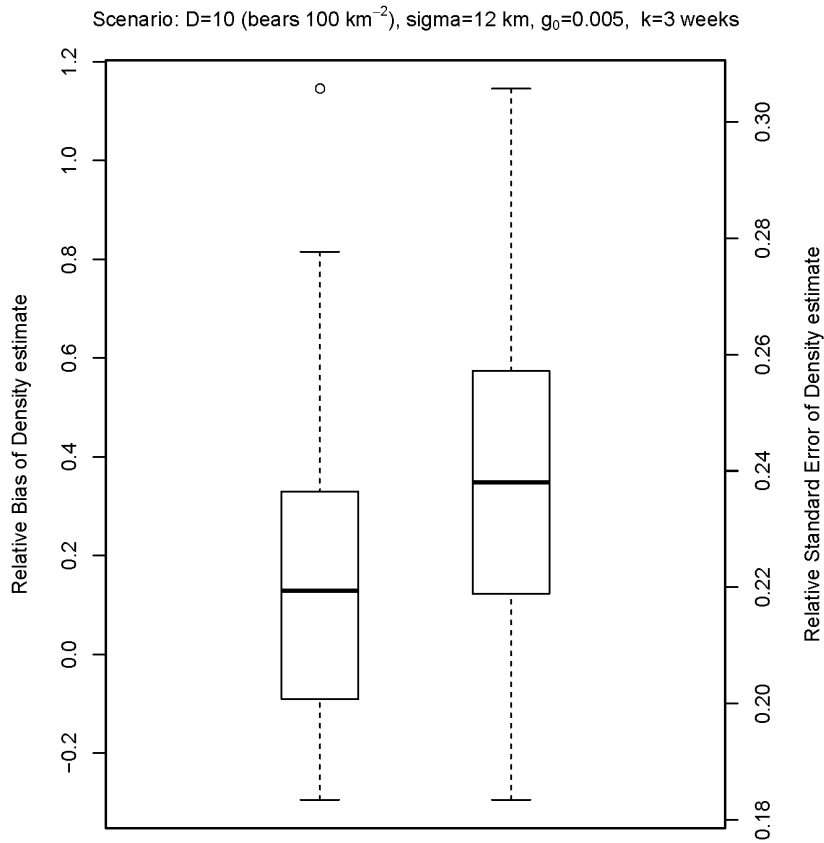


Figure 1.10. Distribution of relative bias (left boxplot) and relative standard error (right boxplot) in the density estimate for a simulated scenario of a spatial capture-recapture model ($D = 10$ bears/ 100 km^2 , $\sigma = 12 \text{ km}$, $g_0 = 0.005$, and sampling occurred over 3 weeks).

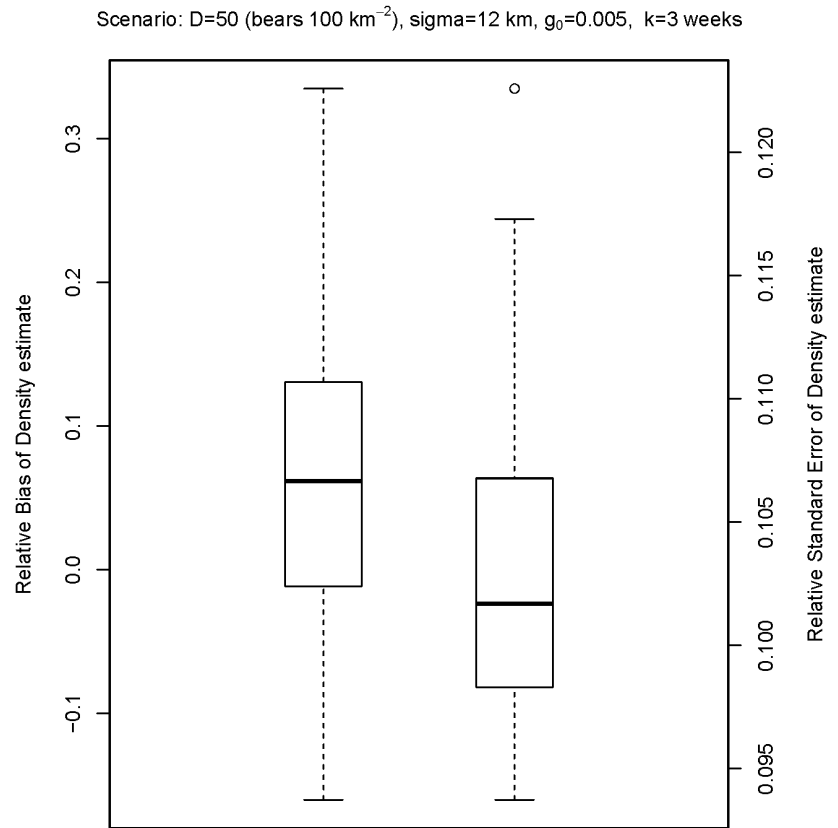


Figure 1.11. Distribution of relative bias (left boxplot) and relative standard error (right boxplot) in the density estimate for a simulated scenario of a spatial capture-recapture model ($D = 50$ bears/ 100 km^2 , $\sigma = 12 \text{ km}$, $g_0 = 0.005$, and sampling occurred over 3 weeks).

Scenario: $D=100$ (bears 100 km^{-2}), $\sigma=12 \text{ km}$, $g_0=0.005$, $k=3$ weeks

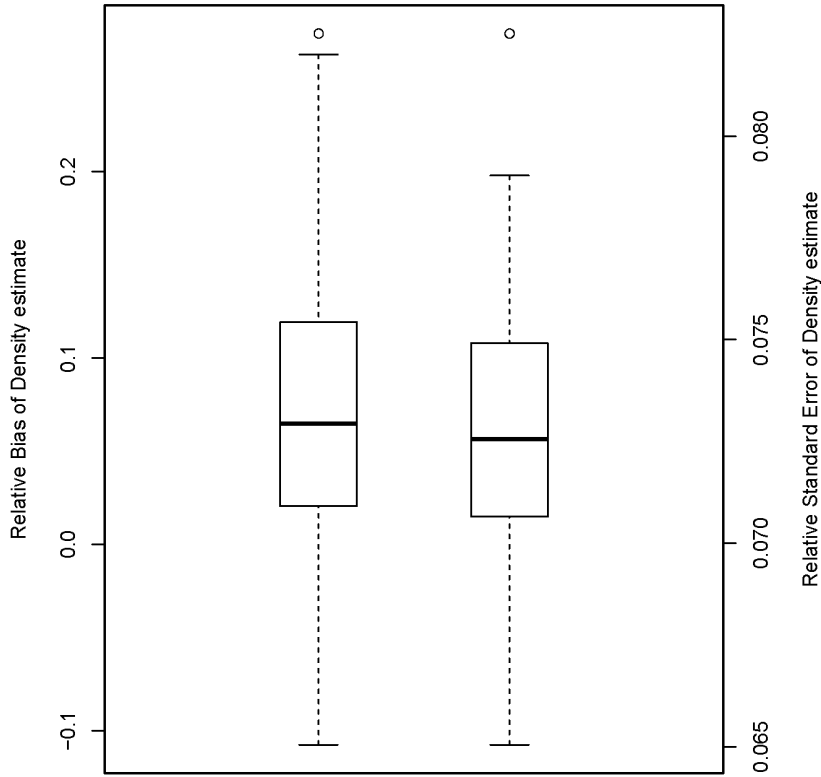


Figure 1.12. Distribution of relative bias (left boxplot) and relative standard error (right boxplot) in the density estimate for a simulated scenario of a spatial capture-recapture model ($D = 100$ bears/ 100 km^2 , $\sigma = 12 \text{ km}$, $g_0 = 0.005$, and sampling occurred over 3 weeks).

Scenario: $D=10$ (bears 100 km^{-2}), $\sigma=2 \text{ km}$, $g_0=0.02$, $k=3$ weeks

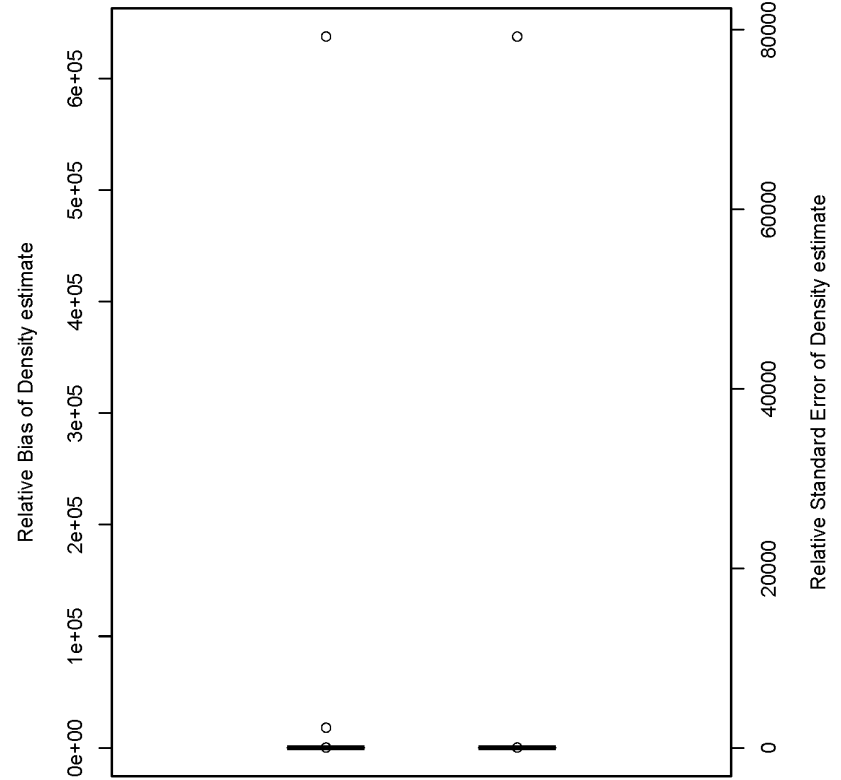


Figure 1.13. Distribution of relative bias (left boxplot) and relative standard error (right boxplot) in the density estimate for a simulated scenario of a spatial capture-recapture model ($D = 10$ bears/ 100 km^2 , $\sigma = 2 \text{ km}$, $g_0 = 0.02$, and sampling occurred over 3 weeks).

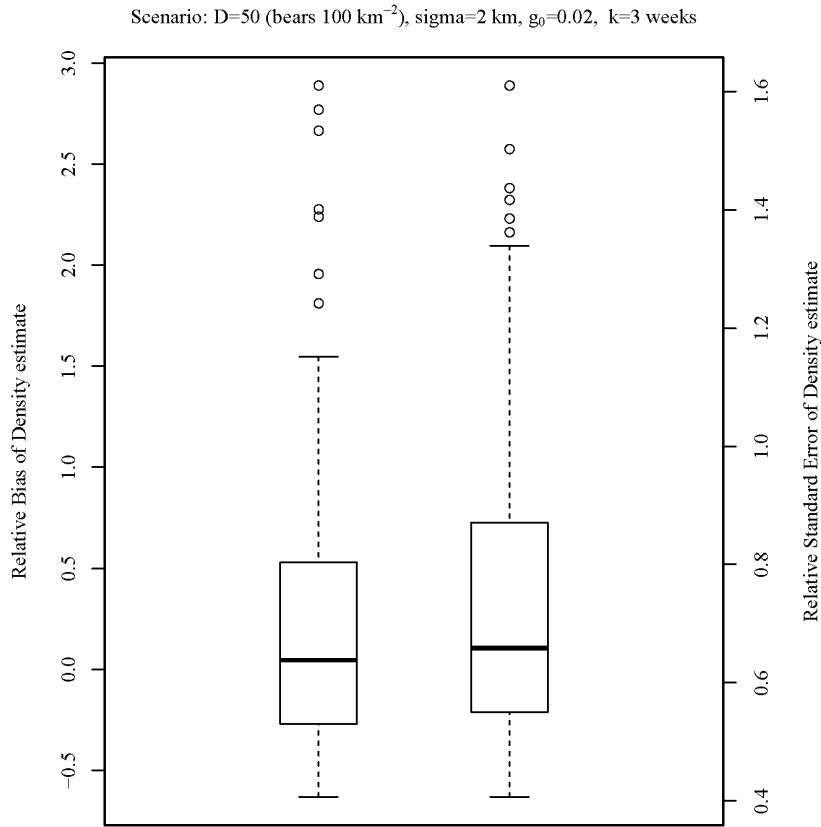


Figure 1.14. Distribution of relative bias (left boxplot) and relative standard error (right boxplot) in the density estimate for a simulated scenario of a spatial capture-recapture model ($D = 50$ bears/ 100 km^2 , $\sigma = 2 \text{ km}$, $g_0 = 0.02$, and sampling occurred over 3 weeks).

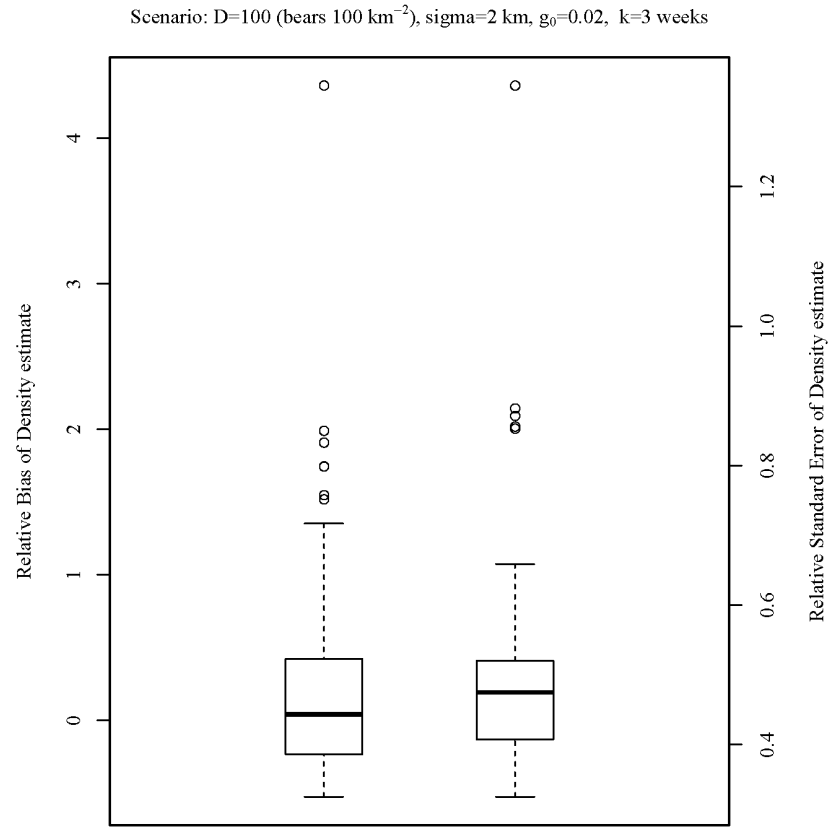


Figure 1.15. Distribution of relative bias (left boxplot) and relative standard error (right boxplot) in the density estimate for a simulated scenario of a spatial capture-recapture model ($D = 100$ bears/ 100 km^2 , $\sigma = 2 \text{ km}$, $g_0 = 0.02$, and sampling occurred over 3 weeks).

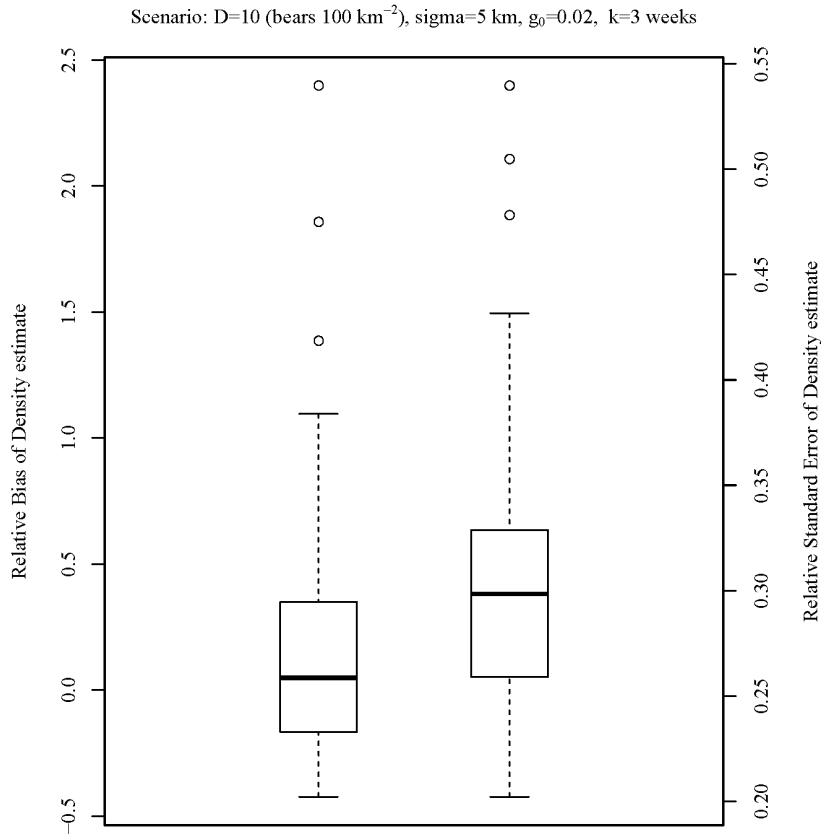


Figure 1.16. Distribution of relative bias (left boxplot) and relative standard error (right boxplot) in the density estimate for a simulated scenario of a spatial capture-recapture model ($D = 10$ bears/ 100 km^2 , $\sigma = 5 \text{ km}$, $g_0 = 0.02$, and sampling occurred over 3 weeks).

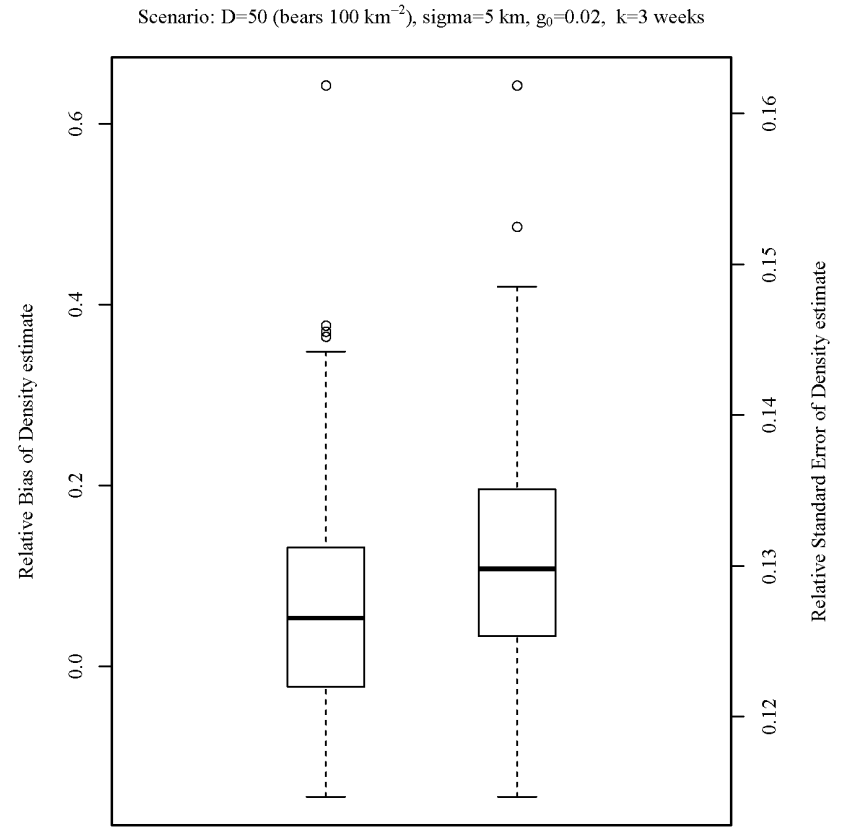


Figure 1.17. Distribution of relative bias (left boxplot) and relative standard error (right boxplot) in the density estimate for a simulated scenario of a spatial capture-recapture model ($D = 50$ bears/ 100 km^2 , $\sigma = 5 \text{ km}$, $g_0 = 0.02$, and sampling occurred over 3 weeks).

Scenario: $D=100$ (bears 100 km^{-2}), $\sigma=5 \text{ km}$, $g_0=0.02$, $k=3$ weeks

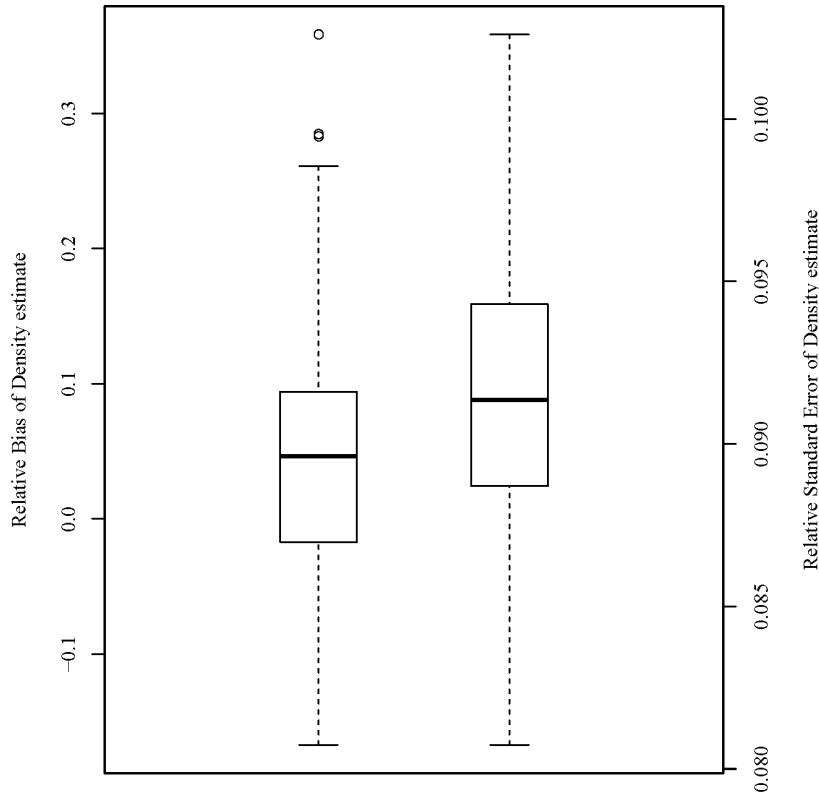


Figure 1.18. Distribution of relative bias (left boxplot) and relative standard error (right boxplot) in the density estimate for a simulated scenario of a spatial capture-recapture model ($D = 100$ bears/ 100 km^2 , $\sigma = 5 \text{ km}$, $g_0 = 0.02$, and sampling occurred over 3 weeks).

Scenario: $D=10$ (bears 100 km^{-2}), $\sigma=12 \text{ km}$, $g_0=0.02$, $k=3$ weeks

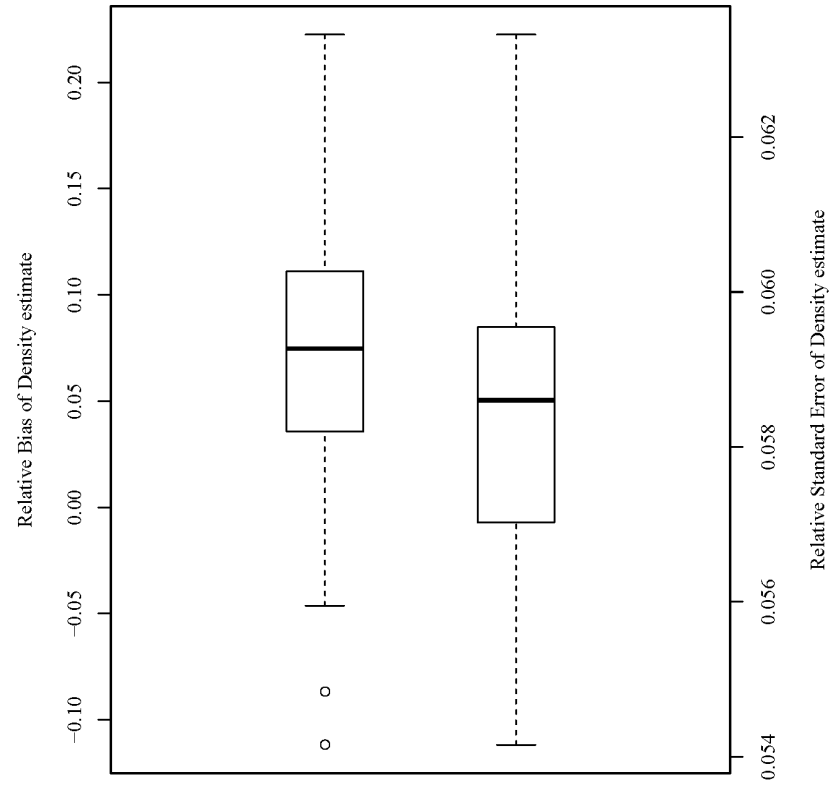


Figure 1.19. Distribution of relative bias (left boxplot) and relative standard error (right boxplot) in the density estimate for a simulated scenario of a spatial capture-recapture model ($D = 10$ bears/ 100 km^2 , $\sigma = 12 \text{ km}$, $g_0 = 0.02$, and sampling occurred over 3 weeks).

Scenario: $D=50$ (bears 100 km^{-2}), $\sigma=12 \text{ km}$, $g_0=0.02$, $k=3$ weeks

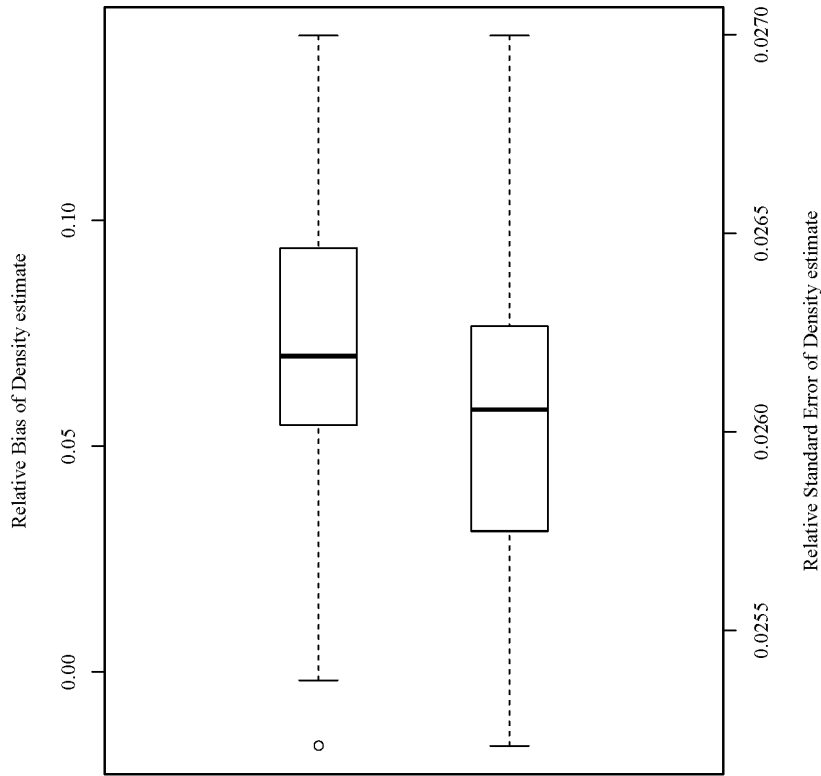


Figure 1.20. Distribution of relative bias (left boxplot) and relative standard error (right boxplot) in the density estimate for a simulated scenario of a spatial capture-recapture model ($D = 50$ bears/ 100 km^2 , $\sigma = 12 \text{ km}$, $g_0 = 0.02$, and sampling occurred over 3 weeks).

Scenario: $D=100$ (bears 100 km^{-2}), $\sigma=12 \text{ km}$, $g_0=0.02$, $k=3$ weeks

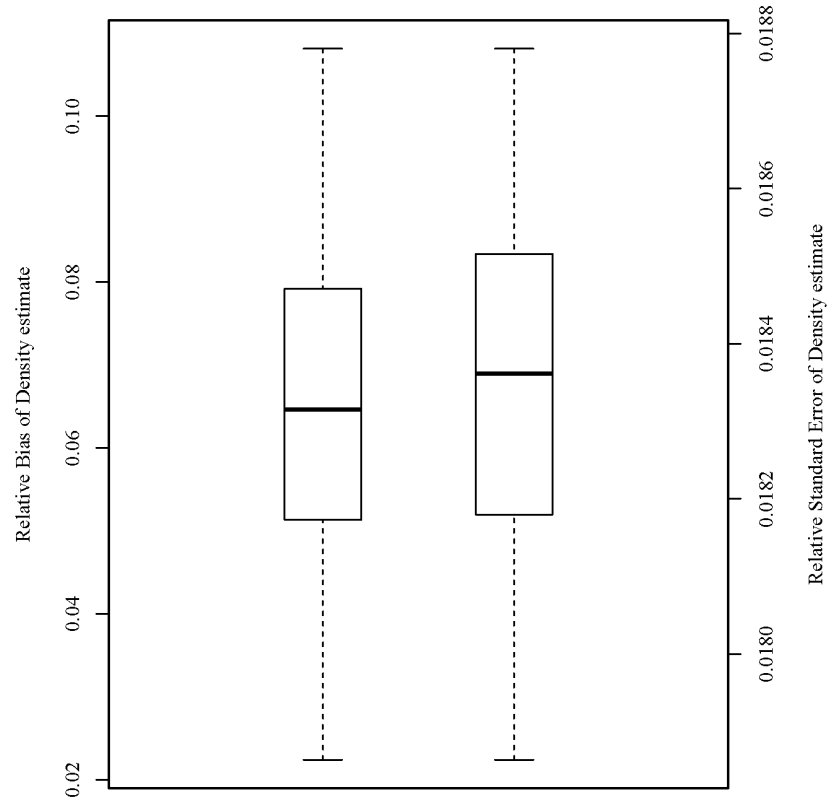


Figure 1.21. Distribution of relative bias (left boxplot) and relative standard error (right boxplot) in the density estimate for a simulated scenario of a spatial capture-recapture model ($D = 100$ bears/ 100 km^2 , $\sigma = 12 \text{ km}$, $g_0 = 0.02$, and sampling occurred over 3 weeks).

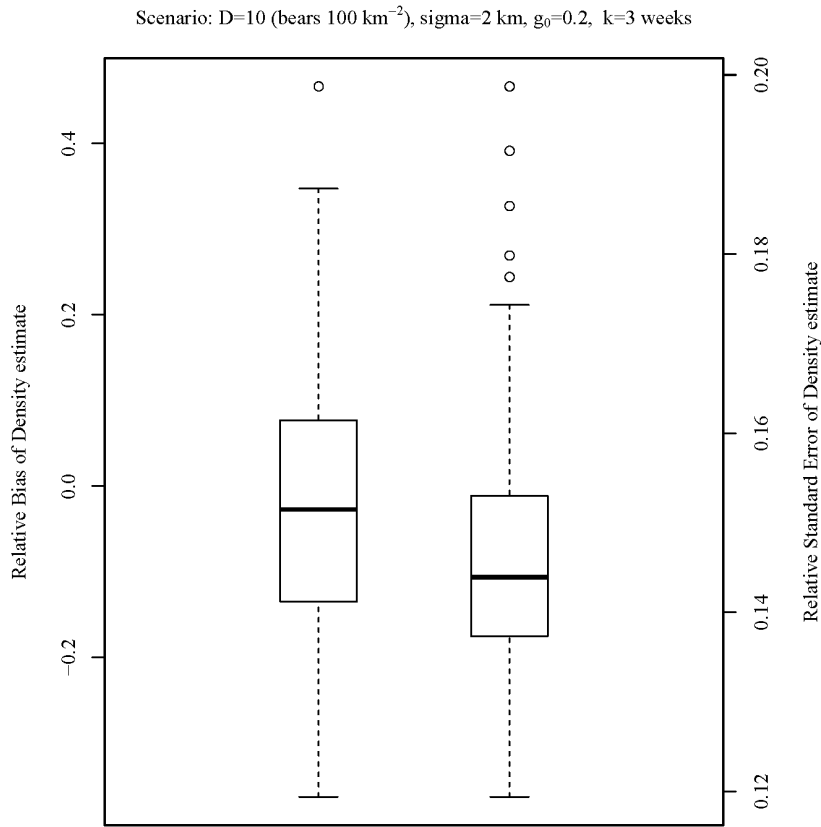


Figure 1.22. Distribution of relative bias (left boxplot) and relative standard error (right boxplot) in the density estimate for a simulated scenario of a spatial capture-recapture model ($D = 10$ bears/ 100 km^2 , $\sigma = 2 \text{ km}$, $g_0 = 0.2$, and sampling occurred over 3 weeks).

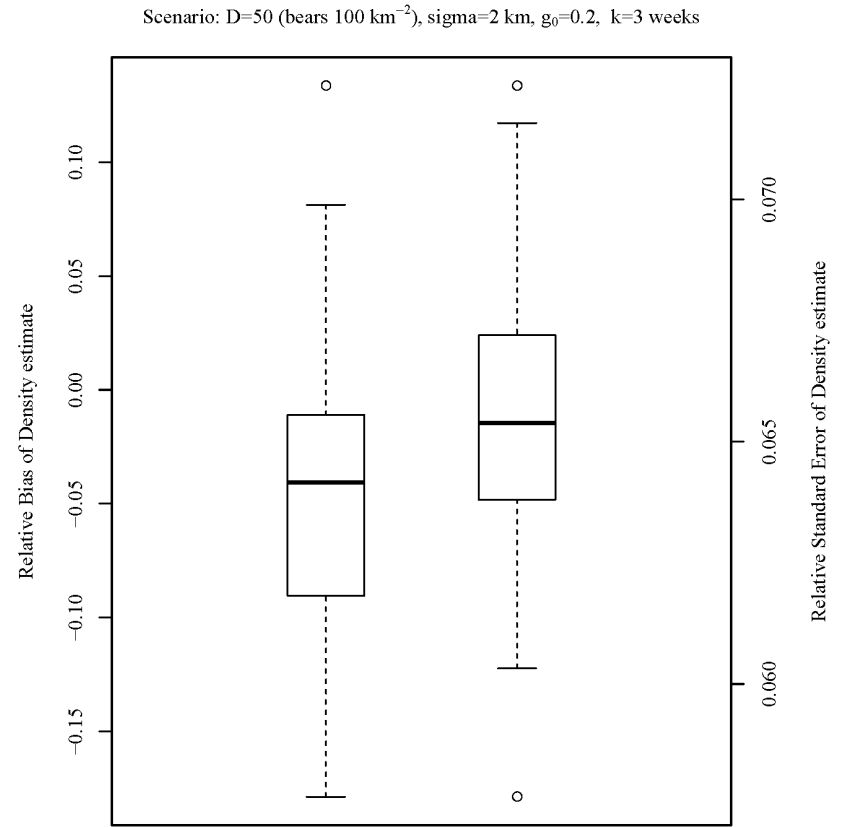


Figure 1.23. Distribution of relative bias (left boxplot) and relative standard error (right boxplot) in the density estimate for a simulated scenario of a spatial capture-recapture model ($D = 50$ bears/ 100 km^2 , $\sigma = 2 \text{ km}$, $g_0 = 0.2$, and sampling occurred over 3 weeks).

Scenario: $D=100$ (bears 100 km^{-2}), $\sigma=2 \text{ km}$, $g_0=0.2$, $k=3$ weeks

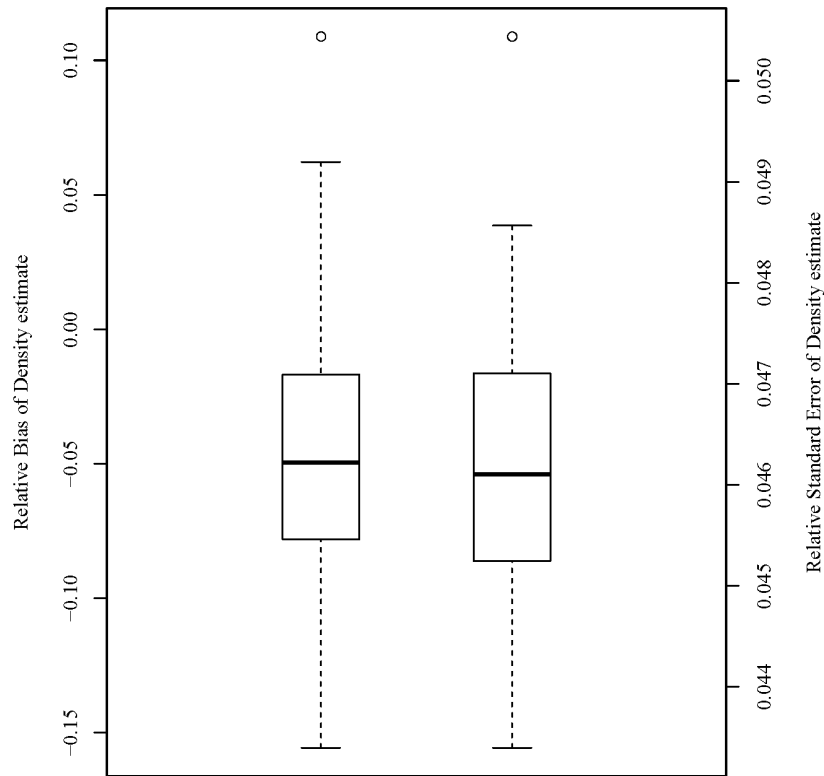


Figure 1.24. Distribution of relative bias (left boxplot) and relative standard error (right boxplot) in the density estimate for a simulated scenario of a spatial capture-recapture model ($D = 100$ bears/ 100 km^2 , $\sigma = 2 \text{ km}$, $g_0 = 0.2$, and sampling occurred over 3 weeks).

Scenario: $D=10$ (bears 100 km^{-2}), $\sigma=5 \text{ km}$, $g_0=0.2$, $k=3$ weeks

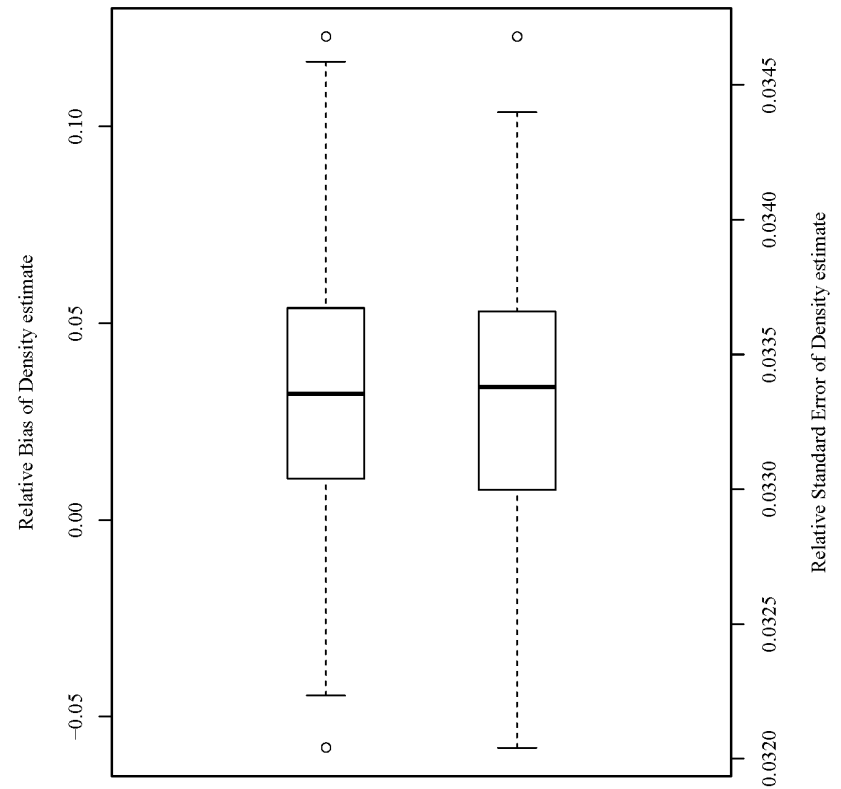


Figure 1.25. Distribution of relative bias (left boxplot) and relative standard error (right boxplot) in the density estimate for a simulated scenario of a spatial capture-recapture model ($D = 10$ bears/ 100 km^2 , $\sigma = 5 \text{ km}$, $g_0 = 0.2$, and sampling occurred over 3 weeks).

Scenario: $D=50$ (bears 100 km^{-2}), $\sigma=5 \text{ km}$, $g_0=0.2$, $k=3$ weeks

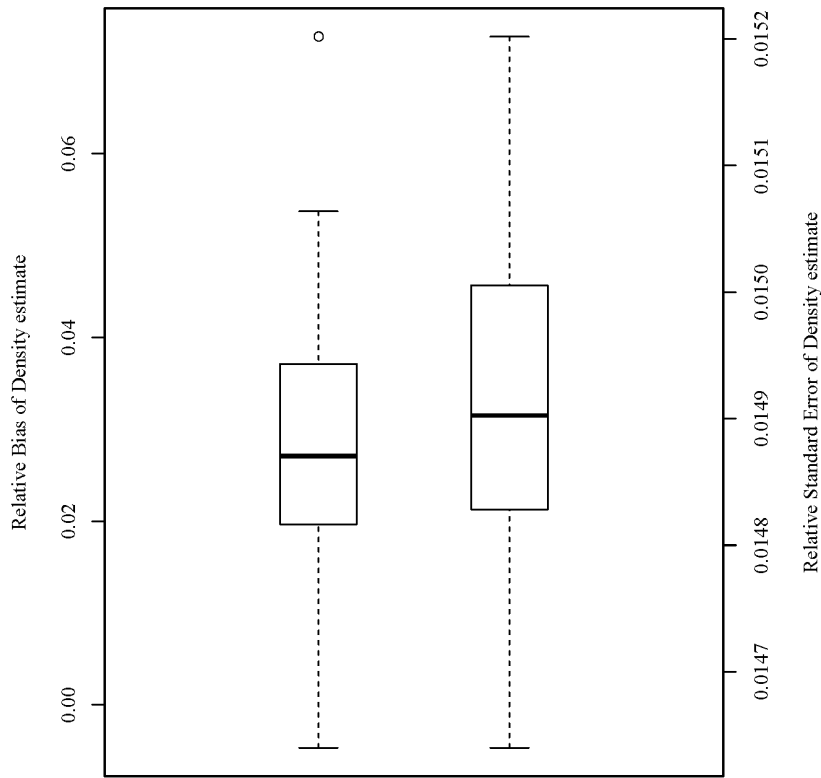


Figure 1.26. Distribution of relative bias (left boxplot) and relative standard error (right boxplot) in the density estimate for a simulated scenario of a spatial capture-recapture model ($D = 50$ bears/ 100 km^2 , $\sigma = 5 \text{ km}$, $g_0 = 0.2$, and sampling occurred over 3 weeks).

Scenario: $D=100$ (bears 100 km^{-2}), $\sigma=5 \text{ km}$, $g_0=0.2$, $k=3$ weeks

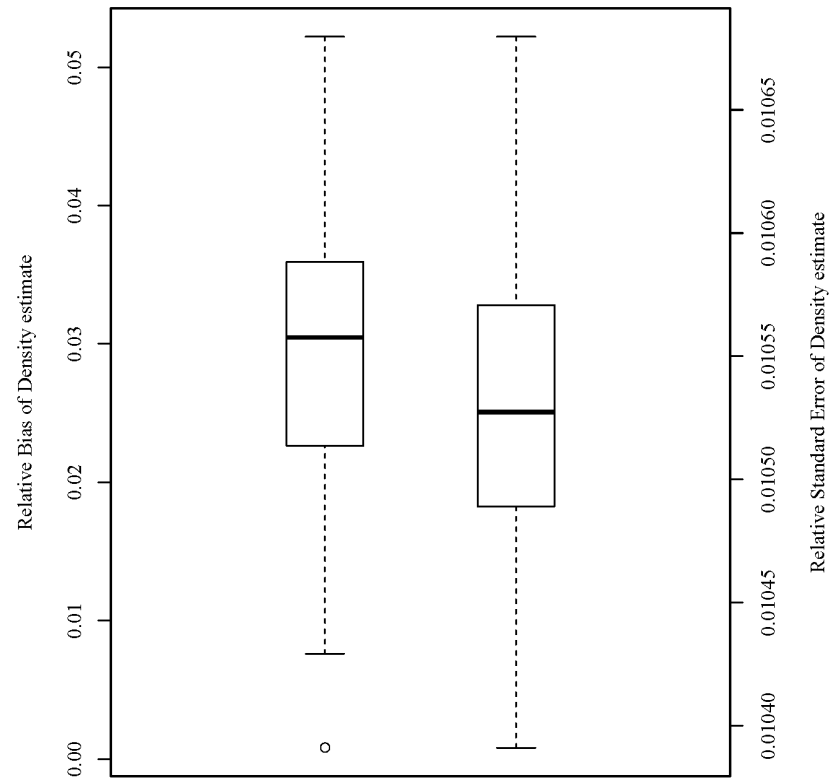


Figure 1.27. Distribution of relative bias (left boxplot) and relative standard error (right boxplot) in the density estimate for a simulated scenario of a spatial capture-recapture model ($D = 100$ bears/ 100 km^2 , $\sigma = 5 \text{ km}$, $g_0 = 0.2$, and sampling occurred over 3 weeks).

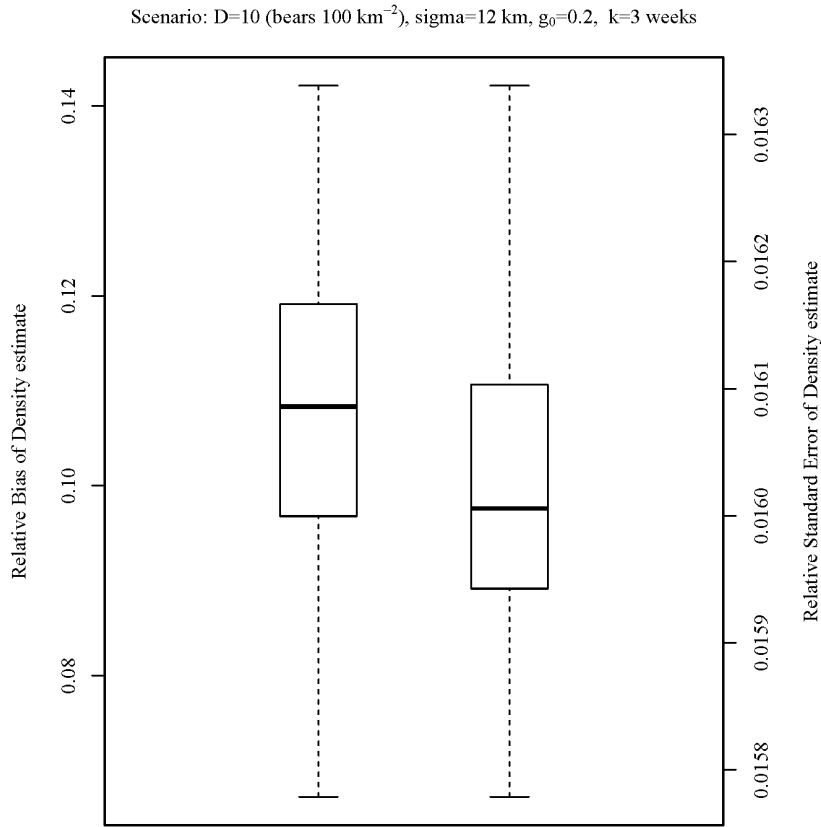


Figure 1.28. Distribution of relative bias (left boxplot) and relative standard error (right boxplot) in the density estimate for a simulated scenario of a spatial capture-recapture model ($D = 10$ bears/ 100 km^2 , $\sigma = 12 \text{ km}$, $g_0 = 0.2$, and sampling occurred over 3 weeks).

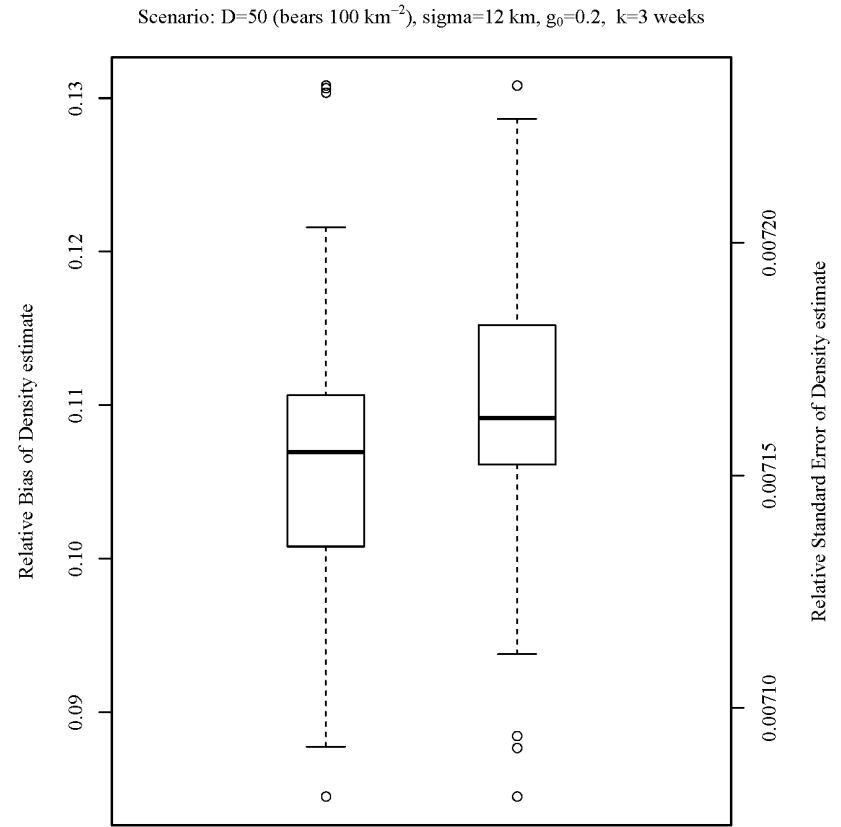


Figure 1.29. Distribution of relative bias (left boxplot) and relative standard error (right boxplot) in the density estimate for a simulated scenario of a spatial capture-recapture model ($D = 50$ bears/ 100 km^2 , $\sigma = 12 \text{ km}$, $g_0 = 0.2$, and sampling occurred over 3 weeks).

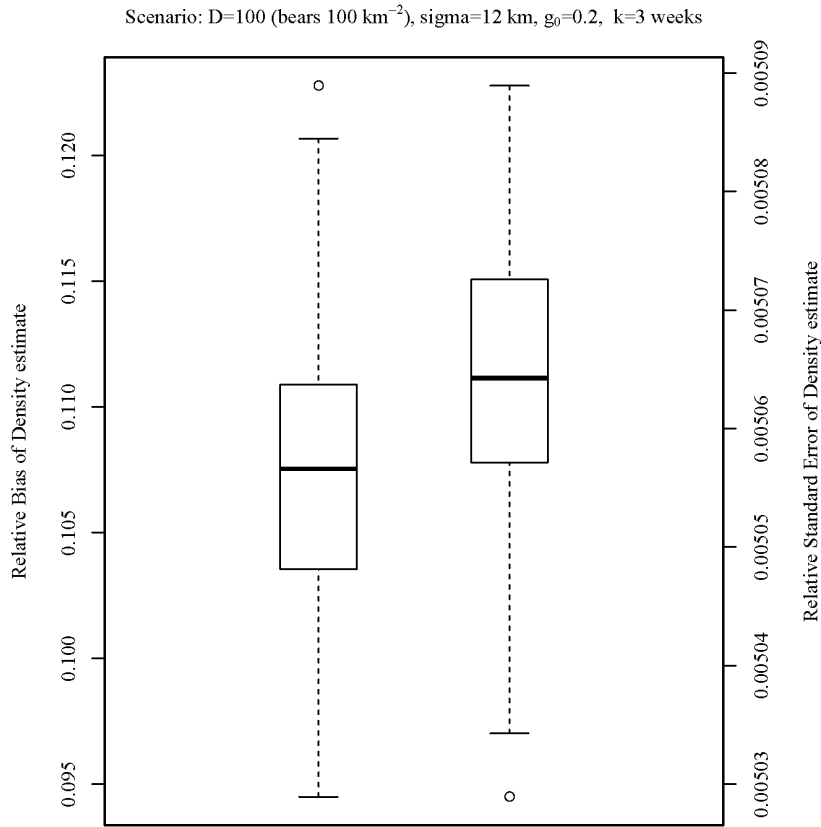


Figure 1.30. Distribution of relative bias (left boxplot) and relative standard error (right boxplot) in the density estimate for a simulated scenario of a spatial capture-recapture model ($D = 100$ bears/ 100 km^2 , $\sigma = 12 \text{ km}$, $g_0 = 0.2$, and sampling occurred over 3 weeks).

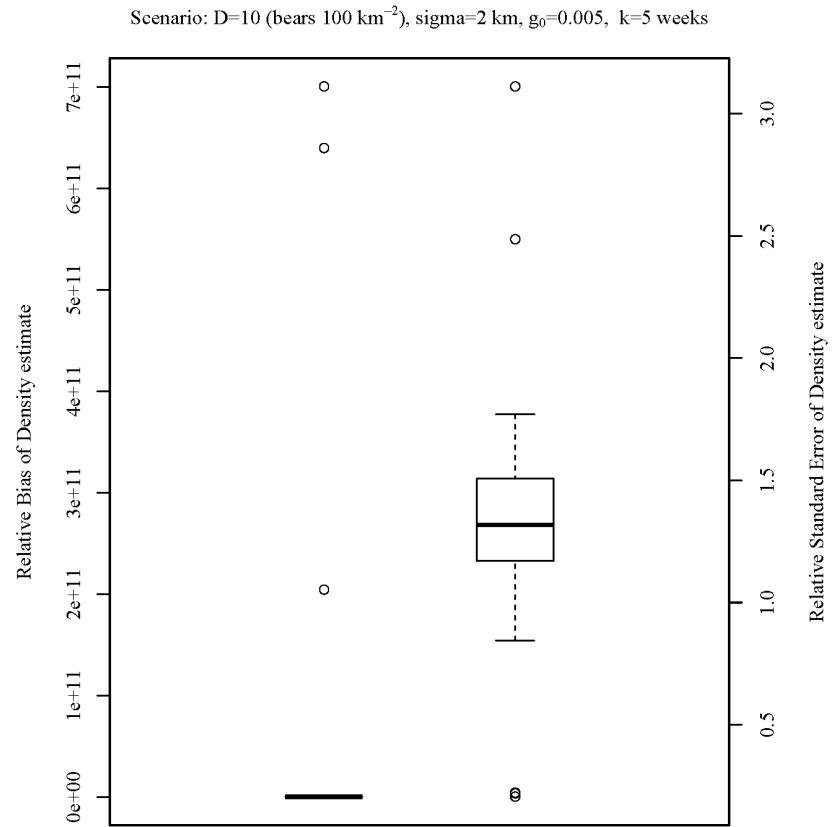


Figure 1.31. Distribution of relative bias (left boxplot) and relative standard error (right boxplot) in the density estimate for a simulated scenario of a spatial capture-recapture model ($D = 10$ bears/ 100 km^2 , $\sigma = 2 \text{ km}$, $g_0 = 0.005$, and sampling occurred over 5 weeks).

Scenario: $D=50$ (bears 100 km^{-2}), $\sigma=2 \text{ km}$, $g_0=0.005$, $k=5$ weeks

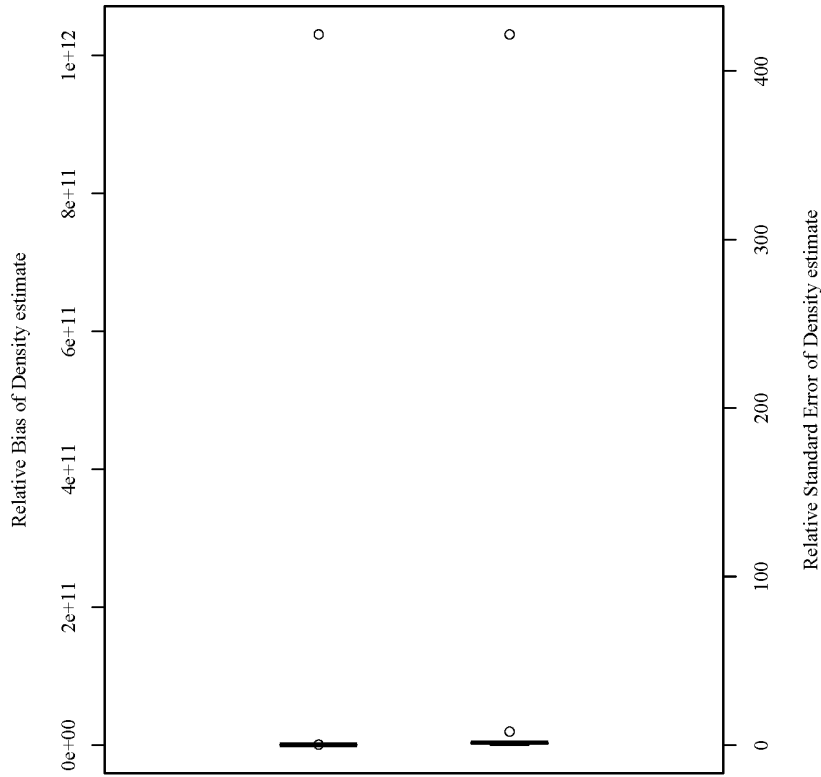


Figure 1.32. Distribution of relative bias (left boxplot) and relative standard error (right boxplot) in the density estimate for a simulated scenario of a spatial capture-recapture model ($D = 50$ bears/ 100 km^2 , $\sigma = 2 \text{ km}$, $g_0 = 0.005$, and sampling occurred over 5 weeks).

Scenario: $D=100$ (bears 100 km^{-2}), $\sigma=2 \text{ km}$, $g_0=0.005$, $k=5$ weeks

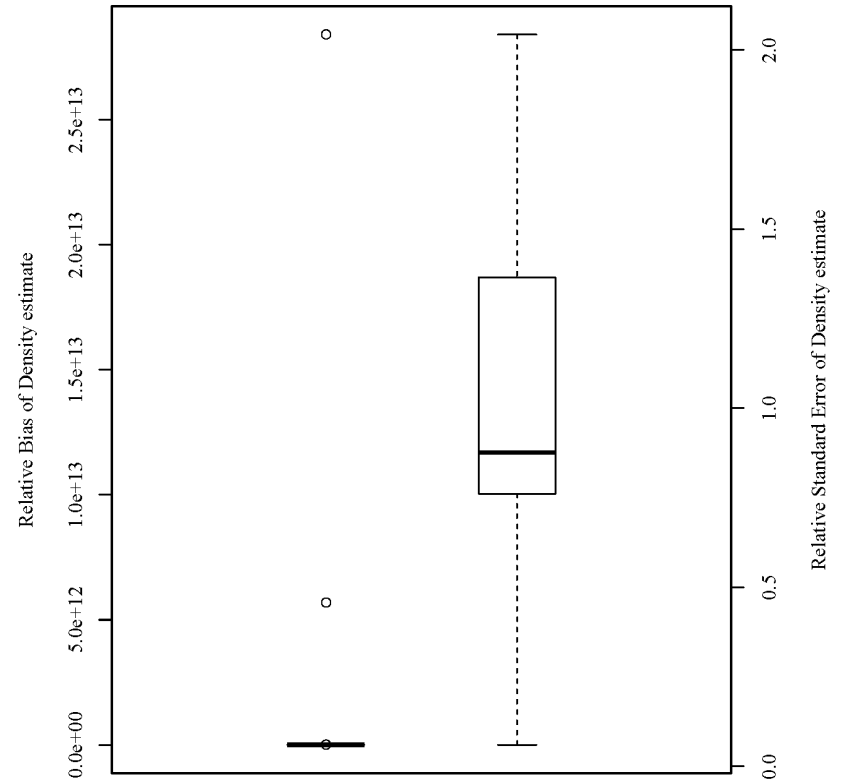


Figure 1.33. Distribution of relative bias (left boxplot) and relative standard error (right boxplot) in the density estimate for a simulated scenario of a spatial capture-recapture model ($D = 100$ bears/ 100 km^2 , $\sigma = 2 \text{ km}$, $g_0 = 0.005$, and sampling occurred over 5 weeks).

Scenario: $D=10$ (bears 100 km^{-2}), $\sigma=5 \text{ km}$, $g_0=0.005$, $k=5$ weeks

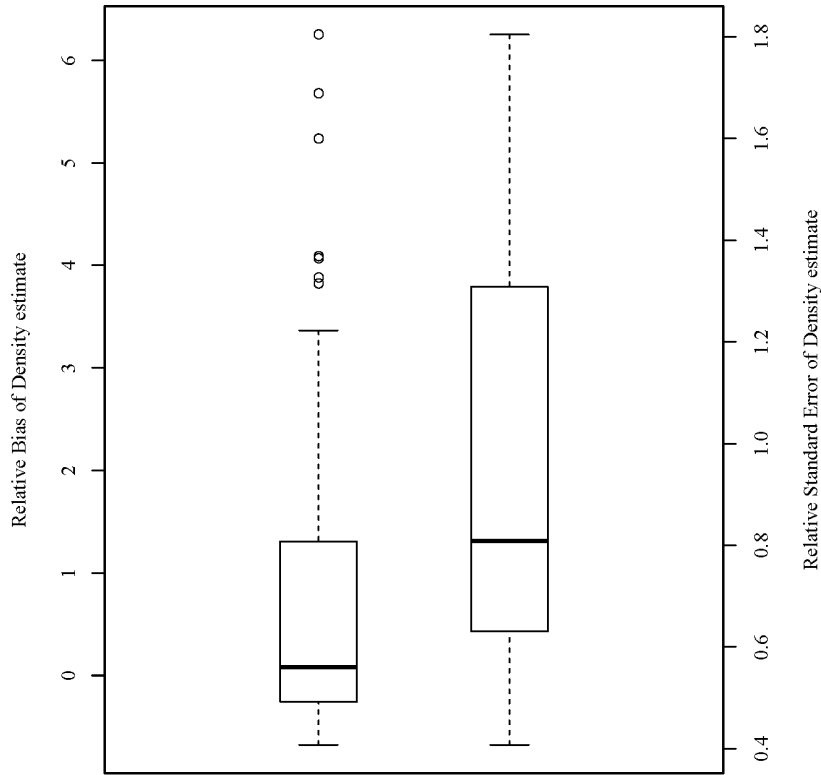


Figure 1.34. Distribution of relative bias (left boxplot) and relative standard error (right boxplot) in the density estimate for a simulated scenario of a spatial capture-recapture model ($D = 10$ bears/ 100 km^2 , $\sigma = 5 \text{ km}$, $g_0 = 0.005$, and sampling occurred over 5 weeks).

Scenario: $D=50$ (bears 100 km^{-2}), $\sigma=5 \text{ km}$, $g_0=0.005$, $k=5$ weeks

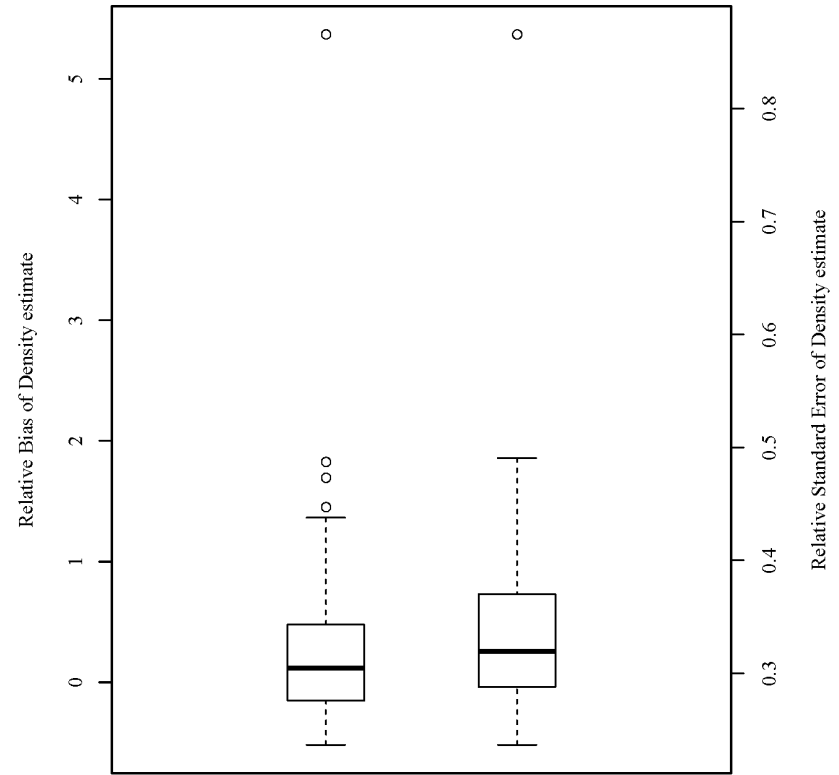


Figure 1.35. Distribution of relative bias (left boxplot) and relative standard error (right boxplot) in the density estimate for a simulated scenario of a spatial capture-recapture model ($D = 50$ bears/ 100 km^2 , $\sigma = 5 \text{ km}$, $g_0 = 0.005$, and sampling occurred over 5 weeks).

Scenario: $D=100$ (bears 100 km^{-2}), $\sigma=5 \text{ km}$, $g_0=0.005$, $k=5$ weeks

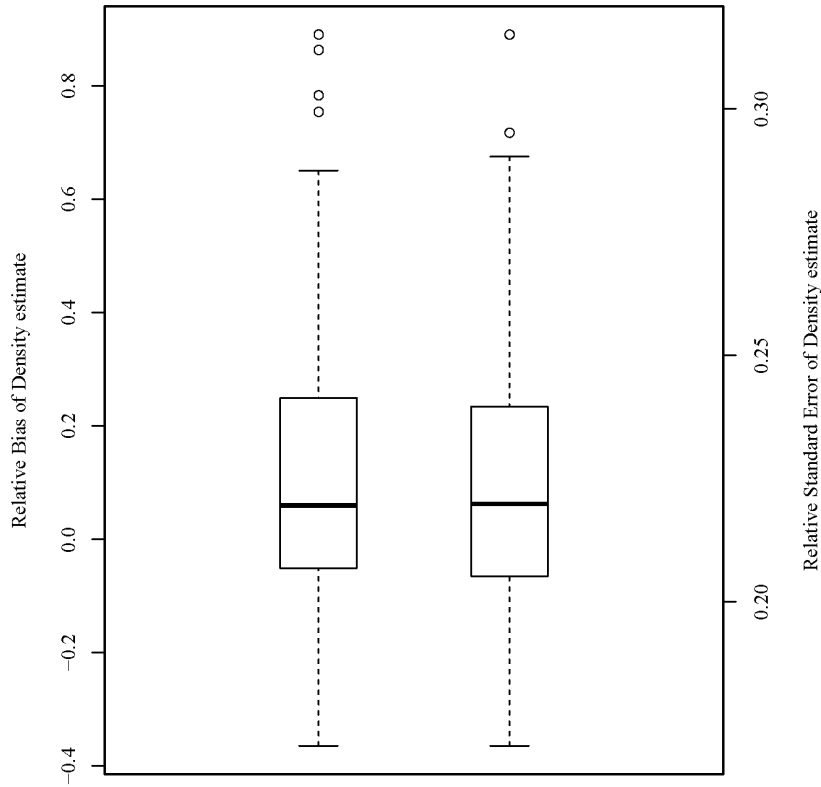


Figure 1.36. Distribution of relative bias (left boxplot) and relative standard error (right boxplot) in the density estimate for a simulated scenario of a spatial capture-recapture model ($D = 100$ bears/ 100 km^2 , $\sigma = 5 \text{ km}$, $g_0 = 0.005$, and sampling occurred over 5 weeks).

Scenario: $D=10$ (bears 100 km^{-2}), $\sigma=12 \text{ km}$, $g_0=0.005$, $k=5$ weeks

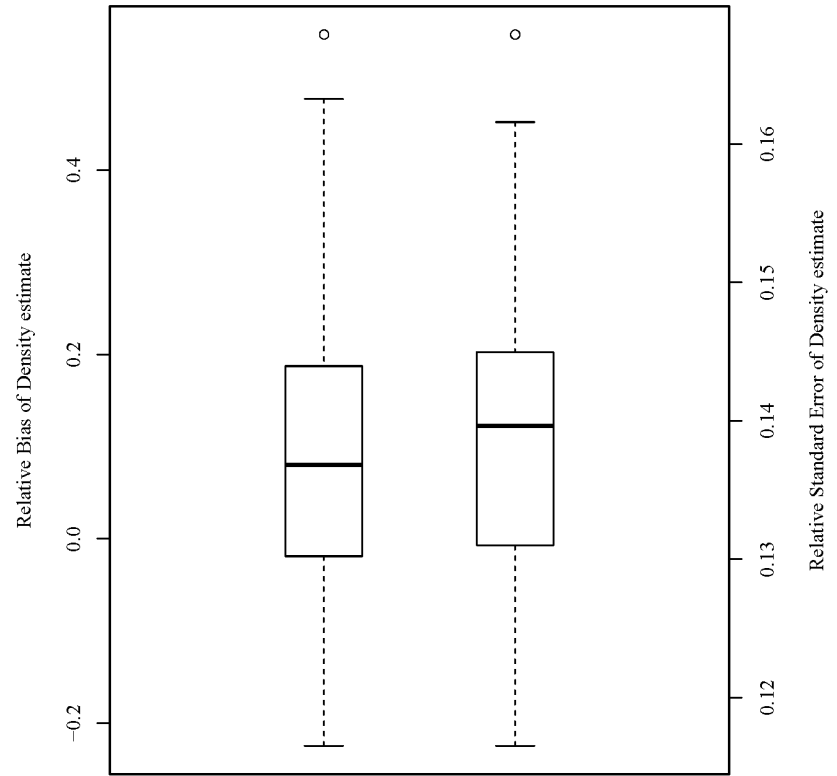


Figure 1.37. Distribution of relative bias (left boxplot) and relative standard error (right boxplot) in the density estimate for a simulated scenario of a spatial capture-recapture model ($D = 10$ bears/ 100 km^2 , $\sigma = 12 \text{ km}$, $g_0 = 0.005$, and sampling occurred over 5 weeks).

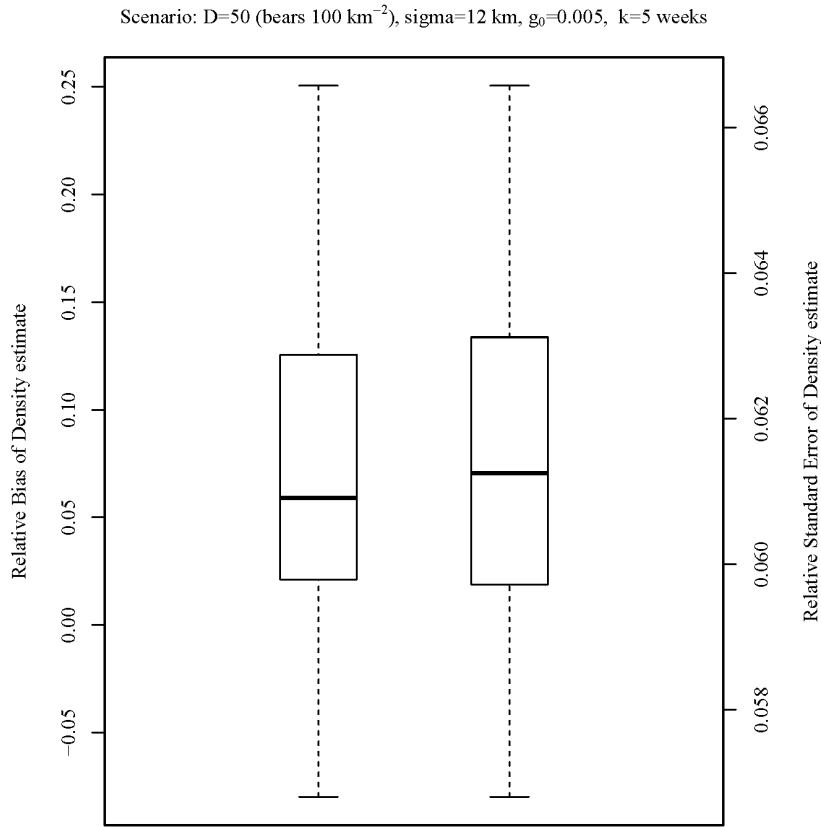


Figure 1.38. Distribution of relative bias (left boxplot) and relative standard error (right boxplot) in the density estimate for a simulated scenario of a spatial capture-recapture model ($D = 50$ bears/ 100 km^2 , $\sigma = 12 \text{ km}$, $g_0 = 0.005$, and sampling occurred over 5 weeks).

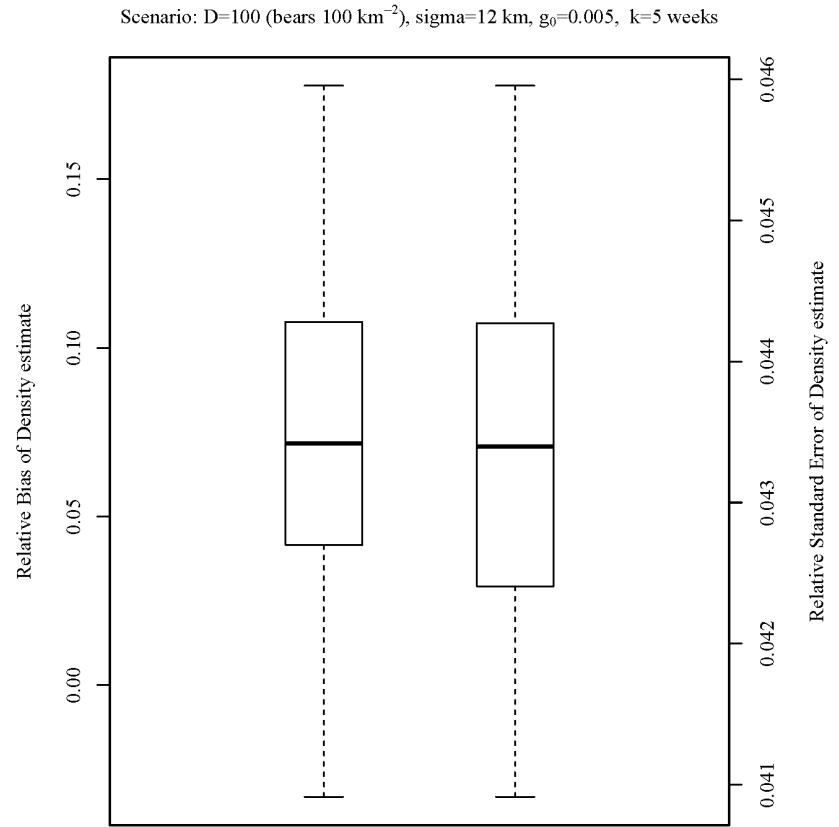


Figure 1.39. Distribution of relative bias (left boxplot) and relative standard error (right boxplot) in the density estimate for a simulated scenario of a spatial capture-recapture model ($D = 100$ bears/ 100 km^2 , $\sigma = 12 \text{ km}$, $g_0 = 0.005$, and sampling occurred over 5 weeks).

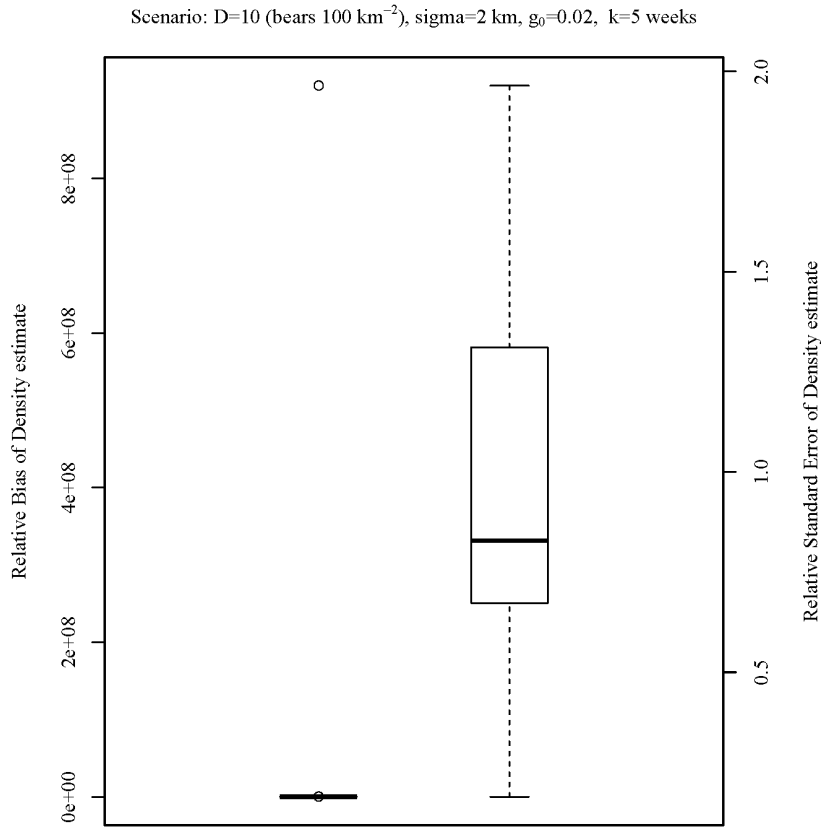


Figure 1.40. Distribution of relative bias (left boxplot) and relative standard error (right boxplot) in the density estimate for a simulated scenario of a spatial capture-recapture model ($D = 10$ bears/ 100 km^2 , $\sigma = 2 \text{ km}$, $g_0 = 0.02$, and sampling occurred over 5 weeks).

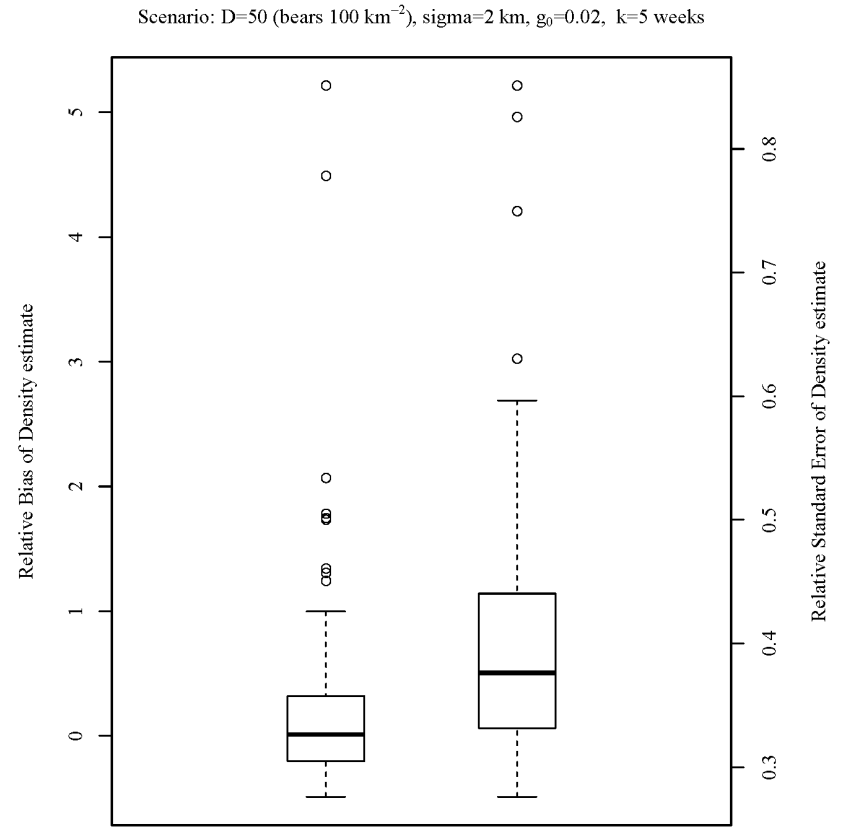


Figure 1.41. Distribution of relative bias (left boxplot) and relative standard error (right boxplot) in the density estimate for a simulated scenario of a spatial capture-recapture model ($D = 50$ bears/ 100 km^2 , $\sigma = 2 \text{ km}$, $g_0 = 0.02$, and sampling occurred over 5 weeks).

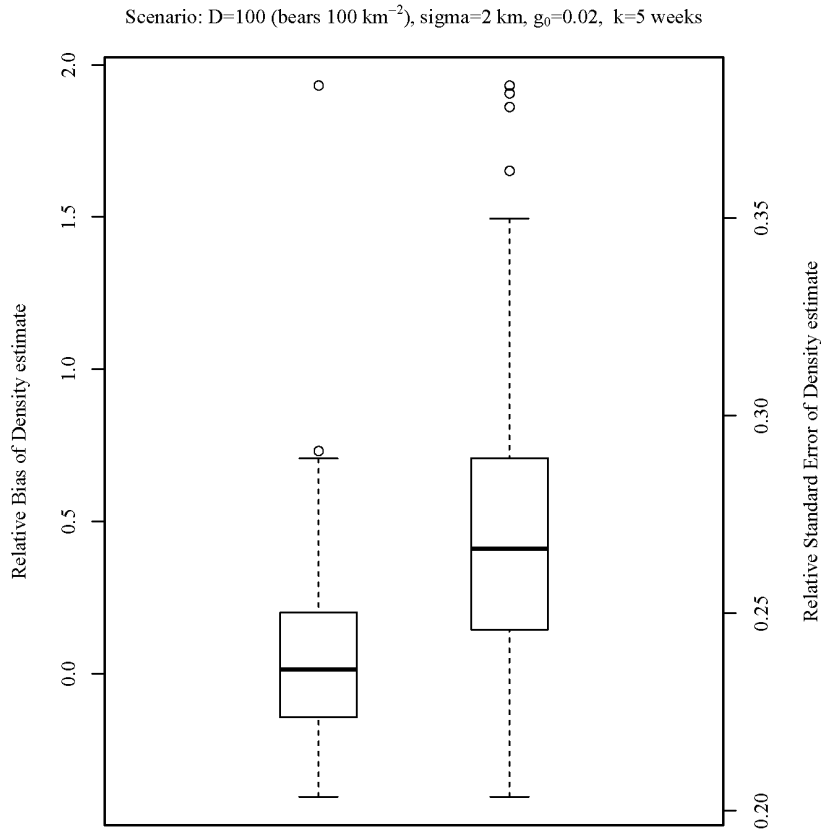


Figure 1.42. Distribution of relative bias (left boxplot) and relative standard error (right boxplot) in the density estimate for a simulated scenario of a spatial capture-recapture model ($D = 100$ bears/ 100 km^2 , $\sigma = 2 \text{ km}$, $g_0 = 0.02$, and sampling occurred over 5 weeks).

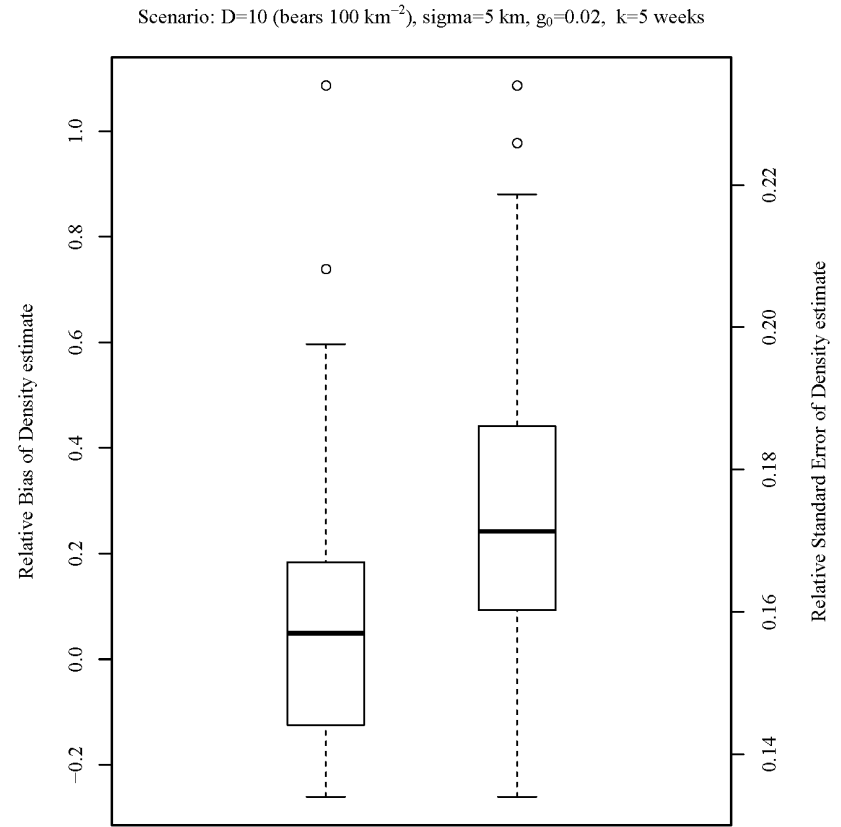


Figure 1.43. Distribution of relative bias (left boxplot) and relative standard error (right boxplot) in the density estimate for a simulated scenario of a spatial capture-recapture model ($D = 10$ bears/ 100 km^2 , $\sigma = 5 \text{ km}$, $g_0 = 0.02$, and sampling occurred over 5 weeks).

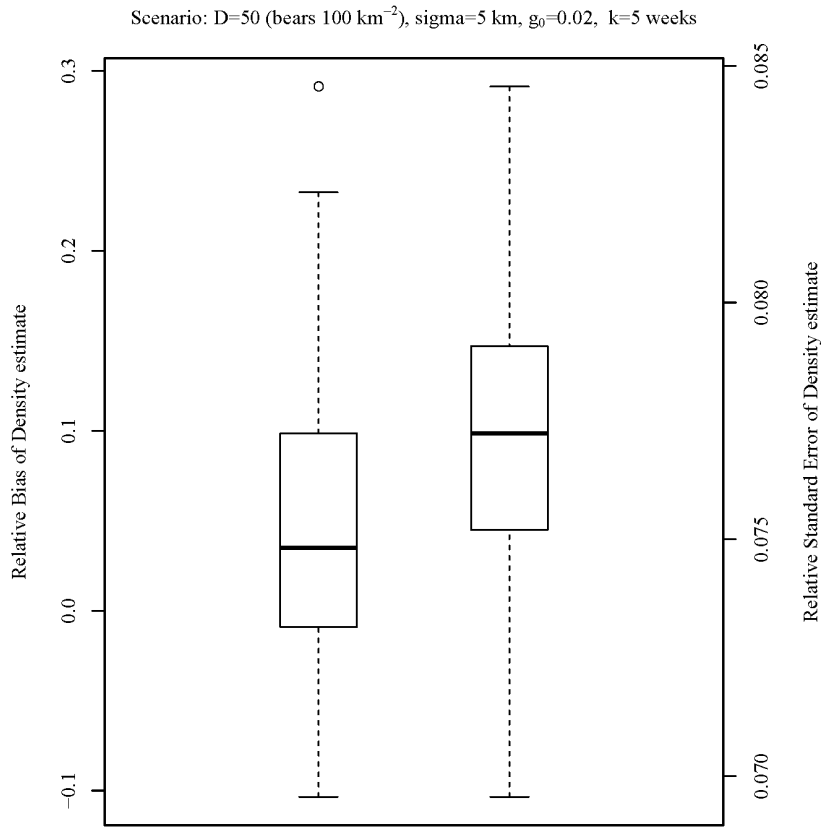


Figure 1.44. Distribution of relative bias (left boxplot) and relative standard error (right boxplot) in the density estimate for a simulated scenario of a spatial capture-recapture model ($D = 50$ bears/ 100 km^2 , $\sigma = 5 \text{ km}$, $g_0 = 0.02$, and sampling occurred over 5 weeks).

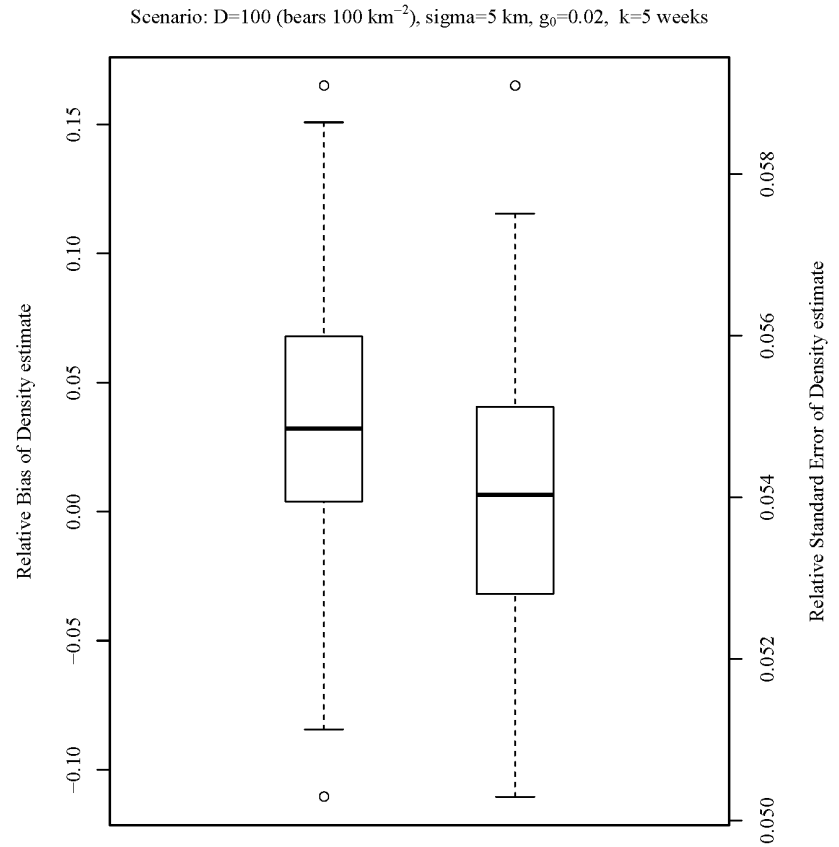


Figure 1.45. Distribution of relative bias (left boxplot) and relative standard error (right boxplot) in the density estimate for a simulated scenario of a spatial capture-recapture model ($D = 100$ bears/ 100 km^2 , $\sigma = 5 \text{ km}$, $g_0 = 0.02$, and sampling occurred over 5 weeks).

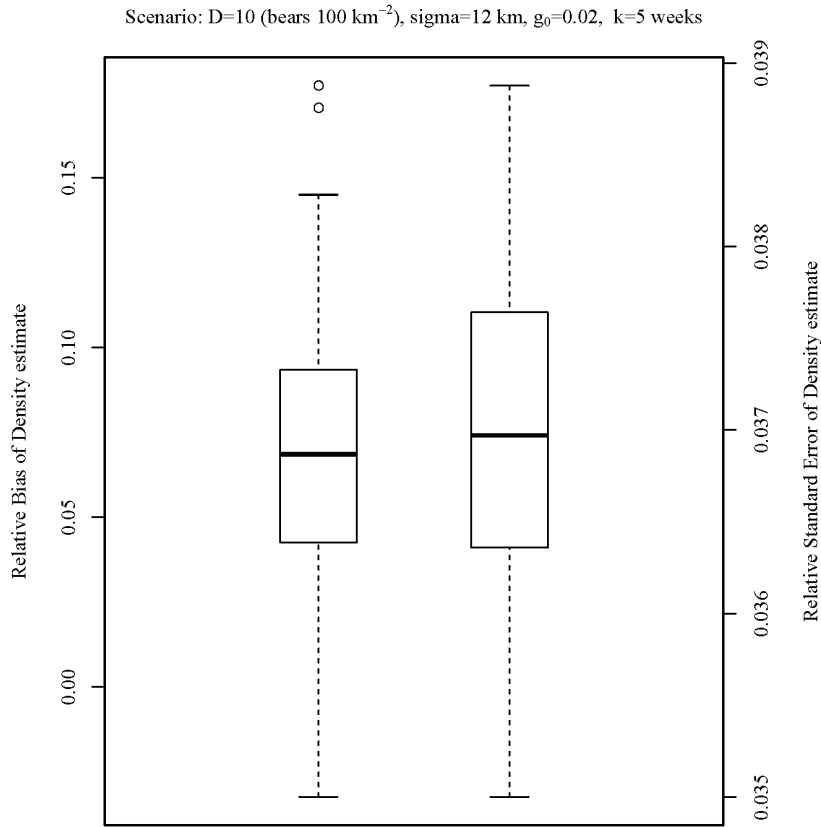


Figure 1.46. Distribution of relative bias (left boxplot) and relative standard error (right boxplot) in the density estimate for a simulated scenario of a spatial capture-recapture model ($D = 10$ bears/ 100 km^2 , $\sigma = 12 \text{ km}$, $g_0 = 0.02$, and sampling occurred over 5 weeks).

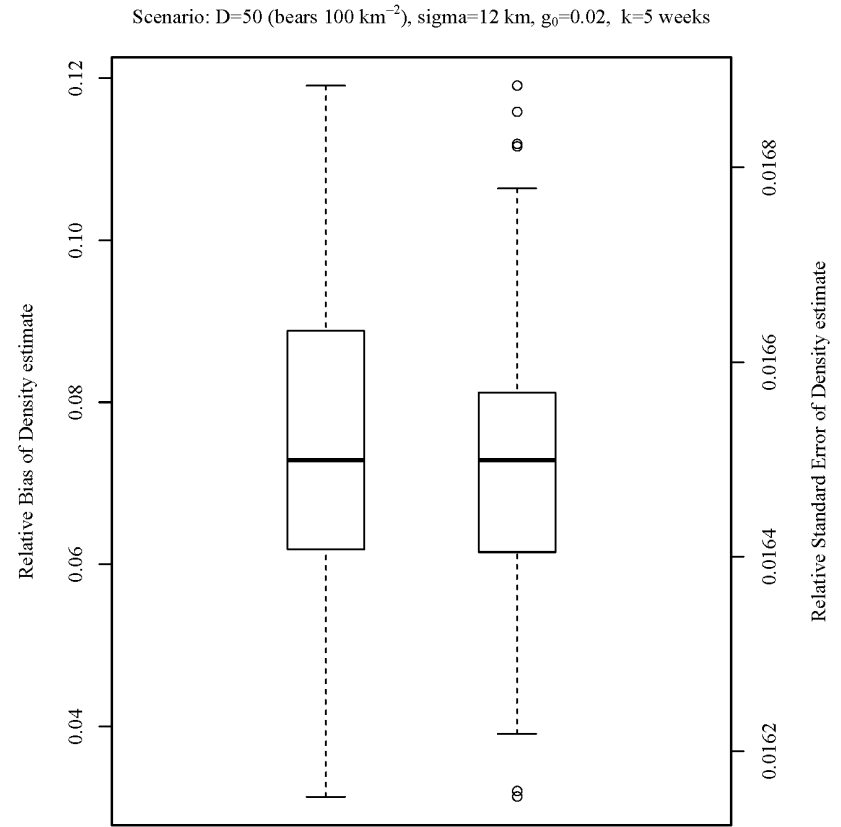


Figure 1.47. Distribution of relative bias (left boxplot) and relative standard error (right boxplot) in the density estimate for a simulated scenario of a spatial capture-recapture model ($D = 50$ bears/ 100 km^2 , $\sigma = 12 \text{ km}$, $g_0 = 0.02$, and sampling occurred over 5 weeks).

Scenario: $D=100$ (bears 100 km^{-2}), $\sigma=12 \text{ km}$, $g_0=0.02$, $k=5$ weeks

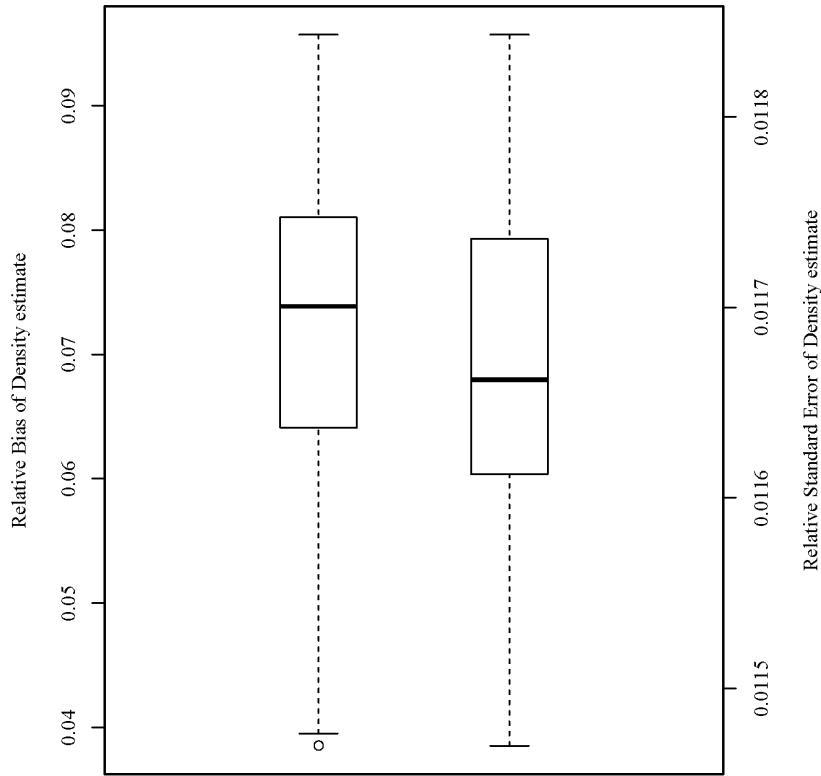


Figure 1.48. Distribution of relative bias (left boxplot) and relative standard error (right boxplot) in the density estimate for a simulated scenario of a spatial capture-recapture model ($D = 100$ bears/ 100 km^2 , $\sigma = 12 \text{ km}$, $g_0 = 0.02$, and sampling occurred over 5 weeks).

Scenario: $D=10$ (bears 100 km^{-2}), $\sigma=2 \text{ km}$, $g_0=0.2$, $k=5$ weeks

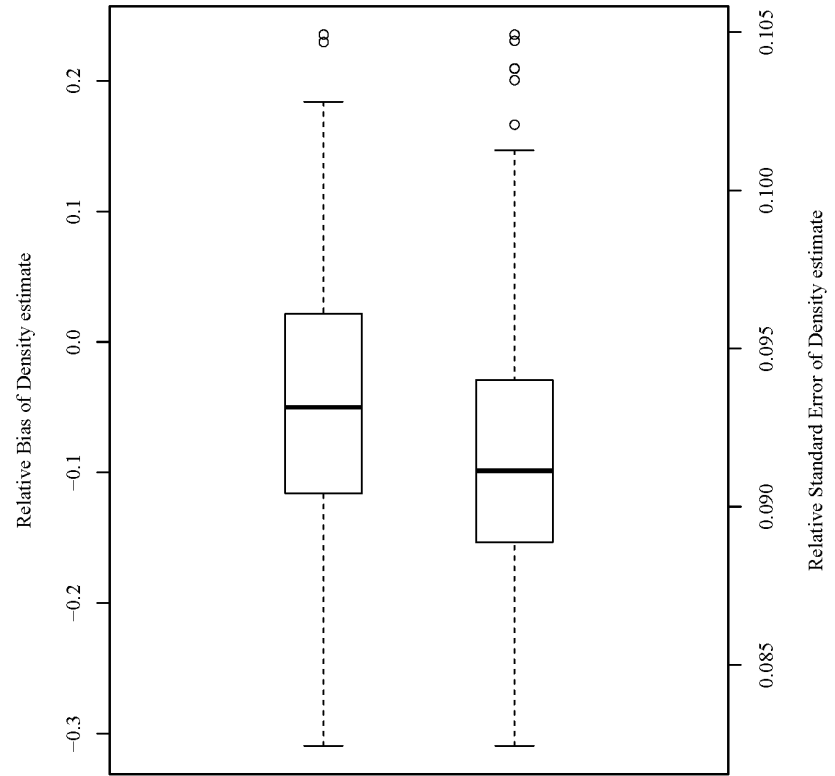


Figure 1.49. Distribution of relative bias (left boxplot) and relative standard error (right boxplot) in the density estimate for a simulated scenario of a spatial capture-recapture model ($D = 10$ bears/ 100 km^2 , $\sigma = 2 \text{ km}$, $g_0 = 0.2$, and sampling occurred over 5 weeks).

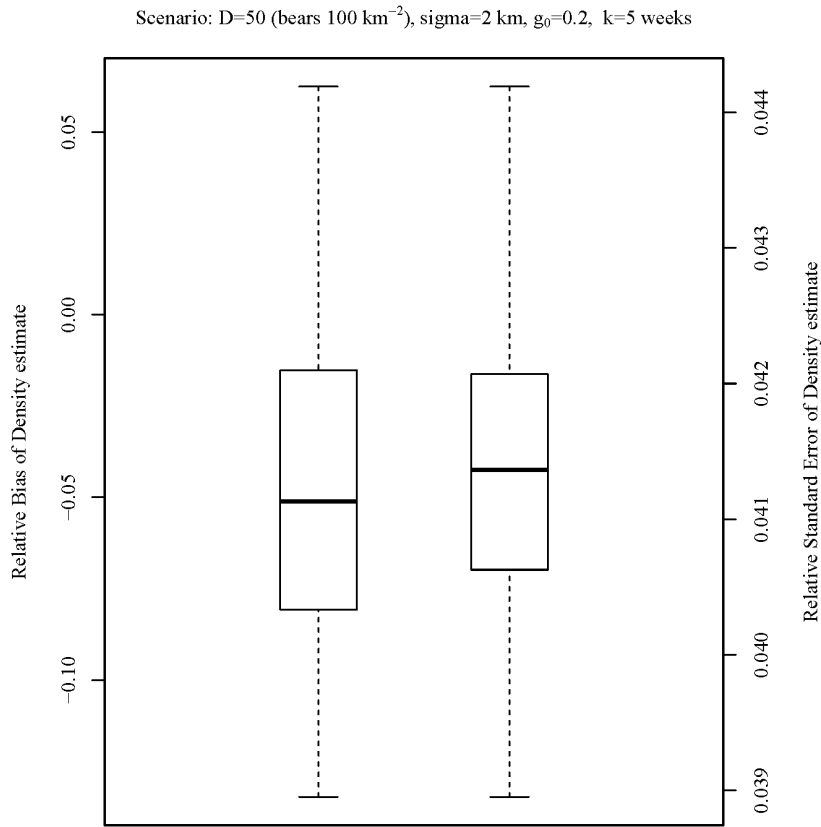


Figure 1.50. Distribution of relative bias (left boxplot) and relative standard error (right boxplot) in the density estimate for a simulated scenario of a spatial capture-recapture model ($D = 50$ bears/ 100 km^2 , $\sigma = 2 \text{ km}$, $g_0 = 0.2$, and sampling occurred over 5 weeks).

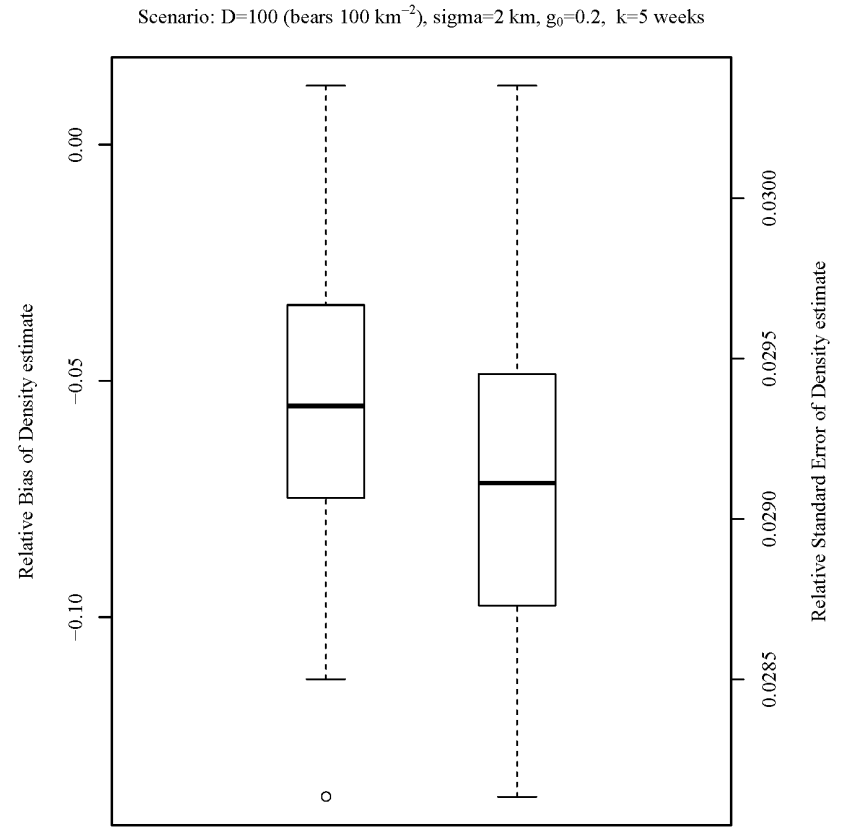


Figure 1.51. Distribution of relative bias (left boxplot) and relative standard error (right boxplot) in the density estimate for a simulated scenario of a spatial capture-recapture model ($D = 100$ bears/ 100 km^2 , $\sigma = 2 \text{ km}$, $g_0 = 0.2$, and sampling occurred over 5 weeks).

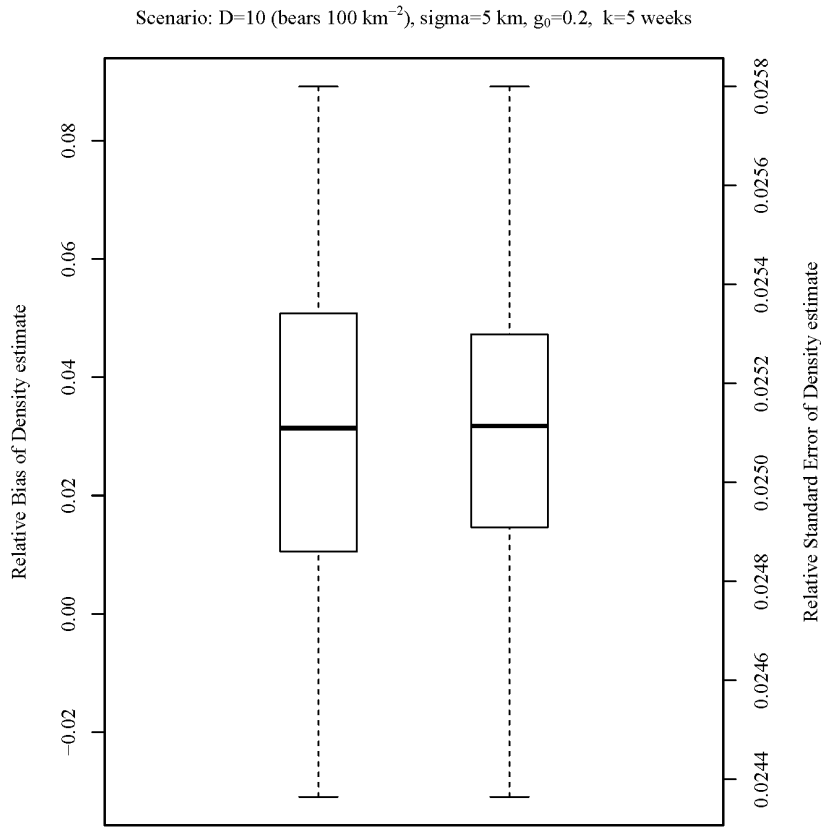


Figure 1.52. Distribution of relative bias (left boxplot) and relative standard error (right boxplot) in the density estimate for a simulated scenario of a spatial capture-recapture model ($D = 10$ bears/ 100 km^2 , $\sigma = 5 \text{ km}$, $g_0 = 0.2$, and sampling occurred over 5 weeks).

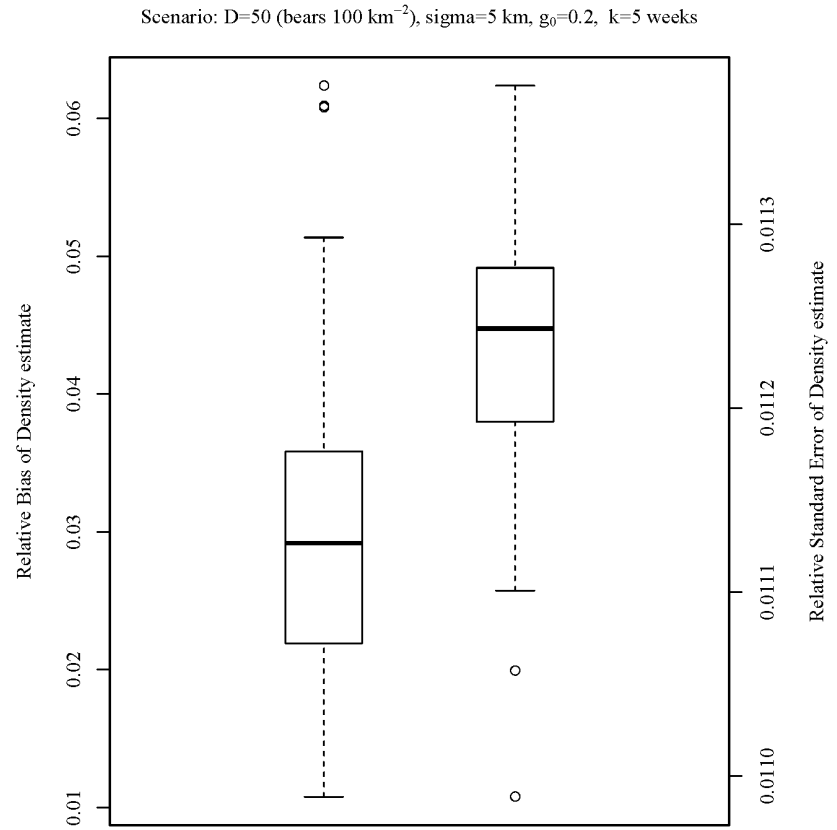


Figure 1.53. Distribution of relative bias (left boxplot) and relative standard error (right boxplot) in the density estimate for a simulated scenario of a spatial capture-recapture model ($D = 50$ bears/ 100 km^2 , $\sigma = 5 \text{ km}$, $g_0 = 0.2$, and sampling occurred over 5 weeks).

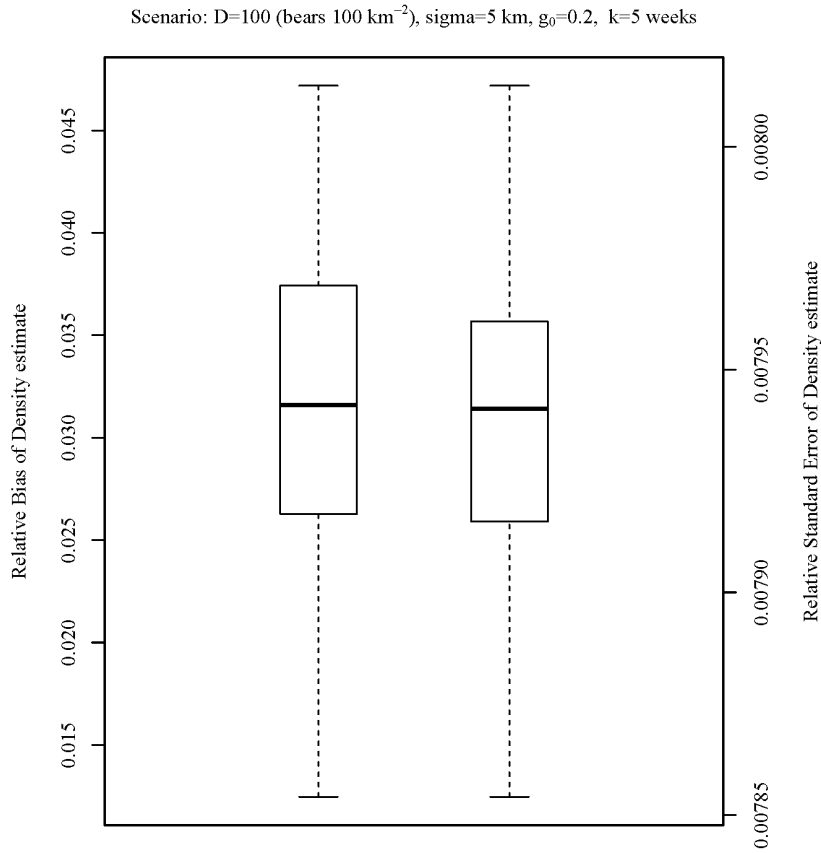


Figure 1.54. Distribution of relative bias (left boxplot) and relative standard error (right boxplot) in the density estimate for a simulated scenario of a spatial capture-recapture model ($D = 100$ bears/ 100 km^2 , $\sigma = 5 \text{ km}$, $g_0 = 0.2$, and sampling occurred over 5 weeks).

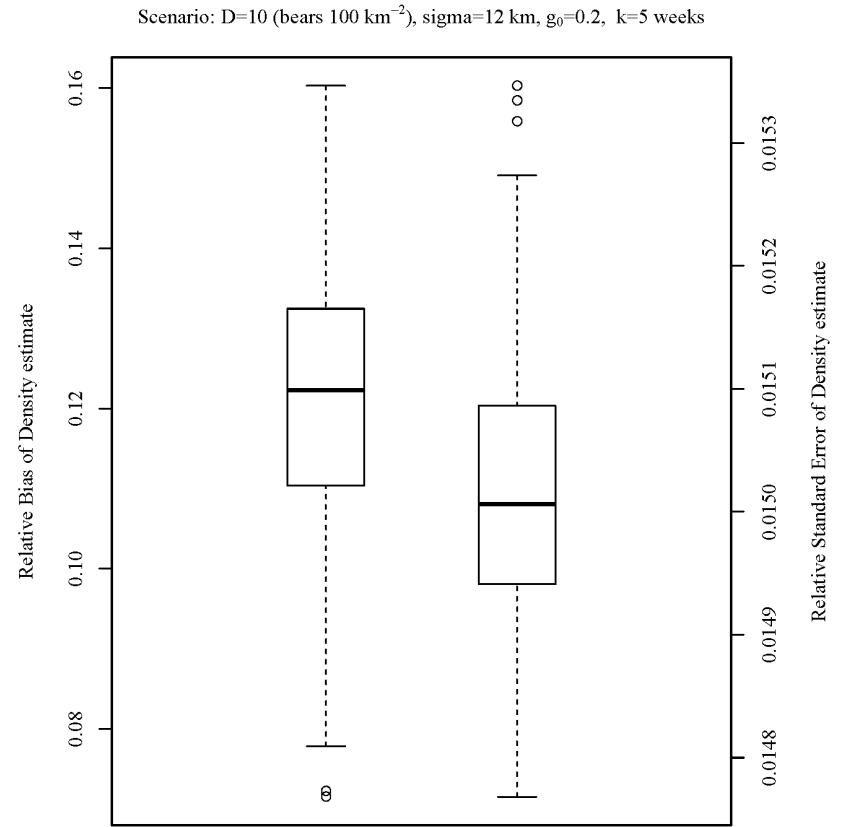


Figure 1.55. Distribution of relative bias (left boxplot) and relative standard error (right boxplot) in the density estimate for a simulated scenario of a spatial capture-recapture model ($D = 10$ bears/ 100 km^2 , $\sigma = 12 \text{ km}$, $g_0 = 0.2$, and sampling occurred over 5 weeks).

Scenario: $D=50$ (bears 100 km^{-2}), $\sigma=12 \text{ km}$, $g_0=0.2$, $k=5$ weeks

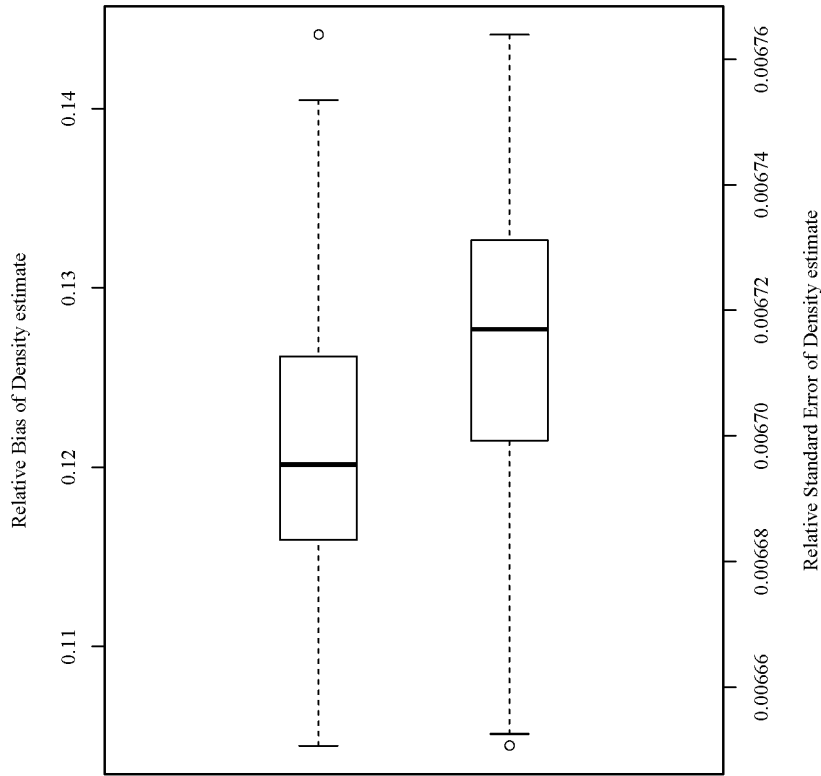


Figure 1.56. Distribution of relative bias (left boxplot) and relative standard error (right boxplot) in the density estimate for a simulated scenario of a spatial capture-recapture model ($D = 50$ bears/ 100 km^2 , $\sigma = 12 \text{ km}$, $g_0 = 0.2$, and sampling occurred over 5 weeks).

Scenario: $D=100$ (bears 100 km^{-2}), $\sigma=12 \text{ km}$, $g_0=0.2$, $k=5$ weeks

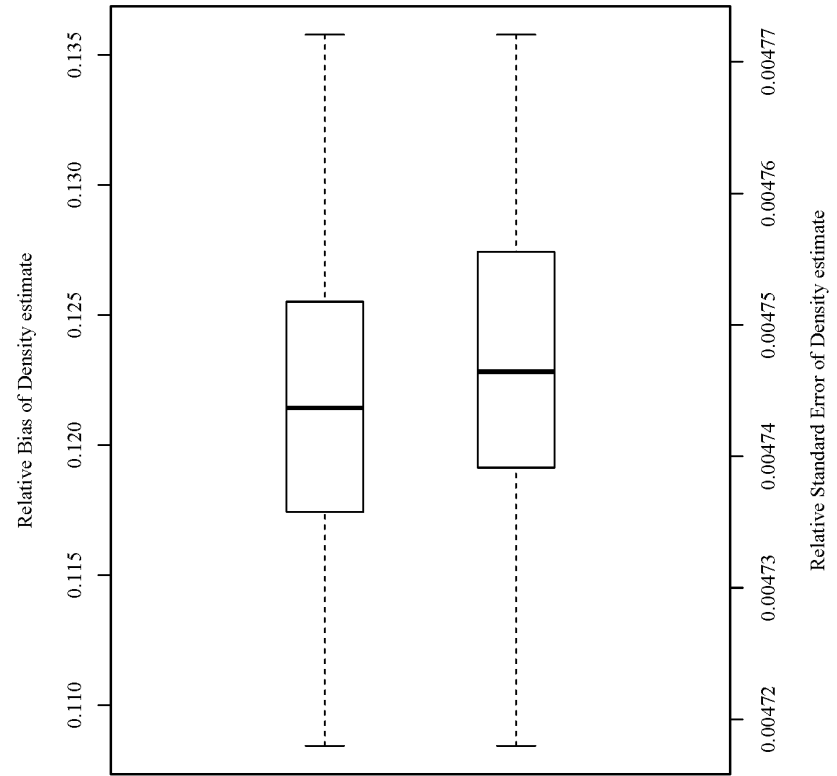


Figure 1.57. Distribution of relative bias (left boxplot) and relative standard error (right boxplot) in the density estimate for a simulated scenario of a spatial capture-recapture model ($D = 100$ bears/ 100 km^2 , $\sigma = 12 \text{ km}$, $g_0 = 0.2$, and sampling occurred over 5 weeks).

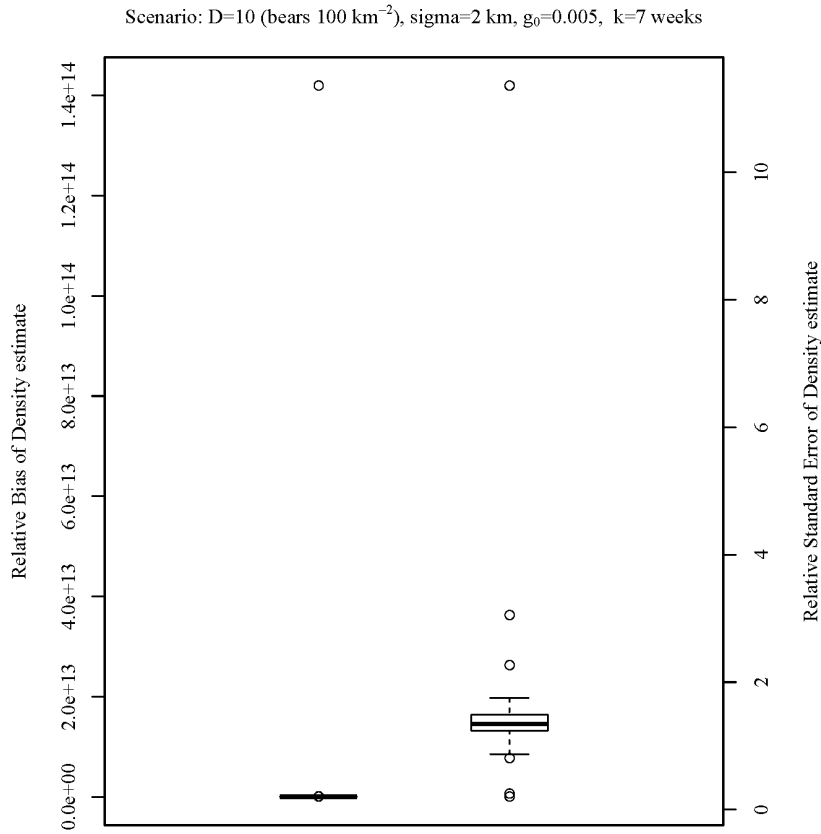


Figure 1.58. Distribution of relative bias (left boxplot) and relative standard error (right boxplot) in the density estimate for a simulated scenario of a spatial capture-recapture model ($D = 10$ bears/ 100 km^2 , $\sigma = 2 \text{ km}$, $g_0 = 0.005$, and sampling occurred over 7 weeks).

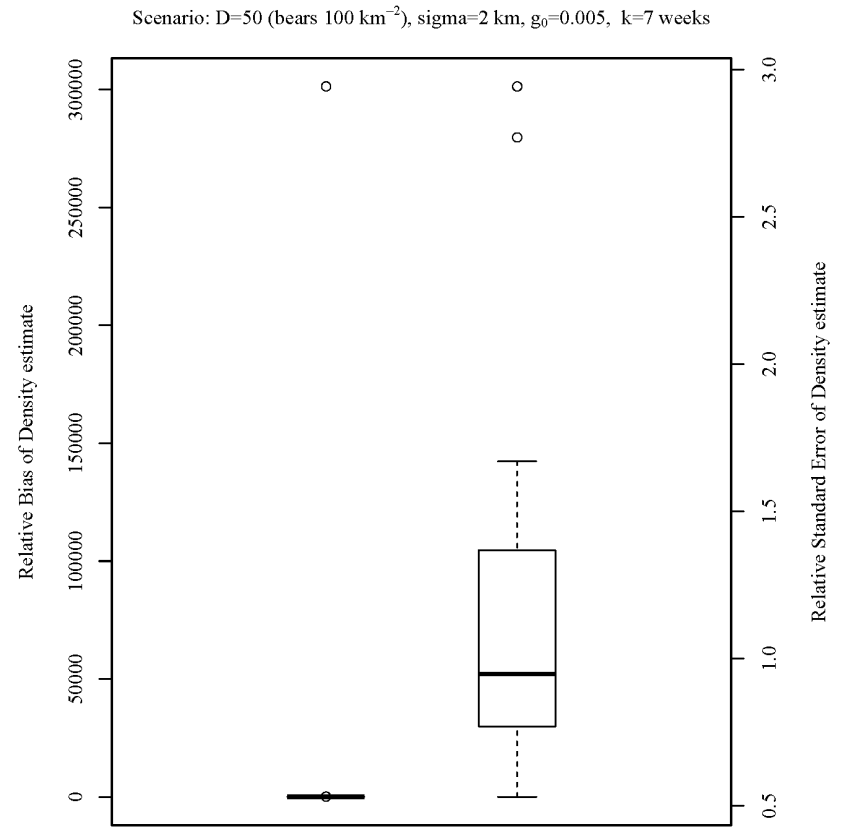


Figure 1.59. Distribution of relative bias (left boxplot) and relative standard error (right boxplot) in the density estimate for a simulated scenario of a spatial capture-recapture model ($D = 50$ bears/ 100 km^2 , $\sigma = 2 \text{ km}$, $g_0 = 0.005$, and sampling occurred over 7 weeks).

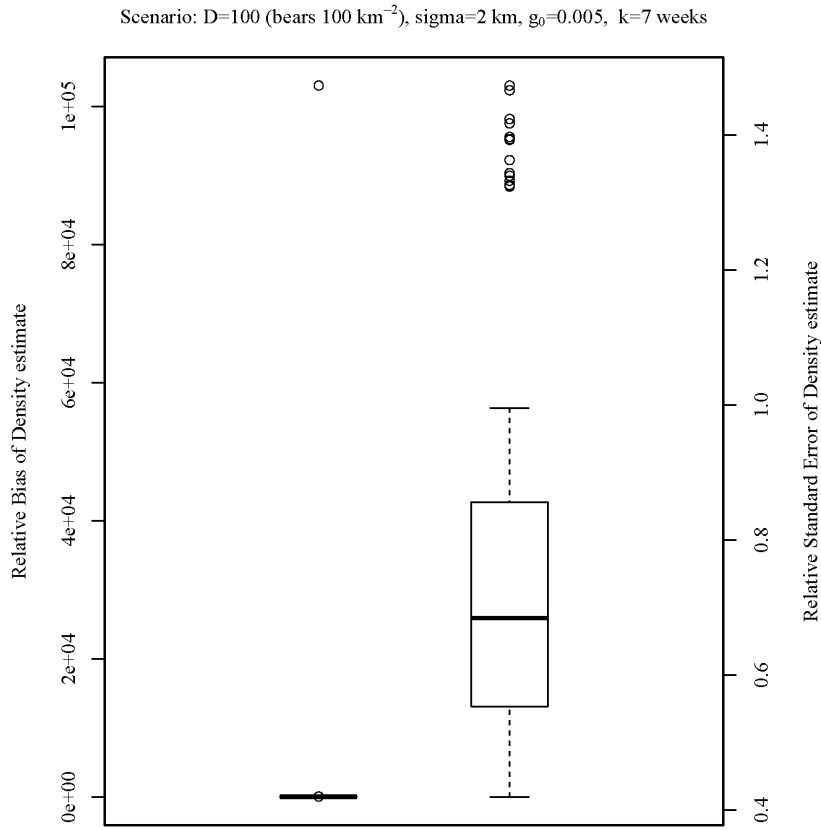


Figure 1.60. Distribution of relative bias (left boxplot) and relative standard error (right boxplot) in the density estimate for a simulated scenario of a spatial capture-recapture model ($D = 100$ bears/ 100 km^2 , $\sigma = 2 \text{ km}$, $g_0 = 0.005$, and sampling occurred over 7 weeks).

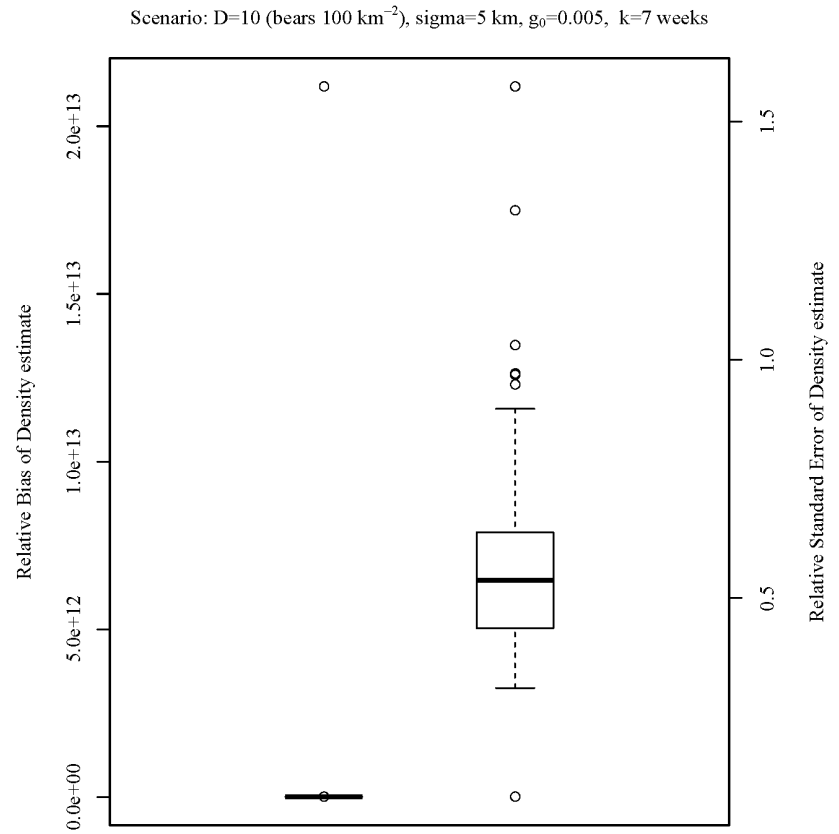


Figure 1.61. Distribution of relative bias (left boxplot) and relative standard error (right boxplot) in the density estimate for a simulated scenario of a spatial capture-recapture model ($D = 10$ bears/ 100 km^2 , $\sigma = 5 \text{ km}$, $g_0 = 0.005$, and sampling occurred over 7 weeks).

Scenario: $D=50$ (bears 100 km^{-2}), $\sigma=5 \text{ km}$, $g_0=0.005$, $k=7$ weeks

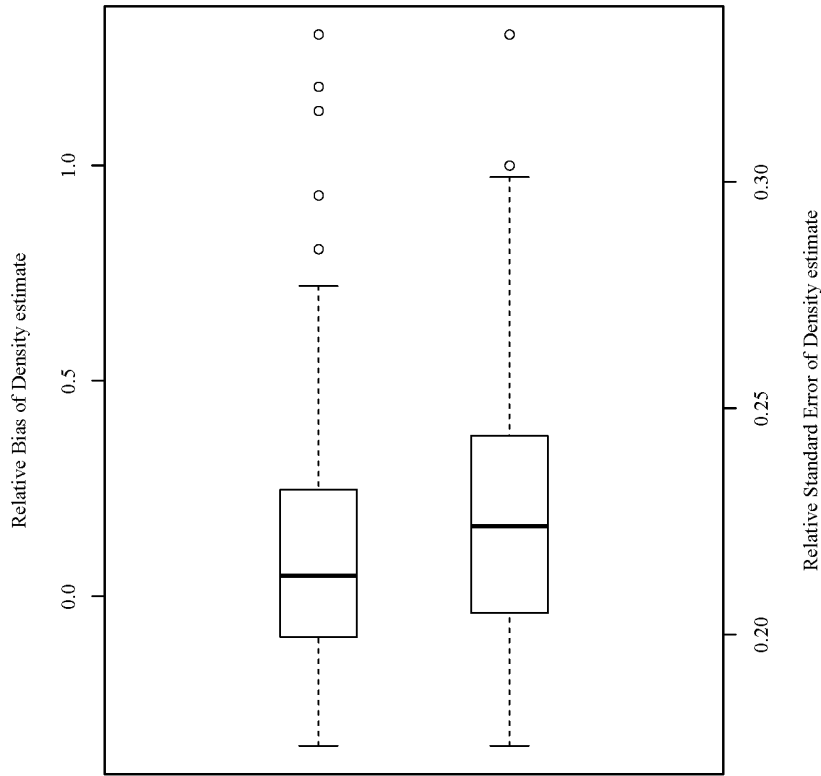


Figure 1.62. Distribution of relative bias (left boxplot) and relative standard error (right boxplot) in the density estimate for a simulated scenario of a spatial capture-recapture model ($D = 50$ bears/ 100 km^2 , $\sigma = 5 \text{ km}$, $g_0 = 0.005$, and sampling occurred over 7 weeks).

Scenario: $D=100$ (bears 100 km^{-2}), $\sigma=5 \text{ km}$, $g_0=0.005$, $k=7$ weeks

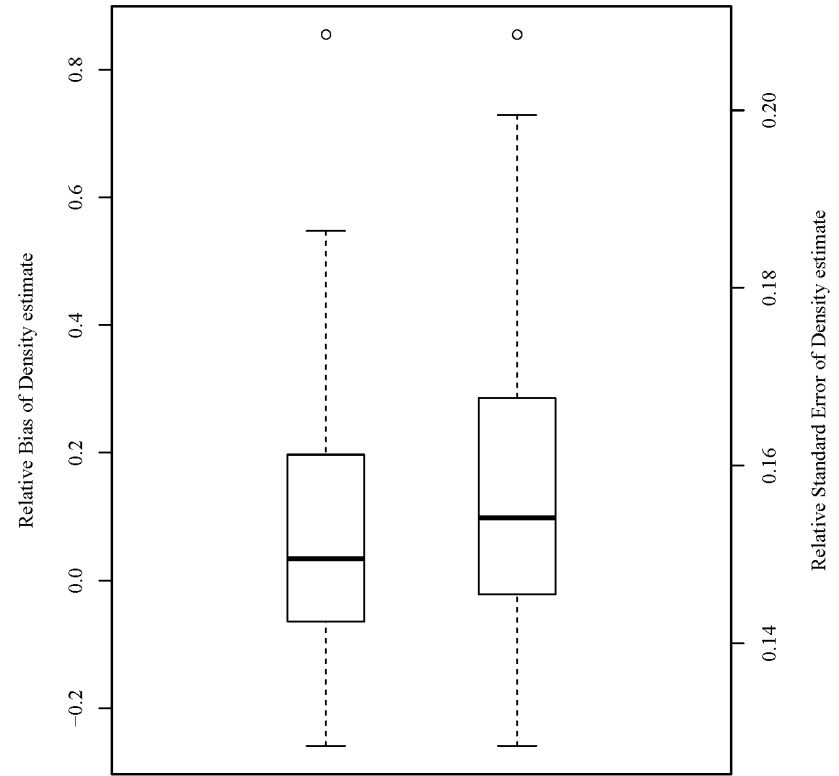


Figure 1.63. Distribution of relative bias (left boxplot) and relative standard error (right boxplot) in the density estimate for a simulated scenario of a spatial capture-recapture model ($D = 100$ bears/ 100 km^2 , $\sigma = 5 \text{ km}$, $g_0 = 0.005$, and sampling occurred over 7 weeks).

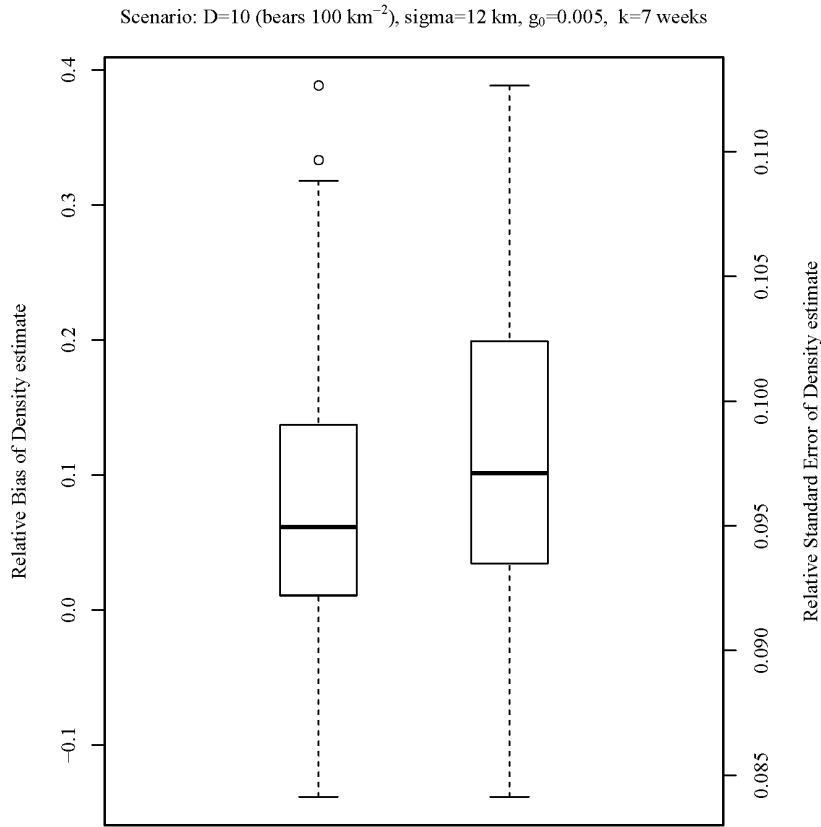


Figure 1.64. Distribution of relative bias (left boxplot) and relative standard error (right boxplot) in the density estimate for a simulated scenario of a spatial capture-recapture model ($D = 10$ bears/ 100 km^2 , $\sigma = 12 \text{ km}$, $g_0 = 0.005$, and sampling occurred over 7 weeks).

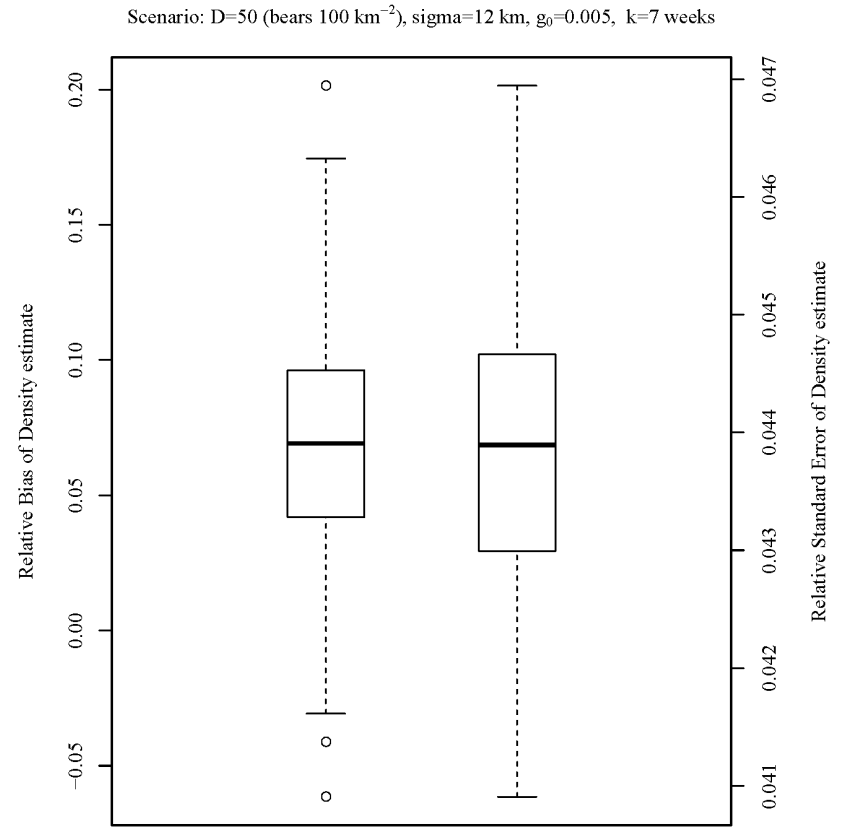


Figure 1.65. Distribution of relative bias (left boxplot) and relative standard error (right boxplot) in the density estimate for a simulated scenario of a spatial capture-recapture model ($D = 50$ bears/ 100 km^2 , $\sigma = 12 \text{ km}$, $g_0 = 0.005$, and sampling occurred over 7 weeks).

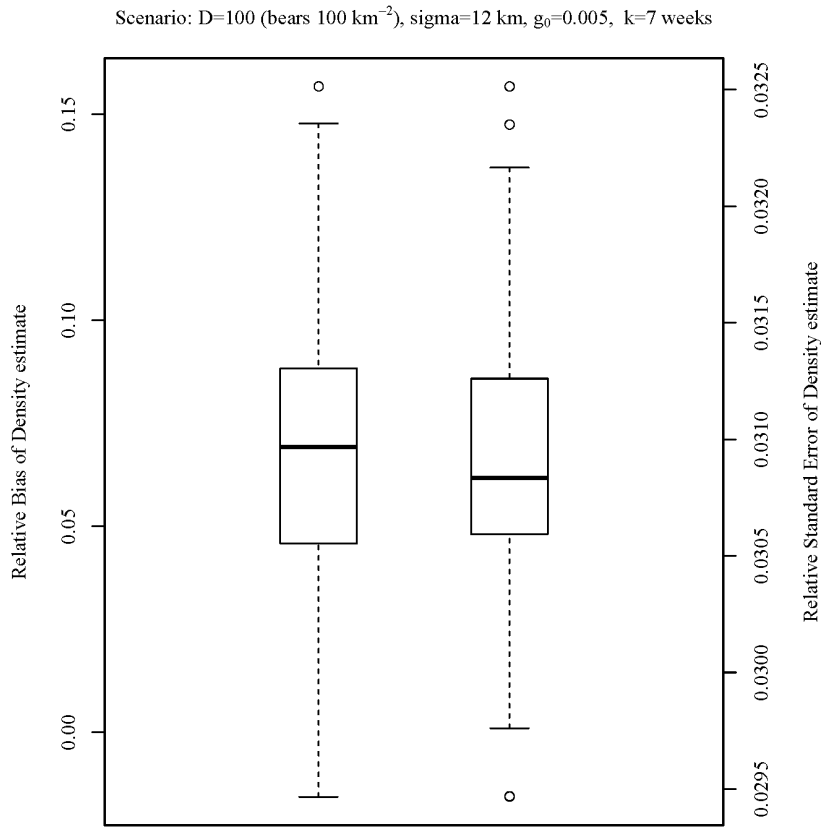


Figure 1.66. Distribution of relative bias (left boxplot) and relative standard error (right boxplot) in the density estimate for a simulated scenario of a spatial capture-recapture model ($D = 100$ bears/ 100 km^2 , $\sigma = 12 \text{ km}$, $g_0 = 0.005$, and sampling occurred over 7 weeks).

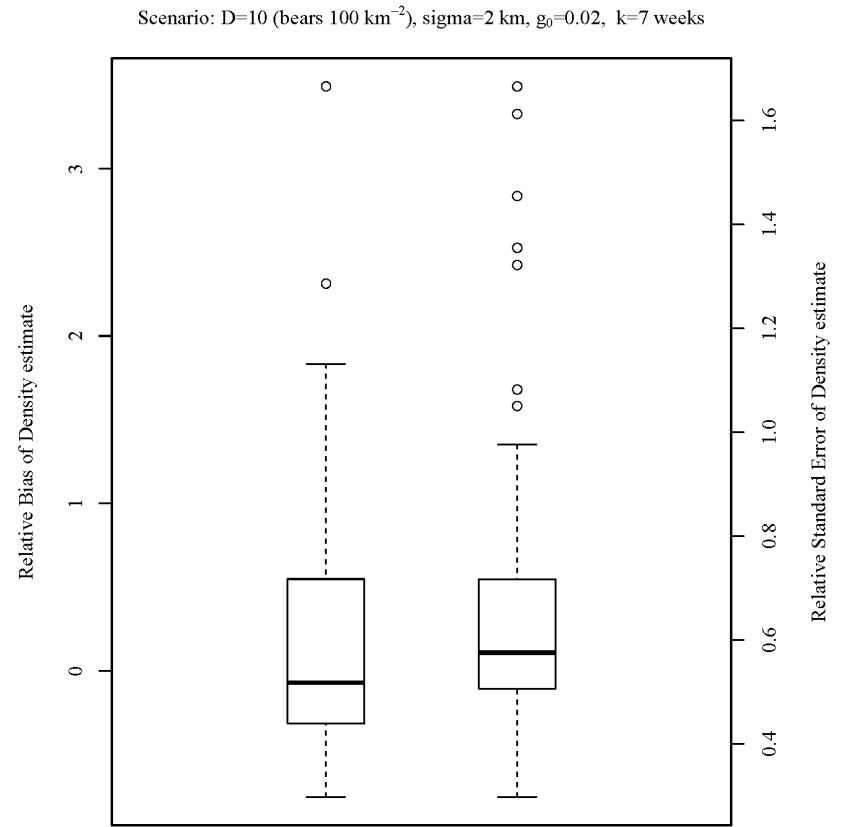


Figure 1.67. Distribution of relative bias (left boxplot) and relative standard error (right boxplot) in the density estimate for a simulated scenario of a spatial capture-recapture model ($D = 10$ bears/ 100 km^2 , $\sigma = 2 \text{ km}$, $g_0 = 0.02$, and sampling occurred over 7 weeks).

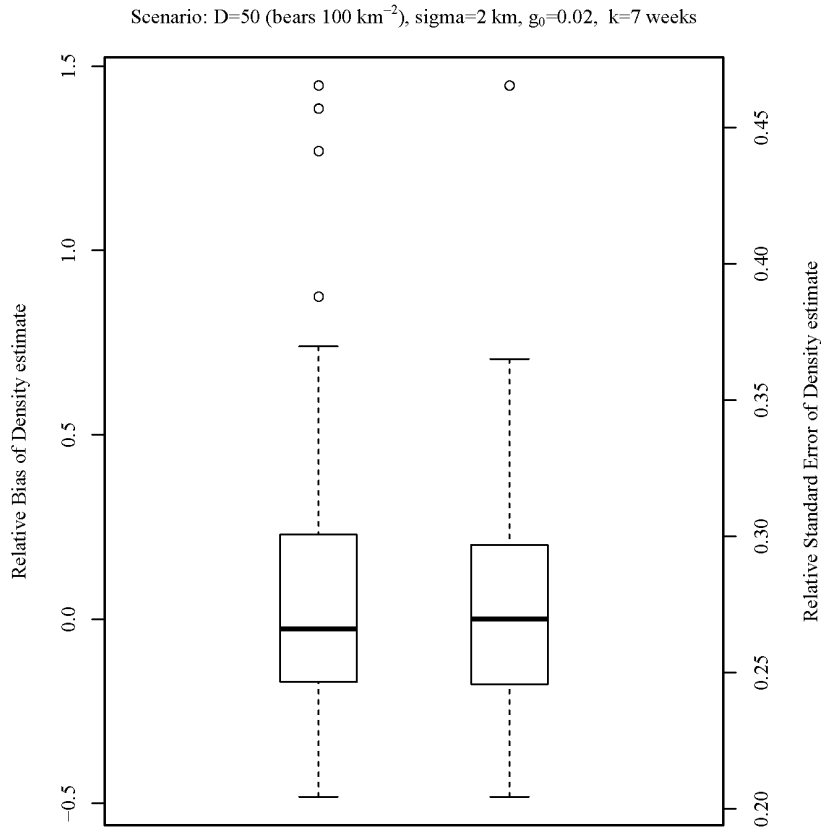


Figure 1.68. Distribution of relative bias (left boxplot) and relative standard error (right boxplot) in the density estimate for a simulated scenario of a spatial capture-recapture model ($D = 50$ bears/ 100 km^2 , $\sigma = 2 \text{ km}$, $g_0 = 0.02$, and sampling occurred over 7 weeks).

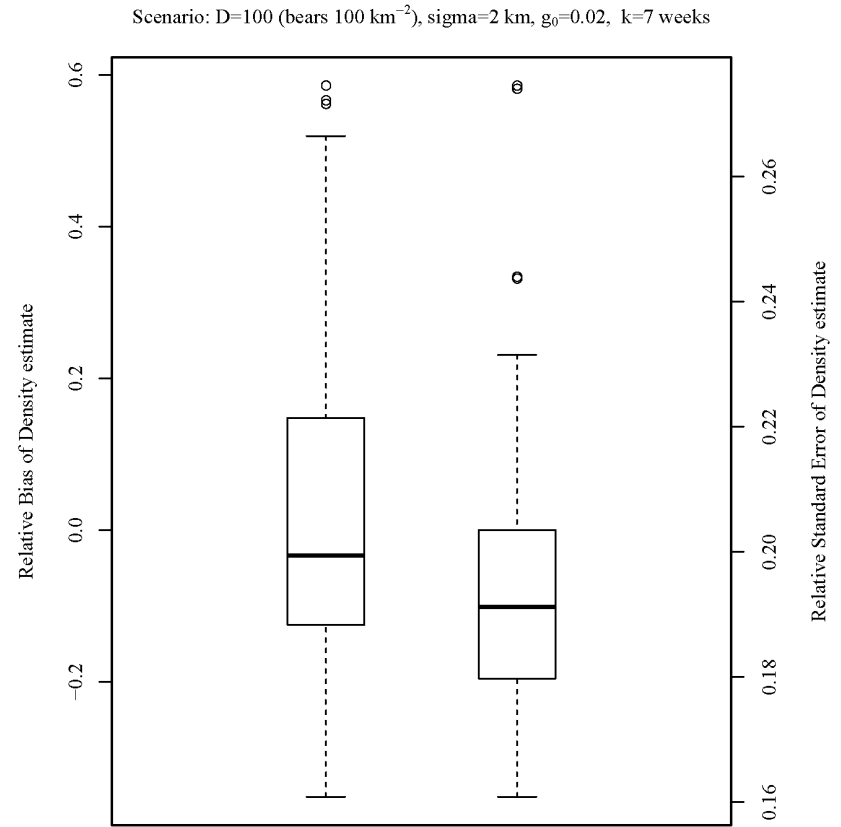


Figure 1.69. Distribution of relative bias (left boxplot) and relative standard error (right boxplot) in the density estimate for a simulated scenario of a spatial capture-recapture model ($D = 100$ bears/ 100 km^2 , $\sigma = 2 \text{ km}$, $g_0 = 0.02$, and sampling occurred over 7 weeks).

Scenario: $D=10$ (bears 100 km^{-2}), $\sigma=5 \text{ km}$, $g_0=0.02$, $k=7$ weeks

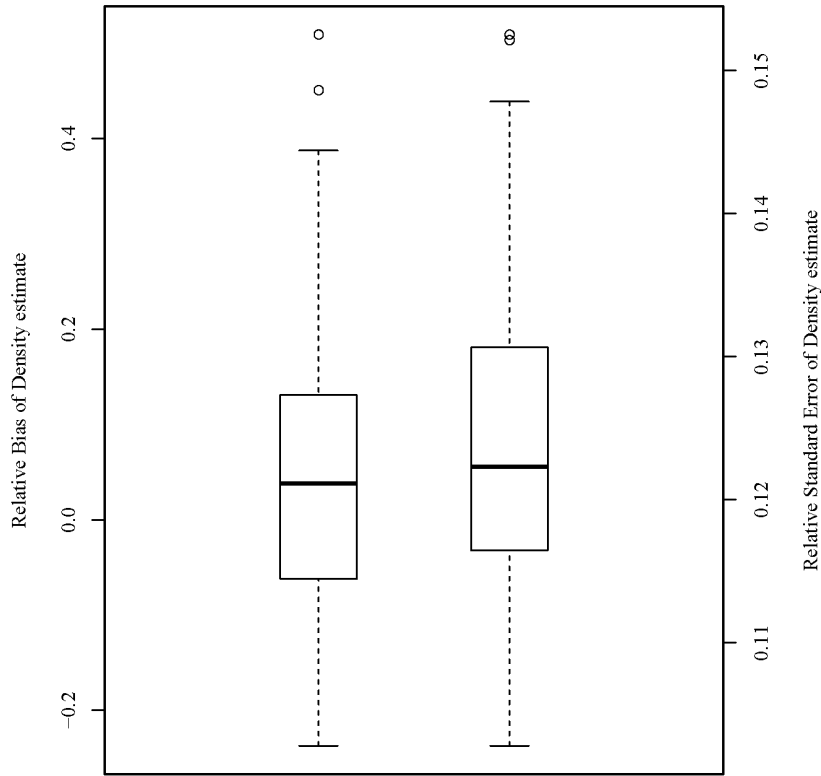


Figure 1.70. Distribution of relative bias (left boxplot) and relative standard error (right boxplot) in the density estimate for a simulated scenario of a spatial capture-recapture model ($D = 10$ bears/ 100 km^2 , $\sigma = 5 \text{ km}$, $g_0 = 0.02$, and sampling occurred over 7 weeks).

Scenario: $D=50$ (bears 100 km^{-2}), $\sigma=5 \text{ km}$, $g_0=0.02$, $k=7$ weeks

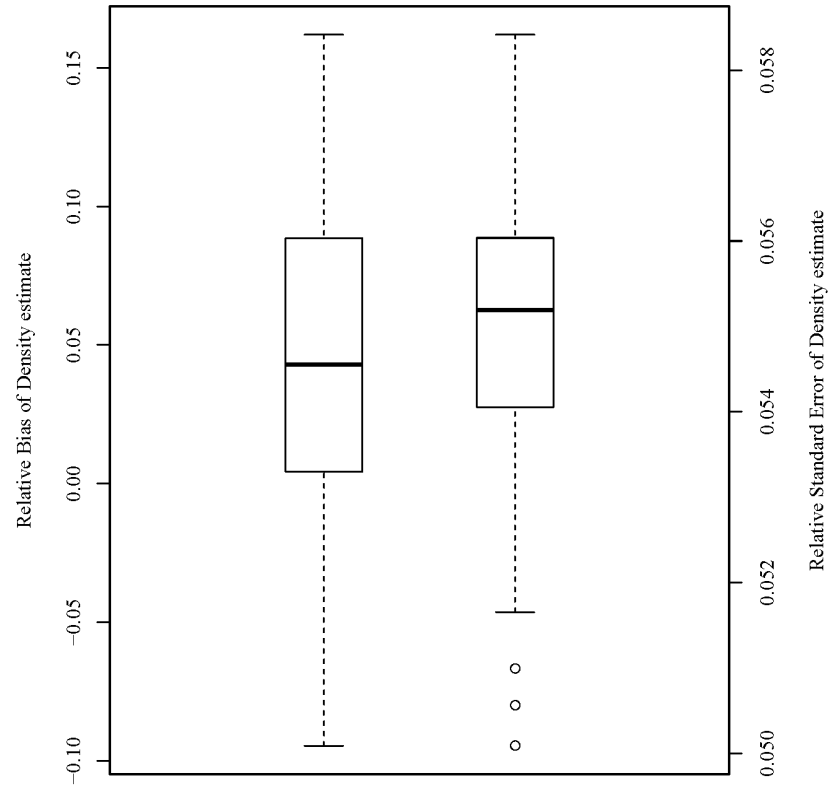


Figure 1.71. Distribution of relative bias (left boxplot) and relative standard error (right boxplot) in the density estimate for a simulated scenario of a spatial capture-recapture model ($D = 50$ bears/ 100 km^2 , $\sigma = 5 \text{ km}$, $g_0 = 0.02$, and sampling occurred over 7 weeks).

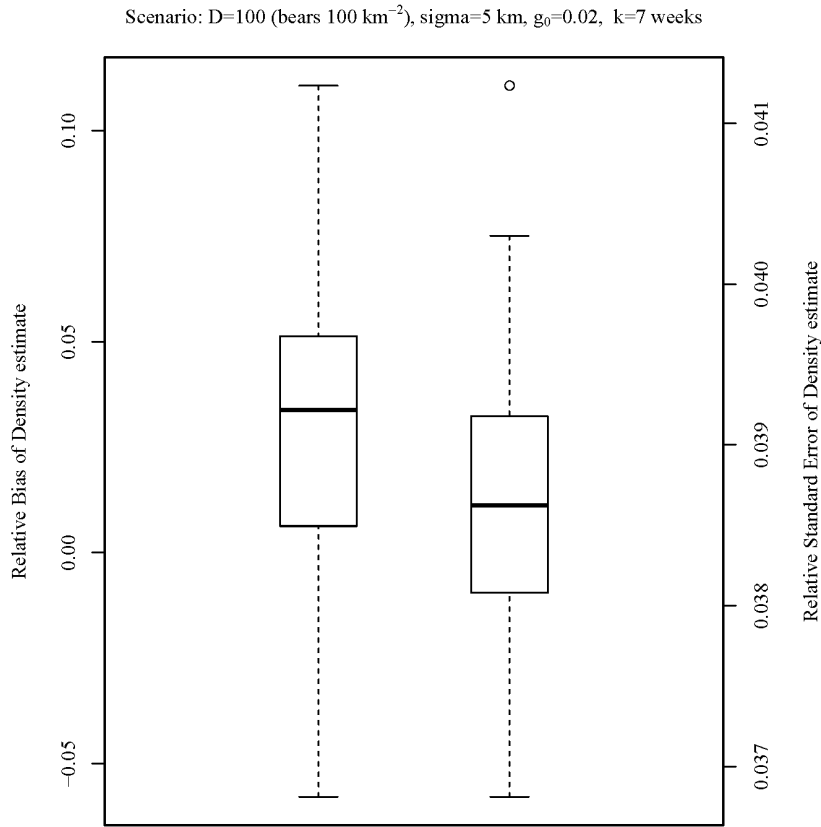


Figure 1.72. Distribution of relative bias (left boxplot) and relative standard error (right boxplot) in the density estimate for a simulated scenario of a spatial capture-recapture model ($D = 100$ bears/ 100 km^2 , $\sigma = 5 \text{ km}$, $g_0 = 0.02$, and sampling occurred over 7 weeks).

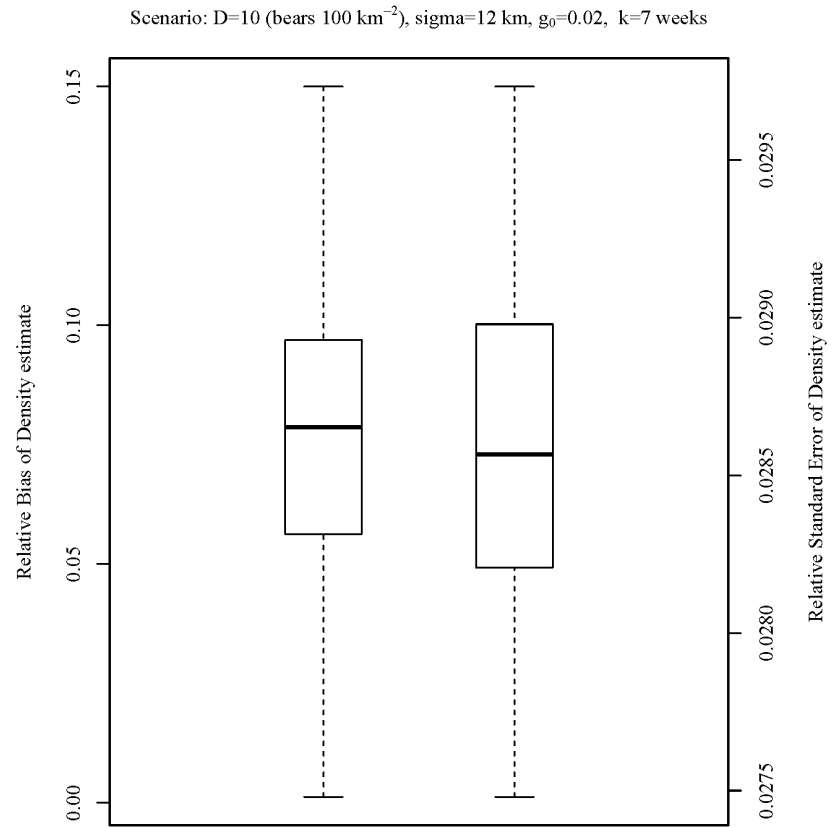


Figure 1.73. Distribution of relative bias (left boxplot) and relative standard error (right boxplot) in the density estimate for a simulated scenario of a spatial capture-recapture model ($D = 10$ bears/ 100 km^2 , $\sigma = 12 \text{ km}$, $g_0 = 0.02$, and sampling occurred over 7 weeks).

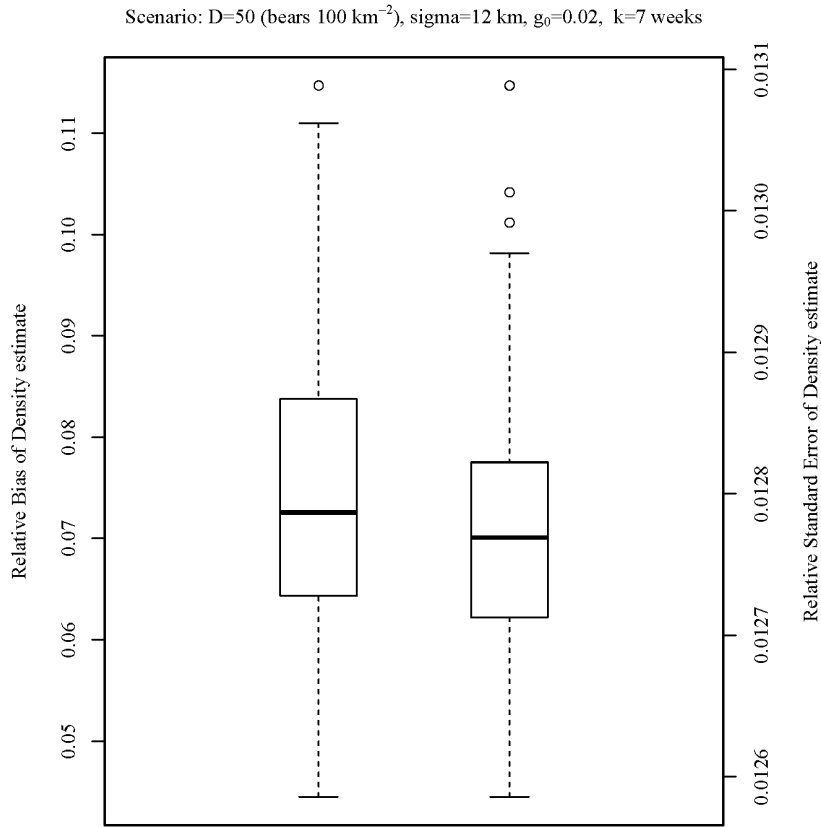


Figure 1.74. Distribution of relative bias (left boxplot) and relative standard error (right boxplot) in the density estimate for a simulated scenario of a spatial capture-recapture model ($D = 50$ bears/ 100 km^2 , $\sigma = 12 \text{ km}$, $g_0 = 0.02$, and sampling occurred over 7 weeks).

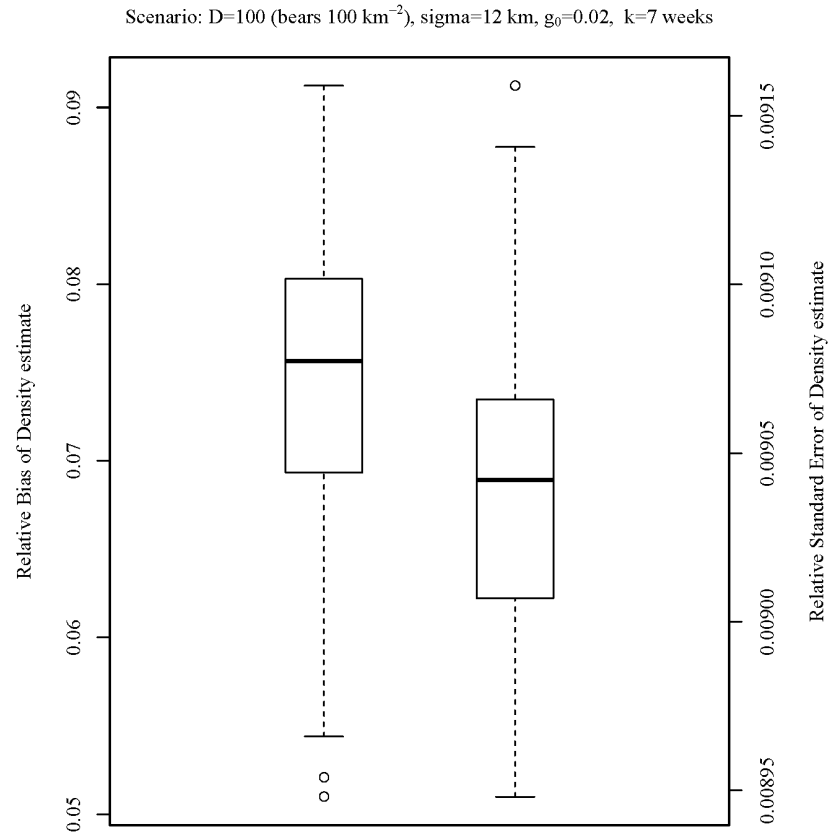


Figure 1.75. Distribution of relative bias (left boxplot) and relative standard error (right boxplot) in the density estimate for a simulated scenario of a spatial capture-recapture model ($D = 100$ bears/ 100 km^2 , $\sigma = 12 \text{ km}$, $g_0 = 0.02$, and sampling occurred over 7 weeks).

Scenario: $D=10$ (bears 100 km^{-2}), $\sigma=2 \text{ km}$, $g_0=0.2$, $k=7$ weeks

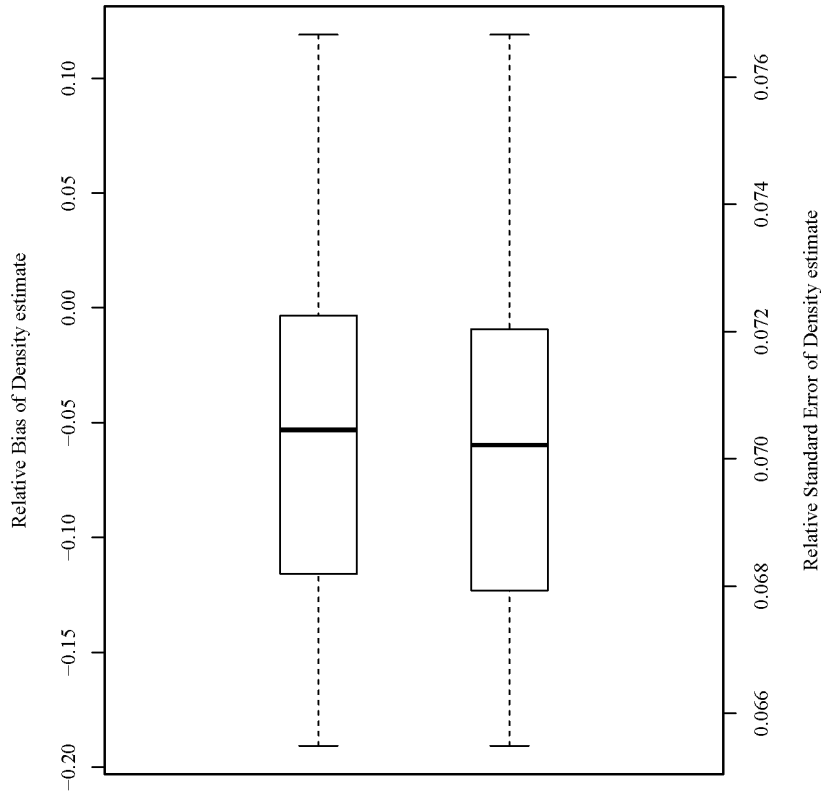


Figure 1.76. Distribution of relative bias (left boxplot) and relative standard error (right boxplot) in the density estimate for a simulated scenario of a spatial capture-recapture model ($D = 10$ bears/ 100 km^2 , $\sigma = 2 \text{ km}$, $g_0 = 0.2$, and sampling occurred over 7 weeks).

Scenario: $D=50$ (bears 100 km^{-2}), $\sigma=2 \text{ km}$, $g_0=0.2$, $k=7$ weeks

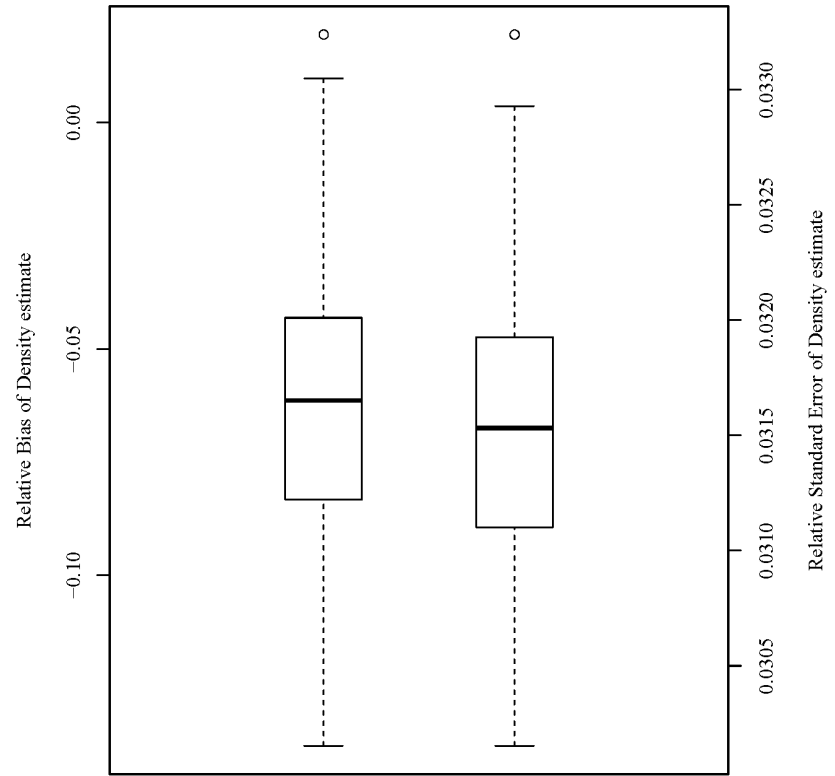


Figure 1.77. Distribution of relative bias (left boxplot) and relative standard error (right boxplot) in the density estimate for a simulated scenario of a spatial capture-recapture model ($D = 50$ bears/ 100 km^2 , $\sigma = 2 \text{ km}$, $g_0 = 0.2$, and sampling occurred over 7 weeks).

Scenario: $D=100$ (bears 100 km^{-2}), $\sigma=2 \text{ km}$, $g_0=0.2$, $k=7$ weeks

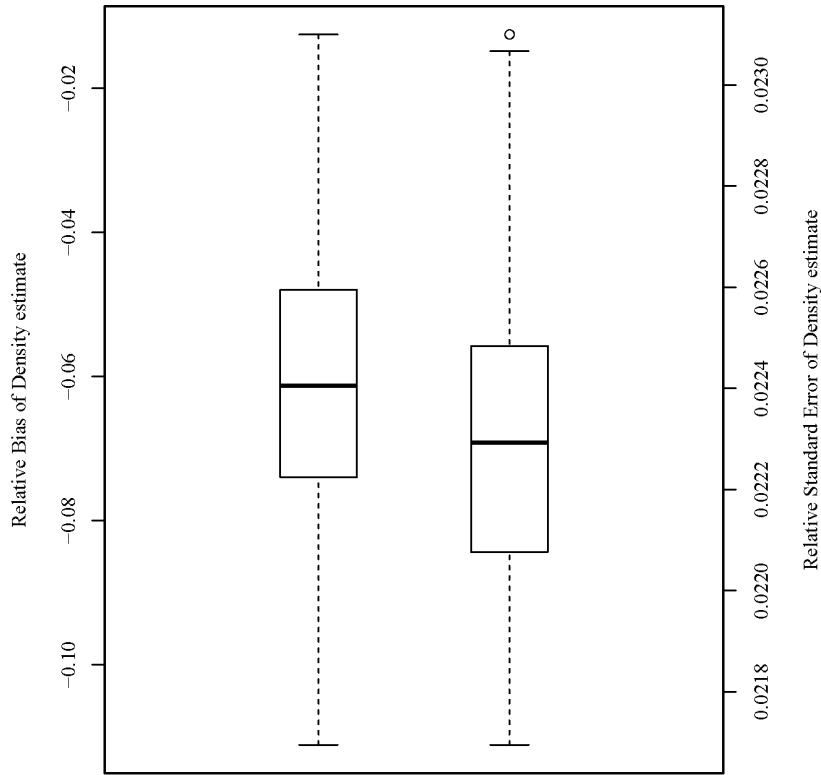


Figure 1.78. Distribution of relative bias (left boxplot) and relative standard error (right boxplot) in the density estimate for a simulated scenario of a spatial capture-recapture model ($D = 100$ bears/ 100 km^2 , $\sigma = 2 \text{ km}$, $g_0 = 0.2$, and sampling occurred over 7 weeks).

Scenario: $D=10$ (bears 100 km^{-2}), $\sigma=5 \text{ km}$, $g_0=0.2$, $k=7$ weeks

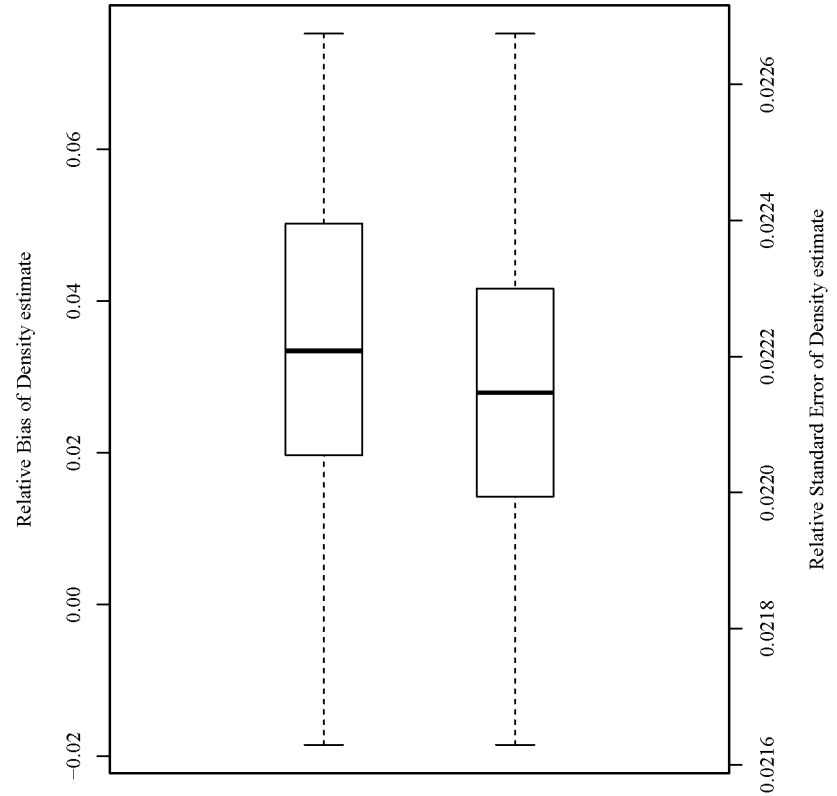


Figure 1.79. Distribution of relative bias (left boxplot) and relative standard error (right boxplot) in the density estimate for a simulated scenario of a spatial capture-recapture model ($D = 10$ bears/ 100 km^2 , $\sigma = 5 \text{ km}$, $g_0 = 0.2$, and sampling occurred over 7 weeks).

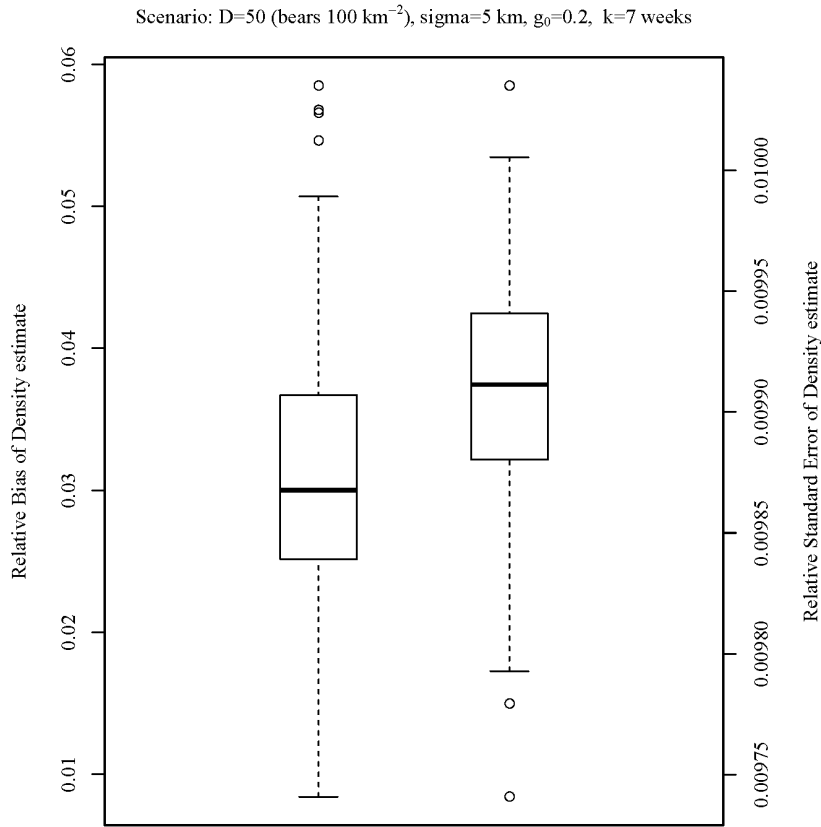


Figure 1.80. Distribution of relative bias (left boxplot) and relative standard error (right boxplot) in the density estimate for a simulated scenario of a spatial capture-recapture model ($D = 50$ bears/ 100 km^2 , $\sigma = 5 \text{ km}$, $g_0 = 0.2$, and sampling occurred over 7 weeks).

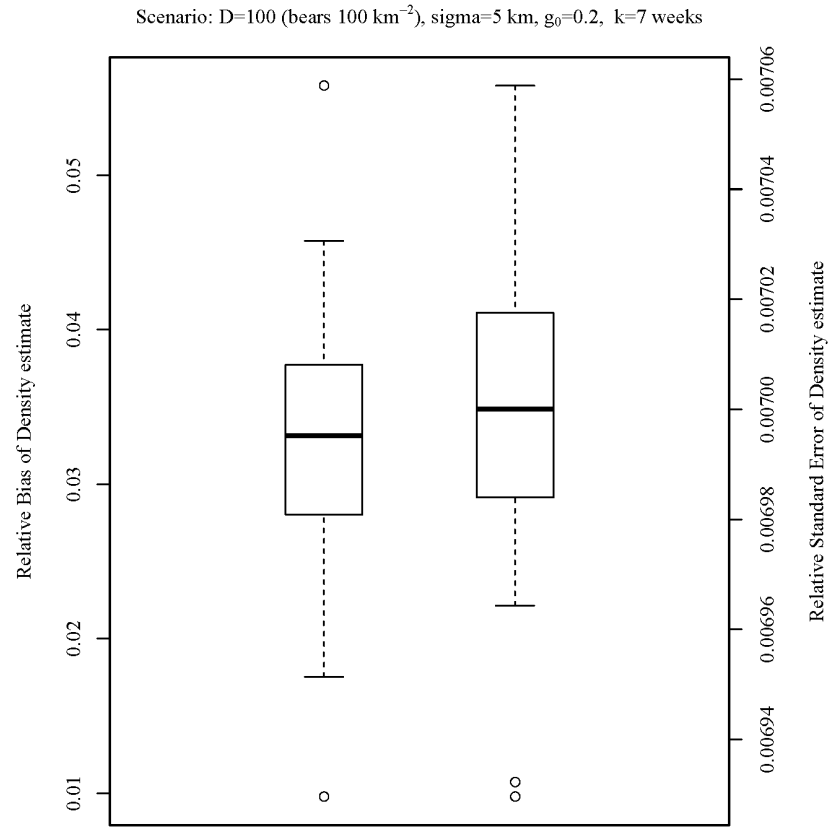


Figure 1.81. Distribution of relative bias (left boxplot) and relative standard error (right boxplot) in the density estimate for a simulated scenario of a spatial capture-recapture model ($D = 100$ bears/ 100 km^2 , $\sigma = 5 \text{ km}$, $g_0 = 0.2$, and sampling occurred over 7 weeks).

Scenario: $D=10$ (bears 100 km^{-2}), $\sigma=12 \text{ km}$, $g_0=0.2$, $k=7$ weeks

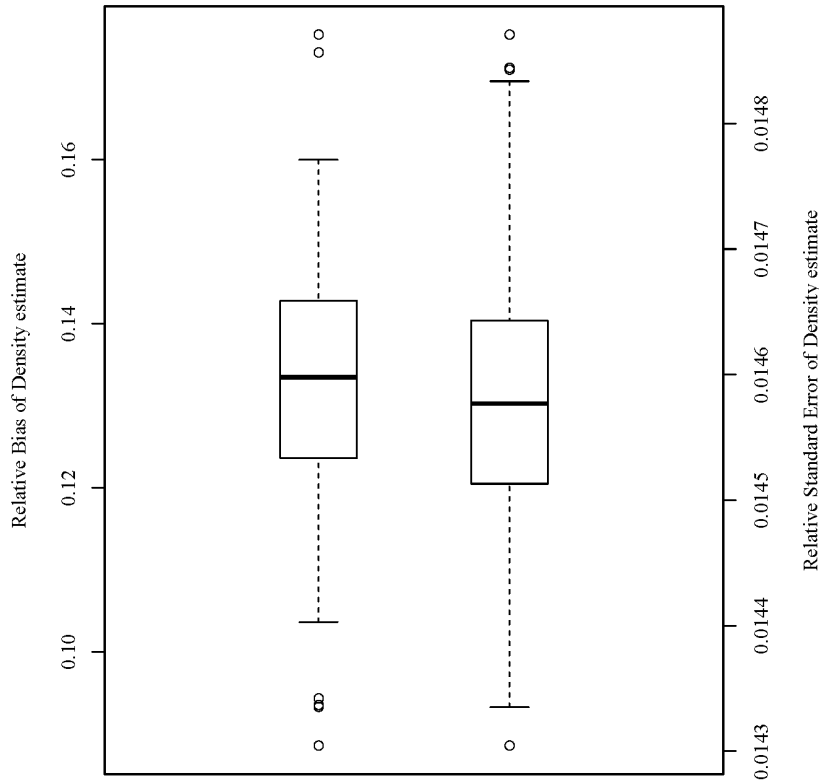


Figure 1.82. Distribution of relative bias (left boxplot) and relative standard error (right boxplot) in the density estimate for a simulated scenario of a spatial capture-recapture model ($D = 10$ bears/ 100 km^2 , $\sigma = 12 \text{ km}$, $g_0 = 0.2$, and sampling occurred over 7 weeks).

Scenario: $D=50$ (bears 100 km^{-2}), $\sigma=12 \text{ km}$, $g_0=0.2$, $k=7$ weeks

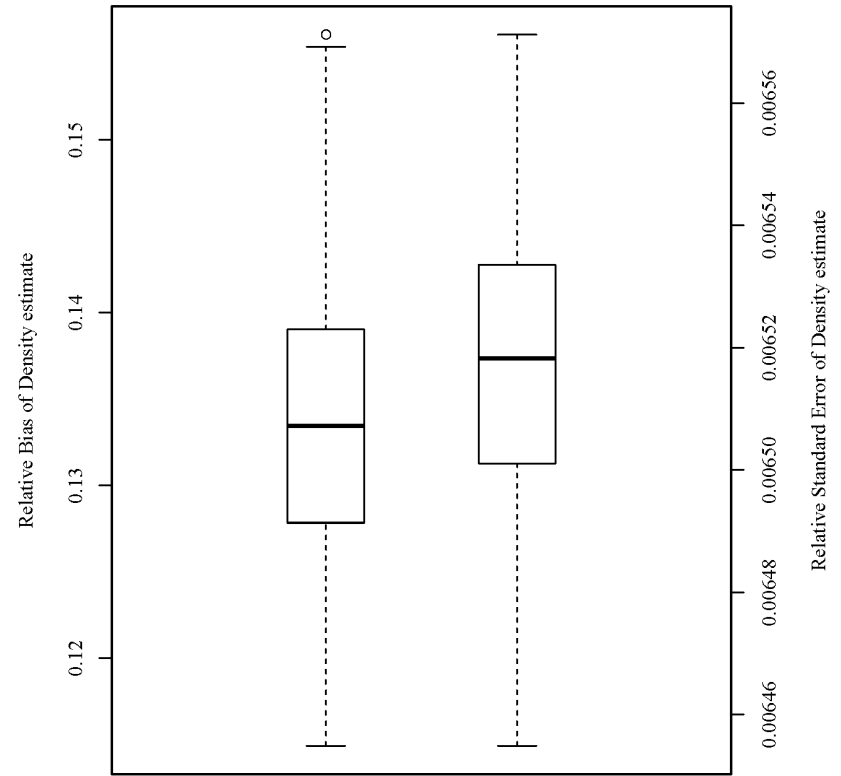


Figure 1.83. Distribution of relative bias (left boxplot) and relative standard error (right boxplot) in the density estimate for a simulated scenario of a spatial capture-recapture model ($D = 50$ bears/ 100 km^2 , $\sigma = 12 \text{ km}$, $g_0 = 0.2$, and sampling occurred over 7 weeks).

Scenario: $D=100$ (bears 100 km^{-2}), $\sigma=12 \text{ km}$, $g_0=0.2$, $k=7$ weeks

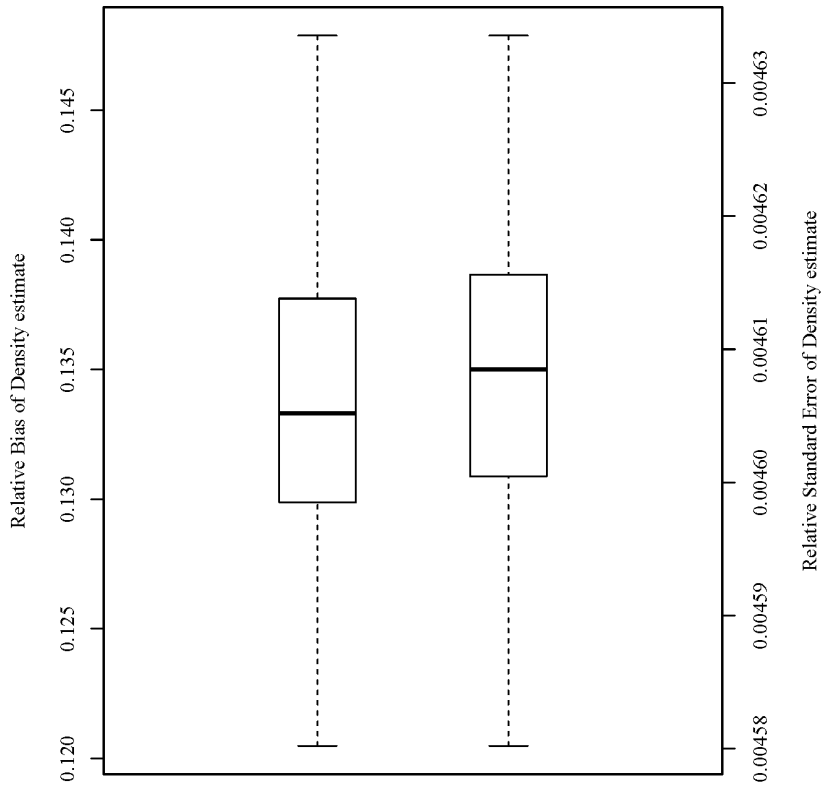


Figure 1.84. Distribution of relative bias (left boxplot) and relative standard error (right boxplot) in the density estimate for a simulated scenario of a spatial capture-recapture model ($D = 100$ bears/ 100 km^2 , $\sigma = 12 \text{ km}$, $g_0 = 0.2$, and sampling occurred over 7 weeks).

LITERATURE CITED

LITERATURE CITED

- Borchers, D. L., and M. G. Efford. 2008. Spatially explicit maximum likelihood methods for capture-recapture studies. *Biometrics* 64:377–385.
- Boulanger, J., B. N. McLellan, J. G. Woods, M. F. Proctor, and C. Strobeck. 2004. Sampling design and bias in DNA-based capture-mark-recapture population and density estimates of grizzly bears. *The Journal of Wildlife Management* 68: 457–469.
- Brown, J. H. 1984. On the relationship between abundance and distribution of species. *The American Naturalist* 124:255–279.
- Chandler, R. B., and J. D. Clark. 2014. Spatially explicit integrated population models. *Methods in Ecology and Evolution* 5:1351–1360.
- Dreher, B. P., S. R. Winterstein, K.T. Scribner, P. M. Lukacs, D. R. Etter, G. J. M. Rosa, V. A. Lopez, S. Libants, and K. B. Filcek. 2007. Noninvasive estimation of black bear abundance incorporating genotyping errors and harvested bear. *The Journal of Wildlife Management* 71:2684–2693.
- Efford, M. G., and R. M. Fewster. 2013. Estimating population size by spatially explicit capture–recapture. *Oikos* 122:918–928.
- Gardner, B., J. A. Royle, and M. T. Wegan. 2009. Hierarchical models for estimating density from DNA mark–recapture studies. *Ecology* 90:1106–1115.
- Howe, E. J., M. E. Obbard, and C. J. Kyle. 2013. Combining data from 43 standardized surveys to estimate densities of female American black bears by spatially explicit capture–recapture. *Population Ecology* 55:595–607.
- Kendall, W. L. 1999. Robustness of closed capture-recapture methods to violations of the closure assumption. *Ecology* 80:2517–25125.
- Pollock, K. H., J. D. Nichols, C. Brownie, and J. E. Hines. 1990. Statistical inference for capture–recapture experiments. *Wildlife Monographs* 107:3–97.
- Reppucci, J., B. Gardner, and M. Lucherini. 2011. Estimating detection and density of the Andean cat in the high Andes. *Journal of Mammalogy* 92:140–147.
- Royle J. A., and B. Gardner. 2011. Hierarchical spatial capture–recapture models for estimating density from trapping arrays. Pages 163 – 190 *in* A. F. O’Connell, J. D. Nichols, K. U. Karanth, editors. *Camera traps in animal ecology: methods and analyses*. Springer-Verlag, New York, New York, USA.

- Royle J. A., R. B. Chandler, R. Sollmann, and B. Gardner. 2014. Spatial capture-recapture. Academic Press, Waltham, Massachusetts, USA.
- Smith, J. B. 2018. Context matters for black bears: evaluating spatially explicit density estimates and trade-offs in resource selection. Thesis, Michigan State University, East Lansing, Michigan, USA.
- Sollmann, R., M. M. Furtado, B. Gardner, H. Hofer, A. T. A. Jácomo, N. M. Tôrres, and L. Silveira. 2011. Improving density estimates for elusive carnivores: accounting for sex-specific detection and movements using spatial capture–recapture models for jaguars in central Brazil. *Biological Conservation* 144:1017–1024.
- Sollmann, R., B. Gardner, and J. L. Belant. 2012. How does spatial study design influence density estimates from spatial capture-recapture models? *PloS ONE* 7(4):e34575.
- Sollmann, R., B. Gardner, A. W. Parsons, J. J. Stocking, B. T. McClintock, T. R. Simons, K. H. Pollock, and A. F. O’Connell. 2013. A spatial mark—resight model augmented with telemetry data. *Ecology* 94:553–559.
- Sun, C. C., A. K. Fuller, and J. A. Royle. 2014. Trap configuration and spacing influences parameter estimates in spatial capture-recapture models. *PLoS ONE* 9(2):e88025.
- Wilton, C. M., E. E. Puckett, J. Beringer, B. Gardner, L. S. Eggert, and J. L. Belant. 2014. Trap array configuration influences estimates and precision of black bear density and abundance. *PLoS ONE* 9(10):e111257.

CHAPTER 2: CONTEXT MATTERS: VARIATION IN BLACK BEAR USE OF AGRICULTURAL LANDSCAPES

Introduction

Resource selection is a process in which individuals move across landscapes in pursuit of resources (Manly et al. 2002). This movement affects genetic diversity, spread of diseases, and population viability (Tilman 1994, Hess 1996). Quantifying patterns of resource selection allows inference on ecological processes and helps predict distribution of individuals on the landscape (Boyce and Macdonald 1999). Behaviorally, resource selection often results from trade-off decisions; individuals must weigh the perceived costs and benefits of using a resource relative to what is available (Myerud and Ims 1998).

Those trade-off decisions are made in, and driven by, a specific ecological context, which varies as individuals move across the landscape. Ecological context can refer to a suite of environmental covariates, including landscape composition and configuration, anthropogenic features, climate, or population size. Such covariates often drive how species respond to and use resources (e.g., Morris 1989, Apps et al. 2001, Sawyer et al. 2006, Chetkiewicz and Boyce 2009). Many studies, though not all (for example, Hebblewhite and Merrill 2008, Clark et al. 2015), describe selection of a resource as constant across space (Carter et al. 2010, Latham et al. 2011, Tri et al. 2016). Such approaches are important for understanding general patterns of resource selection, but they fail to account for changes in selection behavior as a function of variation in the covariates over space and time. Myerud and Ims (1998) first proposed that selection is not constant but is instead a function of availability of a given resource (i.e., a functional response). Recent research has provided more flexible analytical methodologies for modeling functional responses of selection across diverse ecological contexts (Gillies et al. 2006, Hebblewhite and Merrill 2008, Godvik et al. 2009, Matthiopoulos et al. 2011).

Evaluating variation in patterns of resources selection across different contexts can provide more robust predictions of resource selection and population distributions (Godvik et al. 2009). These predictions can be used to minimize human-wildlife conflicts and identify critical habitat for conservation (Carter et al. 2010). Furthermore, understanding how selection varies with local context will allow us to better predict how species will respond to new or changing landscapes. This knowledge is especially important as habitat fragmentation, urbanization, and climate change continue to alter the landscape and shift distributions of wildlife populations (Pearson and Dawson 2003, Austin and Niel 2011).

Resource selection patterns of black bears (*Ursus americanus*) can be complex (Hiller et al. 2015), in part because this widespread generalist can thrive in a range of ecological contexts, including human-dominated landscapes (Powell et al. 1997, Lyons 2005, Baruch-Mordo et al. 2008). Decades of research have established a few consistent patterns of black bear resource selection behavior, such as preferring forested to open habitats (Wooding and Hardisky 1992, Lyons et al. 2003, Sadeghpour and Ginnett 2011, Tri et al. 2016). However, patterns of selection of agriculture are more variable (Jones and Pelton 2003, Kindall and van Manen 2007, Ditmer 2014).

Agricultural crops offer a valuable source of calories for bears (Ditmer et al. 2016), but the benefit of consuming them is weighed against multiple risks. Agricultural fields lack escape cover (e.g., trees (Fecske et al. 2002)), are associated with humans, and as a concentrated food source, may increase despotic behavior among conspecifics (Ben-David et al. 2004). These characteristics create a complex trade-off situation for black bear use of agriculture and are particularly likely to be influenced by variation in context (Hebblewhite and Merrill 2008).

In Michigan, we know little about black bear resource selection in regions where agriculture is the dominant land use. Black bear populations typically are distributed in the Upper Peninsula and the northern Lower Peninsula (NLP), which are dominated by forested landscapes. However, over the past 5 years, reports of bears have increased in the southern Lower Peninsula, where the landscape is dominated by agriculture and increased urbanization. Complaints from the public and anecdotal knowledge suggest bears occasionally use agricultural fields in the Lower Peninsula. However, the only habitat selection study of black bears in the Lower Peninsula of Michigan found that bears avoided agricultural lands (Carter et al. 2010). That research was based on VHF telemetry from bears that occupied the forested region of the NLP and had limited ability to assess how bears respond to agriculture in other landscape contexts. The uncertainty surrounding use of agriculture by bears in the Lower Peninsula could be explained by uncommon incidences of use, shifts in patterns of resource selection, or context-dependent use of agriculture, which has yet to be quantified. Given the paucity of information and the potential for bear-human conflicts in the southern Lower Peninsula, we investigated resource selection by black bears in the Lower Peninsula of Michigan. Our specific objectives were to 1) identify predictive variables of black bear use of agricultural landscapes and 2) quantify how use of agriculture varies as a function of context.

Methods

Study area

Our study area was defined by a 12 km buffer around all used and available points. This boundary encompassed 7,030 km² across seven counties in the west-central Lower Peninsula of Michigan (Fig 2.1). This region of the NLP contains both relatively high bear abundance and presence of agriculture. The region is a northern Laurentian mixed forest (Bailey 1995),

characterized by a mix of dry sand prairies, northern hardwood and oak forests, pine barrens, and multiple large rivers (Albert 1995). Elevation ranged from 175 to 526 m and average annual precipitation was 86 cm (data collected between 1971 – 2000, Natural Resources Conservation Service 2008). Land cover composition included 51% forest, 19% agriculture, 13% wetlands, and 7% developed (NLCD 2011). Habitat patch size distribution was strongly right-skewed ($\bar{x} = 0.12 \text{ km}^2$, $sd = 7.12 \text{ km}^2$, $median = 0.012 \text{ km}^2$); 66% of patches in the study area were 0.01 – 0.02 km^2 . Black bears are hunted in the Lower Peninsula from mid-September until late October. In our study area, approximately 300 bears were harvested from 2011 – 2015.

Black bear location data

Between 2011 and 2015, the Michigan Department of Natural Resources captured 15 black bears (7 females, 8 males) in the study area and each bear was equipped with 1 of 2 types of GPS store-on-board collars (LoTek, New Market, Ontario, Canada; Sirtrack, Havelock North, Hawkes Bay, New Zealand). Collar data were retrieved during winter den checks or after collars dropped off an individual. The 2 types of collars were programmed to calculate and store location information at different intervals; however, a majority of fix schedules were every 30 – 40 minutes. Our analysis only used data collected on a 30 – 40 min fix schedule. To balance data reduction and location accuracy we discarded GPS fixes with a dilution of precision greater than 12 (D'eon and Delparte 2005), positional outliers, and any locations recorded post-mortem or after collar drop-off. We restricted our analysis to locations collected between 01 April and 02 November, an active (non-hibernating) period for bears in Lower Michigan (Carter et al. 2010). Finally, 2 male bears made abnormally long-distance movements; these distances were much longer than the typical home range radius for males in this population. These outliers likely represent distinct movement states, with specific motivations and behavioral states (Nathan et al.

2008). To ensure our analysis represented a single movement state, we removed these 2 individuals. After this screening, our dataset consisted of locations for 12 individuals (6 females, 6 males) over the course of 21 bear-years of data (12 female, 9 male).

Availability

One of the perennial challenges of studying resource selection is appropriately defining availability (Johnson 1980, Porter and Church 1987, McClean et al. 1998, Buskirk and Millspaugh 2006). We used a step-selection analysis (Fortin et al. 2005) to define availability in our analysis. Step-selection analyses compare characteristics of used and available steps. A step is defined as the straight-line segment connecting consecutive locations of an individual. The angle between three consecutive fix locations is called the turning angle, which reflects the direction of the animal's movement relative to the previous step (Coulon et al. 2008). In step-selection analyses, the locations and directions defining available steps are randomly drawn from the distribution of observed steps and turning angles. Thus, availability is informed and constrained by the movement patterns of the population of interest. For each observed step in our dataset, five step lengths and turning angles were randomly selected from the empirical distributions to define the five available steps. To avoid issues of circularity, we followed Fortin et al. (2005), in which the step length and turning angle of the available steps for an observed individual are sampled from the distribution of all other individuals (Coulon et al. 2008).

Covariates

We considered 7 covariates in our analysis; all 7 covariates have previously been identified as influential in resource selection patterns of black bears (Kindall and Van Manen 2007, Lewis et al. 2011, Hiller et al. 2015). These covariates included a categorical land cover variable, density of edge between forest and agriculture (m/ha), percent agriculture in the surrounding landscape

(defined below), distance to high-intensity and low-intensity developed covers (km), distance to water (km), and black bear density (bears/100 km²). We tested for multicollinearity in covariates using Spearman's rank correlation and tolerated correlation of < 0.5 (Zuur et al. 2009). Percent of agriculture was highly correlated with forest: agriculture edge density (0.99 and 0.67, respectively), so we removed the latter from our considered covariates.

We obtained land cover data from the National Land Cover Database (NLCD) 2011 (Homer et al. 2015), which provides 30 m data resolution. We reclassified land cover into 5 categories relevant to black bears and our objectives: forest (deciduous, evergreen, and mixed), agriculture (cultivated crops, pasture and hay), developed (open developed space, low, medium and high intensity), shrubs and grasslands, and wetlands (emergent and wooded). We used forest as the reference category in our models. Percent agriculture in the surrounding landscape was derived from the land cover using FRAGSTATS (version 4, <http://www.umass.edu/landeco/research/fragstats/fragstats.html>, accessed 01 January 2017). We defined the surrounding landscape as the area within the mean home range radius for females and males. These radii were based on 95% kernel density estimation, and were estimated as 5 and 12 km, for female and male bears respectively. Thus, percent agriculture was calculated at a 30 m resolution using a 5 and 12 km moving window.

We mapped water features using the Michigan Geographic Framework's hydrographic line database, which included all lakes, ponds, rivers, creeks, and drain features on the landscape (Center for Shared Solutions and Technology Partnerships 2014). Distance to developed covers and to water features were estimated using Euclidean distance at a 30 m resolution in ArcMap 10.3.1 (Environmental Systems Research Institute, Inc., Redlands, CA, USA). Distance to developed covers was subset into distance to low-intensity development or distance to high-

intensity development. Low-intensity developed covers were defined as land cover that consisted of < 50% impervious surfaces, whereas high-intensity developments consisted of \geq 50% impervious surfaces.

Black bear density estimates were derived from a spatially explicit capture-recapture model based on hair snare and harvest data of black bears in the northern Lower Peninsula (David Williams, unpublished data). This model produced a 16 km² (4 km x 4 km) grid of bear densities in the northern Lower Peninsula.

Autocorrelation

We evaluated model residuals for evidence of spatiotemporal autocorrelation. When present, autocorrelation violates the assumption of independence (Johnson et al. 2008) and creates bias in the standard errors of the beta estimates (Nielson et al. 2002). We generated space and time spline correlograms, as outlined by Zuur et al. (2009). Model residuals indicated two patterns of spatial autocorrelation: positive correlation from 0 – 30 m, and minor negative (< -0.1) correlation from 30 – 100 m. However, the positive correlation reflected the 30 m resolution of our land cover data. The observed negative correlation likely reflected the patch structure and classification in our study area; most (75%) patches were < 100 m radius, meaning patch type changed every 30 – 100 m. Thus, we evaluated spatiotemporal autocorrelation in model residuals but did not identify any patterns relevant to this analysis (Appendix II).

Modeling framework

We estimated a resource selection function (RSF) via a use-availability design in a binomial logistic regression for male and female bears separately. We pooled individuals within each sex and evaluated selection within home ranges (third-order selection (Johnson et al. 1980)). We considered two random intercepts for the random effect structure of our models. One intercept

was on individual. The second intercept accounted for the mismatch of scale in our covariates; bear density was quantified at a coarser scale than other covariates. Therefore, we numbered each cell within the grid of bear density and placed a random intercept on the cell number. Likelihood ratio tests supported using a generalized linear modeling (GLM) framework for female bears (no random effects) and a generalized linear mixed effects modeling (GLMM) framework for male bears (Boyce et al. 2002, Manly et al. 2002). For the male RSF, likelihood ratio tests supported a random intercept on the density grid cell. Thus, relative probability of use was estimated by the function $w(x) = \exp(\beta_1x_1 + \beta_2x_2 + \dots + \beta_nx_n)$.

We estimated β coefficients and random effects from the logistic regression equation

$$P_{use} = \frac{\exp(B_0 + B_1x_1 + \dots + B_nx_n + \gamma_j)}{1 + \exp(B_0 + B_1x_1 + \dots + B_nx_n + \gamma_j)}$$

where probability of use is a function of the fixed effect ($\hat{\beta}_1x_1 + \hat{\beta}_2x_2 + \dots + \hat{\beta}_nx_n$) coefficient estimates and, in the male model, γ_j , the random intercept on density grid cell. Models were fit using the lme4 package (version 1.1, <https://cran.r-project.org/package=lme4>, accessed 8 August 2016), in program R (version 3.4.1, www.r-project.org, accessed 8 August 2015). The output of each model consisted of the log-odds ratio (\exp^β) of selection. The odds ratio of land cover variables was relative to the reference land cover category of forest. An odds ratio > 1 indicated selection of that resource, while an odds ratio < 1 indicated avoidance. To model the odds of use, relative to availability, across the range of a covariate (i.e., functional responses), we included four interaction terms (Godvik et al. 2009, Beest et al. 2016). Plotting statistically significant interaction terms allowed us to evaluate variation in selection (e.g., odds of use varied between avoidance and selection over the range of covariate values). We modeled interactions between land cover and one of four covariates: distance to low-intensity development, distance to high-intensity development, bear density, and percent agriculture within the surrounding landscape

(Table 2.1). Thus, the global RSF for females included land cover (categorical variable with five levels), step length, which has been shown to reduce bias in coefficient estimates (Forester et al. 2009), distance to water, bear density, percent agriculture, distance to low-intensity development, distance to high-intensity development, and the interactions. The global model for males consisted of the same fixed-effects structure and a random intercept on density grid number. We used Aikake's Information Criterion model selection on 27 candidate models to identify the top-supported model for each sex (Burnham and Anderson 2004). We considered models within $\leq 2 \Delta AIC$ to be competing. We present the top-supported models for explaining black bear use of agriculture.

Results

GPS collars provided 63,385 use locations for analysis (46,408 from females, 16,979 from males) including 13 years of female location data and 12 years of male location data. Number of locations per female bear-year ranged from 223 to 8,282 ($\bar{x} = 3,867$; $sd = 2,375$). The number of locations across male bear-years ranged from 130 to 5,620 points ($\bar{x} = 1,886$; $sd = 1,774$). Female collars recorded data for 6 months on average, while male collard recorded locations for 5 months on average.

We identified 2 competing models ($\leq 2 \Delta AIC$) for both female and male bears; the two top models for females accounted for 88% of the weight of evidence among the model set, the two top models for male bears accounted for 78% of the weight of evidence (Table 2.2). The top model for females included distance to water and three interaction terms: interactions between land cover and the percent of agriculture within 5 km, land cover and the distance to highly-developed land covers, and land cover and bear density (Table 2.2). The top model for male black bears included distance to water, and interactions between land cover and the percent of

agriculture within 12 km, land cover and the distance to low-intensity developed land covers, and land cover and bear density. The competing model for both sexes did not include distance to water but was otherwise identical to the respective top model. Because distance to water was not predicted to affect bear use of agriculture, and because coefficient estimates and standard errors for all common covariates were virtually identical, we did not average these competing models. All interaction terms between agriculture land cover and covariates in the top model for both sexes were significant ($p < 0.05$) (Tables 2.3 and 2.4).

We observed functional responses in use of agricultural habitat by bears. Odds of using this land cover varied across values of bear density and multiple landscape characteristics. Both male and female bears displayed a density-dependent use of agriculture (Fig 2.2). However, the direction of the functional response was sex-specific. Females avoided agriculture when bear densities were < 3.2 bears/100 km². In locations with relatively higher densities, females shifted from avoiding agricultural lands to selecting for these land covers (Table 2.3 and Fig 2.2; $\beta = 0.359$, SE = 0.058, OR = 1.43, $p < 0.001$). Comparatively, male black bears displayed a negative functional relationship (Table 2.4 and Fig 2.2; $\beta = -0.632$, SE = 0.108, OR = 0.531, $p < 0.001$); males selected for agriculture in areas with relatively low bear densities (< 3.5 bears/100 km²). In areas of relatively high bear density, males shifted from selecting for to avoiding agricultural land covers.

Bears did not use agriculture in proportion to its representation on the landscape. Both females and males were less likely to use agriculture as its representation in the surrounding landscape increased (females: Table 2.3; $\beta = -0.290$, SE = 0.066, OR = 0.75, $p < 0.001$; males: Table 2.4; $\beta = -0.250$, SE = 0.056, OR = 0.779, $p < 0.001$). Although more agriculture in the

surrounding landscape had an overall negative impact on probability of use, black bears did select for agriculture when it made up < 10% of the area within 5 or 12 km (Fig 2.3).

Both sexes were more likely to use agriculture as the distance between the used location and the nearest anthropogenic development increased (Fig 2.4). Both sexes selected for agriculture when they were > 1 km from developed land covers. However, male use of agriculture was predicted by distance to the nearest low-intensity anthropogenic development (Table 2.4; $\beta = 0.369$, SE = 0.051, OR = 1.45, $p < 0.001$), whereas distance to high-intensity development predicted use of agriculture by females (Table 2.3; $\beta = 0.241$, SE = 0.057, OR = 1.27, $p = 0.004$).

Discussion

The benefits to black bears of using agricultural fields are conceivably balanced against multiple risks, including threats from humans (e.g., nuisance wildlife harvest (Hristienko and McDonald 2007)), increased stress from traversing non-forested areas (Ditmer et al. 2015), and encountering conspecifics. Our findings for black bears in the northern Lower Peninsula of Michigan reveal variation in how bears respond to agriculture, and that this response is a function of multiple covariates. In our study area, the probability of black bears using agriculture is a function of bear density within a 16 km² area, the amount of agriculture in the surrounding landscape, and the distance to anthropogenic developments.

Male and female black bears exhibited different density-dependent responses to use of agriculture (Fig 2.2). The sex-specific responses suggest males and females in this study perceive the suitability and the trade-off of using agricultural habitat differently. Female black bears with cubs ($n = 11$ bear-years) face heightened threats from conspecifics (Barber and Lindzey 1983, Garrison et al. 2007), and generally are believed to be more risk averse (Martin et al. 2010,

Ditmer et al. 2015). Infanticide and despotic behavior increase in populations with higher densities and in areas of concentrated food resources (Beckmann and Berger 2003, Ben-David et al. 2004). Thus, when densities are relatively low, intra-specific competition and risk of cub mortality are lower, thereby allowing female bears to select the most suitable habitats.

Absent the pressures of competition or risk of infanticide, female bears avoided agricultural fields, suggesting they perceived agriculture as less suitable than other habitats in our study. This is supported by studies in Minnesota; females with cubs disproportionately avoided foraging in crop fields, and when they crossed these fields, their heart rates indicated acute stress (Ditmer et al. 2015). However, as bear density increases, competition and risk from conspecifics increase, which in turn influences the suitability of the habitat (Fretwell 1972). Our findings suggest relatively higher density areas create an overall context in which suitability of agricultural patches is higher for female bears in this study, which explains the observed shift from avoidance to selection of this resource as density increased.

Areas with relatively lower bear densities create a context in which male bears are less likely to encounter a larger, or more aggressive, conspecific. In this context, it is conceivable the trade-off for male bears of consuming crops, and benefiting from the high caloric intake, outweighed the risk of using exposed habitat. However, in areas of relatively higher bear density, competition increases, and we found the odds of male bears using agriculture declined dramatically. Such patterns of switching habitats are predicted by ideal-free distribution and density-dependent selection theories (Fretwell and Lucas 1970, Rosenzweig 1981), and have been observed in other wildlife species (Beest et al. 2016).

The odds of black bears using agriculture also depended on the amount of agriculture in the surrounding area, and distance to anthropogenic developments. Variation in each of these

characteristics reflects variation in the cost to a black bear of using an agricultural field. Therefore, the covariate values in which avoidance shifts to selection may reflect the landscape composition and configuration that optimizes the cost-benefit of bears using agriculture in this region. For instance, we found males and females increasingly avoided agriculture when it represented $> 10\%$ of the surrounding landscape. Yet bears selected for agriculture when it constituted $< 10\%$ of the cover in the defined radius. In our study area, the remaining landscape is likely composed of forest or wetland cover types. This landscape composition likely not only attracts more bears (McFadden-Hiller et al. 2016), which in itself may increase the chances of a bear using an agriculture patch, but may also buffer the risk of venturing into an exposed habitat patch (Jones and Pelton 2003, Kindall and Van Manen 2007).

Finally, male bears in this study shifted from avoiding to selecting for agriculture as distance to high-intensity human development increased. Females exhibited a similar functional relationship but with distance to low-intensity, rather than high-intensity, human development. High-intensity developments refer to locations with high concentrations of impervious surfaces while low-intensity developments included roads and sparser human structures. Proximity to human developments can stress bears (Støen et al. 2015) and hunted populations often avoid roads to reduce vulnerability to harvest (Brody and Pelton 1989, Fecske et al. 2002, Prokopenko et al. 2017). Although we did not measure stress response, it is possible bears in our study area were not as likely to venture into agricultural covers when travelling relatively close to developed areas because doing so would incur additional risk and stress. It is less obvious why male and female bears respond to different types of development. One possible explanation is due to the spatial structure of our data; male and female bears may be spatially segregated such that distance between males and high-intensity development does not vary enough to influence

probability of use. Mattson (1990) found female bears often foraged closer to human-dominated landscapes because adult males defended more secure foraging areas.

A primary focus of this analysis was quantifying functional responses in selection of agricultural cover types. Hebblewhite and Merrill (2008) noted functional responses are especially common in selection behavior when trade-offs are present. Crops within agricultural fields offer valuable, concentrated, calories (a “high reward”) but consuming them requires moving away from the protection of forested covers, and possibly competing with conspecifics (“high risk”). Thus, the trade-off of using agriculture changes and drives the observed functional responses. Our findings emphasize the importance of quantifying variation in probability of using a resource as a function of predictive environmental variables.

Management implications

Black bear use of agriculture depends on multiple landscape characteristics. Importantly, both male and female black bears demonstrated variation in both selection and use across the range of predictive covariates. In this study, male bears are more likely to use agriculture in areas > 1 km away from low-intensity human developments and with densities < 3 bears/100 km². Females are more likely to use agriculture that is over 4 km away from high-intensity development, and in areas with densities > 3.5 bears/100 km². Both sexes select for agriculture when it is < 10 % of the surrounding landscape. We can use the explicit quantification of these patterns to generate a predictive probability map of bears using agriculture within a region. This knowledge can assist managers in preemptively identifying high-risk areas for conflict between bears and landowners.

APPENDICES

APPENDIX I:

Tables

Table 2.1. Variables used to develop a resource selection function for black bears from 2011 – 2015 in the Lower Peninsula of Michigan.

Variable	Description (units)	Type	Source	Estimation procedure
LC	Land cover	categorical	2011 National Land Cover Database	Reclassified into five categories: forest, shrub and grassland, agriculture, developed, and wetland
step	Euclidean distance between two consecutive locations (m)	continuous	empirical data	Quantified the distance between consecutive locations
PercentAg	Amount of agriculture within average home range (%)	continuous	2011 National Land Cover Database	FRAGSTAS software; moving window radius = 5 km for females and 12 km for males
Dist_HighDev	Distance to high-intensity developed cover (km)	continuous	2011 National Land Cover Database	Calculated minimum Euclidian distance to nearest cover with 50 - 100% impervious surfaces
Dist_LowDev	Distance to low-intensity developed cover (km)	continuous	2011 National Land Cover Database	Calculated minimum Euclidian distance to nearest cover with < 50 % impervious surfaces
Dist_water	Distance to water (km)	continuous	Michigan Geographic Framework; hydrographic line database	Calculated minimum Euclidian distance to nearest water feature
Density	Black bear density (bears/100 km ²)	continuous	David Williams, unpublished data	SECR model estimates informed by hair-snare mark-recapture data and harvest data

Table 2.1. (cont'd)

LC x percentAg	interaction
LC x dist_Highdev	interaction
LC x dist_Lowdev	interaction
LC x density	interaction

Table 2.2. Fixed-effects structure of candidate logistic regression models of female and male black bear resource selection from 2011 – 2015 in the Lower Peninsula, Michigan that are $\leq 10 \Delta$ AIC of the top model. Amount of support (Akaike’s information criterion (AIC and Δ AIC) and model weight (w_i) are shown for each model.

Sex	Model	AIC	Δ AIC	w_i
Female	step + dist_water + LC * PercentAg + LC *Dist_HighDev + LC*Density	250462	0	0.55
Female	step + LC * PercentAg + LC *Dist_HighDev + LC*Density	250463	1	0.33
Female	step +dist_water + LC * PercentAg + LC * Dist_LowDev + LC *Dist_HighDev + LC * Density	250466	4	0.07
Female	step +LC * PercentAg + LC * Dist_LowDev + LC *Dist_HighDev + LC * Density	250467	5	0.05
Male	step +dist_water + LC * PercentAg + LC * Dist_LowDev + LC *Density	91507	0	0.40
Male	step +LC * PercentAg + LC * Dist_LowDev + LC *Density	91507	0	0.38
Male	step +dist_water + LC * PercentAg + LC * Dist_LowDev + LC *Dist_HighDev + LC * Density	91510	3	0.11
Male	step +LC * PercentAg + LC * Dist_LowDev + LC *Dist_HighDev + LC * Density	91510	3	0.10

Note: for variable abbreviations see Table 2.1.

Table 2.3. Summary of the generalized linear logistic regression model for predicting use of agriculture in 12 bear-years of female black bear data from 2011 – 2015 in Lower Peninsula, Michigan.

Fixed Effects	β	Odds Ratio	SE	p-value
(Intercept)	-1.614	0.20	0.006	< 0.001
step	0.015	1.01	0.005	0.004
Distance to nearest water feature	0.009	1.01	0.005	0.092
Shrub and grassland	0.012	1.01	0.019	0.541
Agriculture	-0.043	0.96	0.044	0.323
Developed	-0.549	0.58	0.051	< 0.001
Wetlands	0.115	1.12	0.014	< 0.001
Percent Ag (5km)	-0.003	1.00	0.006	0.588
Distance to nearest high-intensity development	-0.018	0.98	0.006	0.004
Bear density	0.002	1.00	0.006	0.711
Shrubgrassland x Percent Ag (5km)	-0.018	0.98	0.020	0.385
Agriculture x Percent Ag (5km)	-0.290	0.75	0.066	< 0.001
Developed x Percent Ag (5km)	0.286	1.33	0.053	< 0.001
Wetland x Percent Ag (5km)	0.046	1.05	0.014	0.001
Shrubgrassland x distance to nearest high-intensity development	0.028	1.03	0.021	0.187
Agriculture x distance to nearest high-intensity development	0.241	1.27	0.057	< 0.001
Developed x distance to nearest high-intensity development	0.237	1.27	0.049	< 0.001
Wetland x distance to nearest high-intensity development	-0.005	0.99	0.016	0.746
Shrubgrassland x bear density	0.015	1.02	0.018	0.394
Agriculture x bear density	0.359	1.43	0.058	< 0.001
Developed x bear density	-0.070	0.93	0.064	0.275
Wetland x bear density	0.002	1.00	0.015	0.889

Table 2.4. Summary of the generalized linear mixed effect logistic regression model for predicting use of agriculture in 9 bear-years of male black bear data from 2011 – 2015 in Lower Peninsula, Michigan.

Fixed Effects	β	Odds Ratio	SE	p-value
(Intercept)	-1.688	0.18	0.014	< 0.001
step	0.005	1.01	0.009	0.544
Distance to nearest water feature	0.014	1.01	0.010	0.137
Shrub and grassland	0.067	1.07	0.030	0.025
Agriculture	-0.120	0.89	0.053	0.023
Developed	-117.400	0.00	871.700	0.893
Wetlands	0.250	1.28	0.022	< 0.001
Percent Ag (12km)	0.013	1.01	0.016	0.428
Distance to nearest low-intensity development	0.018	1.02	0.014	0.174
Bear density	-0.002	1.00	0.018	0.907
Shrubgrassland x Percent Ag (12km)	0.036	1.04	0.038	0.337
Agriculture x Percent Ag (12km)	-0.250	0.78	0.056	< 0.001
Developed x Percent Ag (12km)	-0.058	0.94	0.131	0.656
Wetland x Percent Ag (12km)	0.012	1.01	0.027	0.649
Shrubgrassland x distance to nearest low-intensity developed cover	0.062	1.06	0.029	0.032
Agriculture x distance to nearest low-intensity developed cover	0.369	1.45	0.051	< 0.001
Developed x distance to nearest low-intensity developed cover	-80.970	0.00	604.400	0.893
Wetland x distance to nearest low-intensity developed cover	-0.052	0.95	0.021	0.012
Shrubgrassland x bear density	0.058	1.06	0.039	0.133
Agriculture x bear density	-0.632	0.53	0.108	< 0.001
Developed x bear density	0.082	1.09	0.130	0.530
Wetland x bear density	0.018	1.02	0.026	0.469
Random Effect	Variance	SD		
Grid cell	0.00143	0.04		

APPENDIX II:

Figures

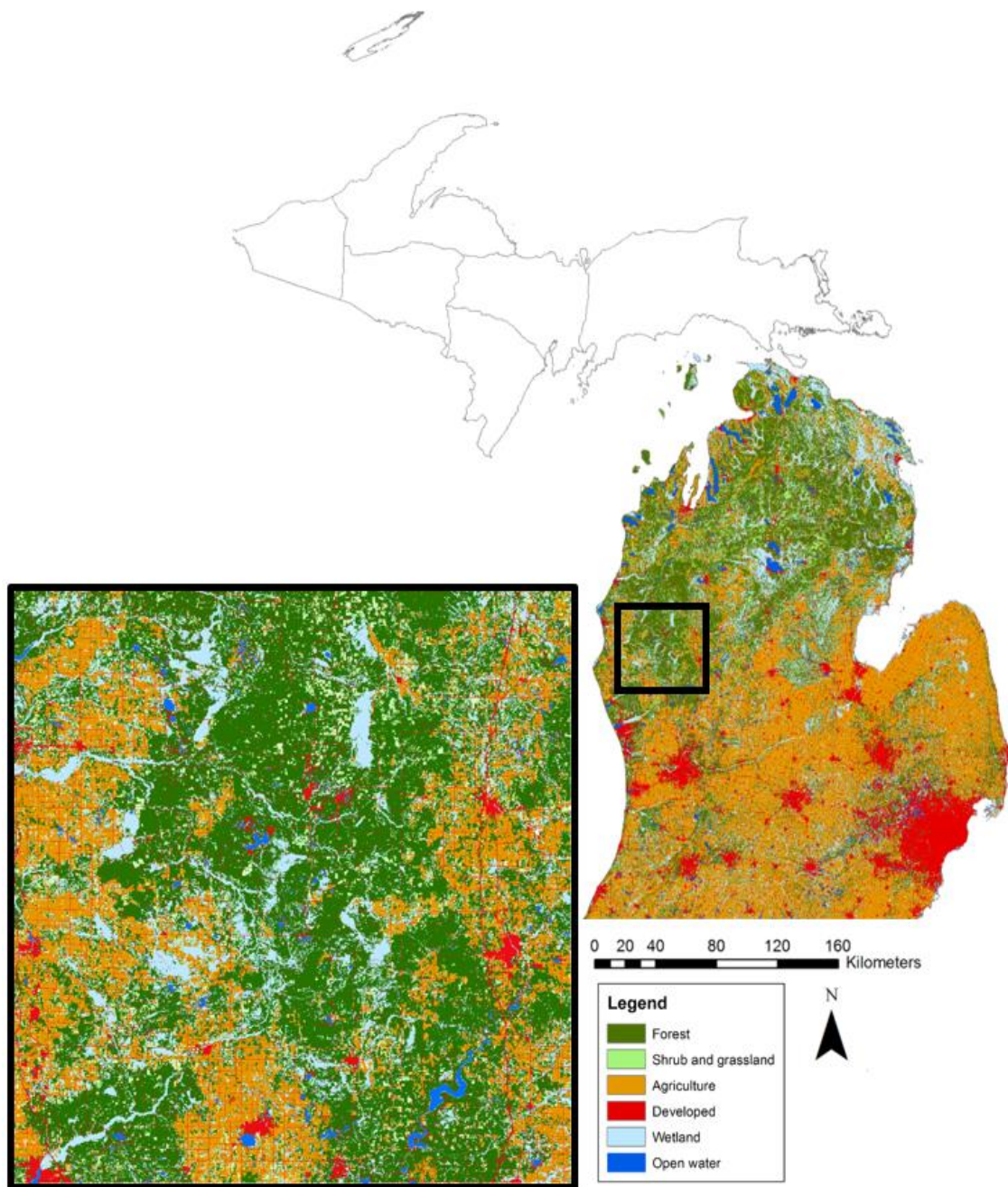


Figure 2.1. Map of the study area (inset) and land covers in which black bear GPS locations occurred in the northern Lower Peninsula of Michigan from 2011 – 2015. Land cover types were reclassified from the 2011 National Land Cover Database.

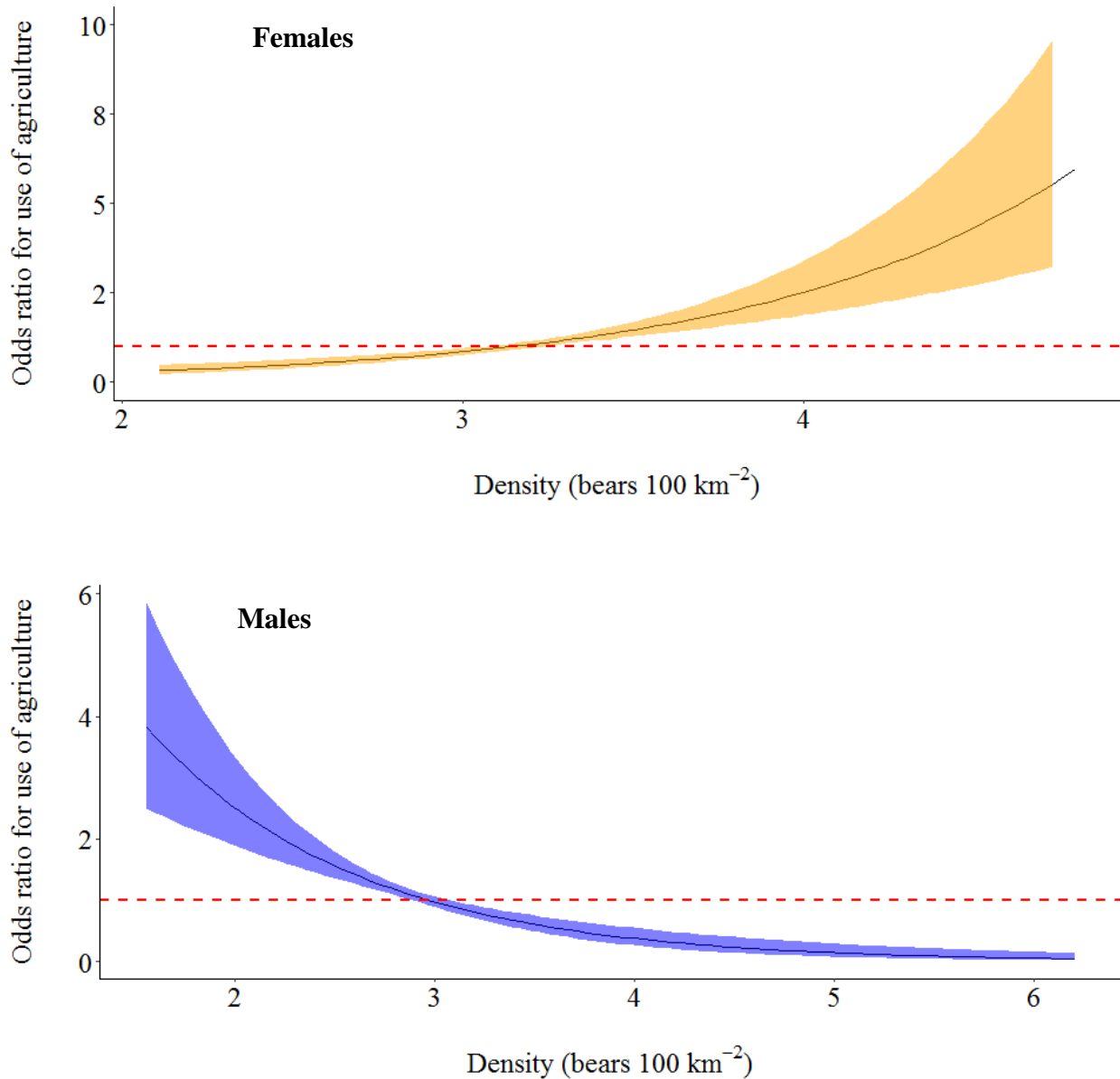


Figure 2.2. Functional response in use of agriculture for female (top) and male (bottom) black bears as bear density varied in the Lower Peninsula of Michigan from 2011 – 2015. The colored ribbons represent the 95% confidence interval around the estimated response (solid black line) for females (orange) and males (blue). The red dashed line indicates odds ratio=1, which is interpreted as having no effect on use.

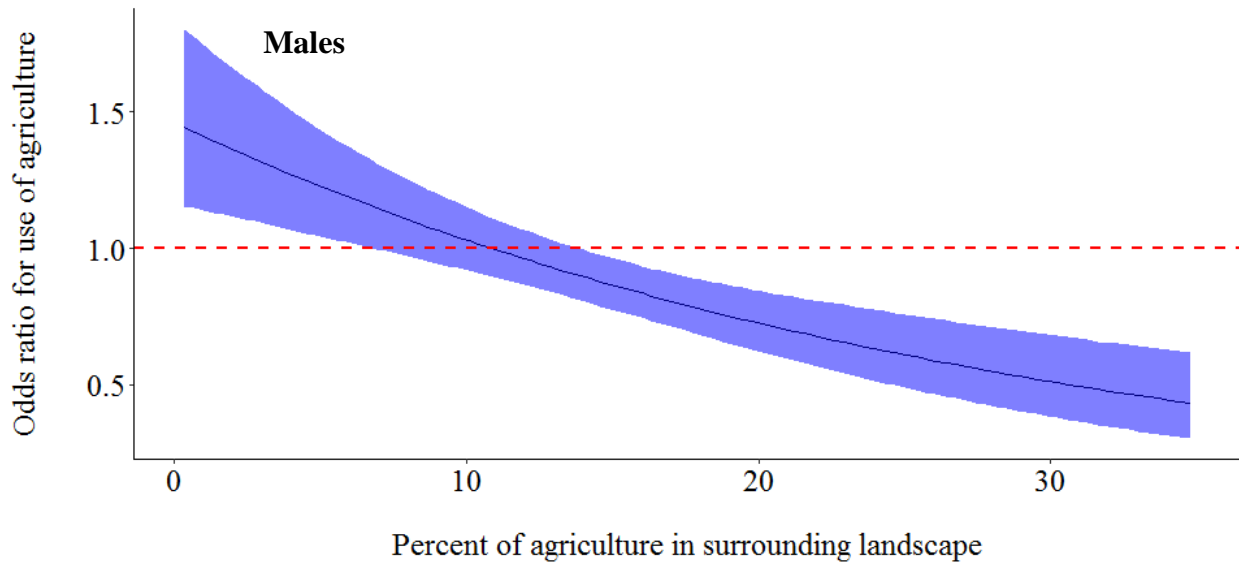
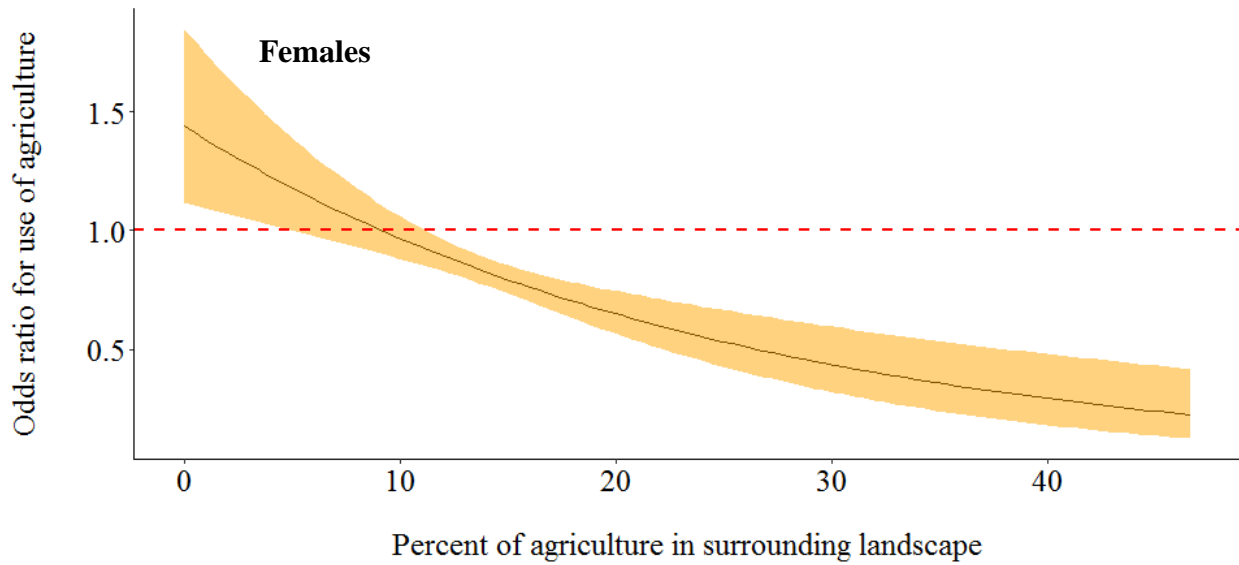


Figure 2.3. Functional response in use of agriculture for female (top) and male (bottom) black bears as the percent agriculture varied within the average sex-specific home range radius (5 km radius for females and 12 km radius for males). GPS locations were collected in the Lower Peninsula of Michigan from 2011 – 2015. The colored ribbons represent the 95% confidence interval around the estimated response (solid black line) for females (orange) and males (blue). The red dashed line indicates odds ratio=1, which is interpreted as having no effect on use.

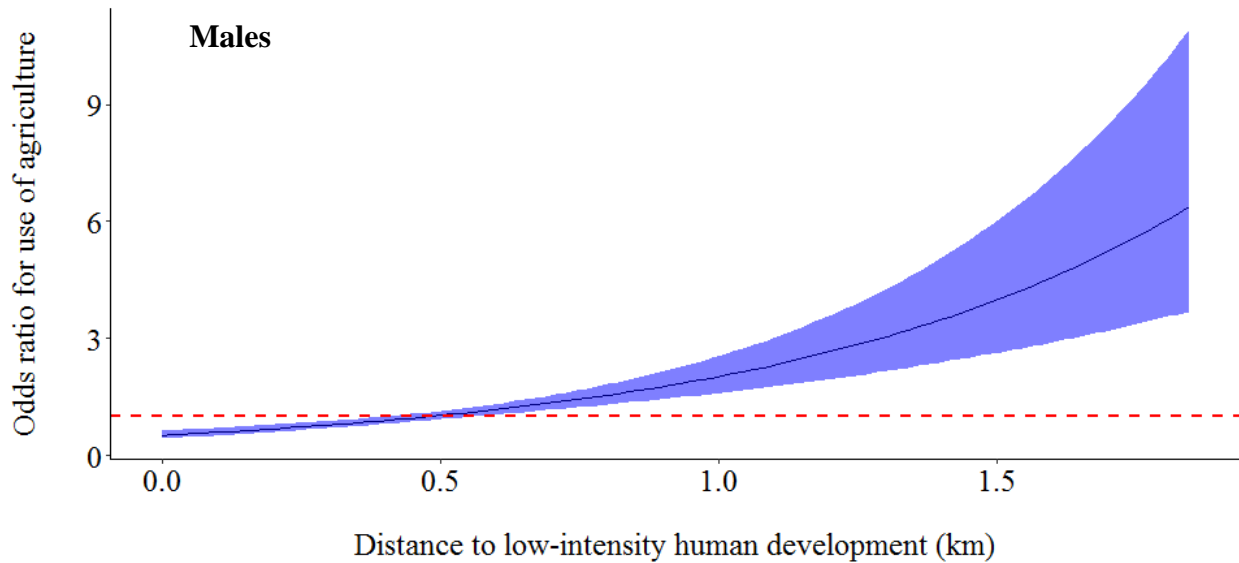
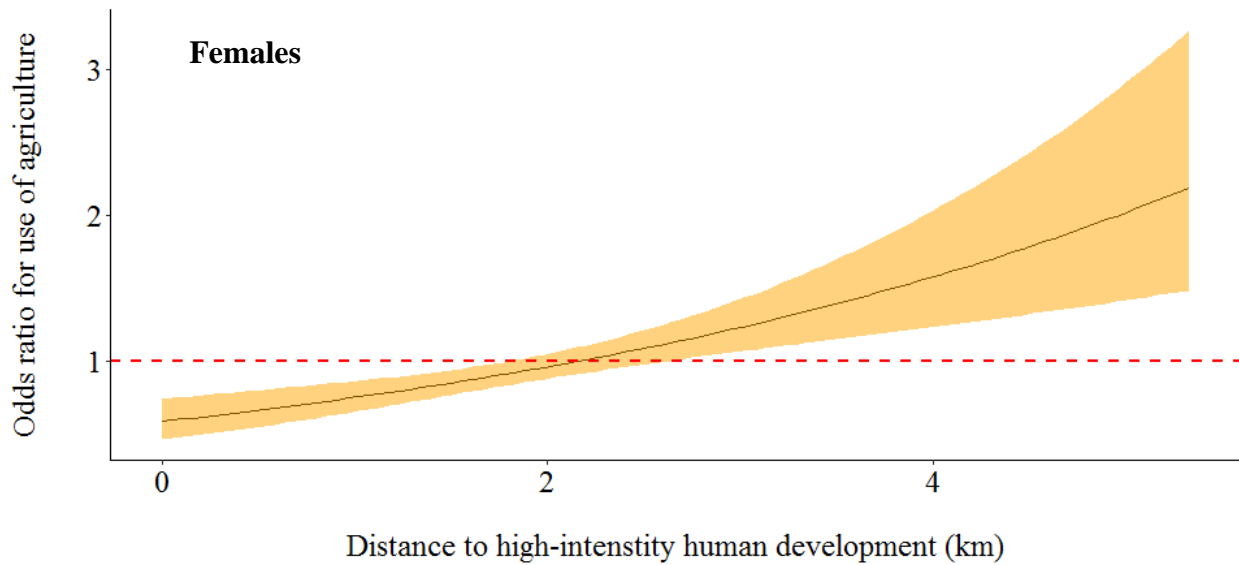


Figure 2.4. Functional response in use of agriculture for female (top) and male (bottom) black bears as distance to high-intensity (top) or low-intensity (bottom) human development varied in the Lower Peninsula of Michigan from 2011 – 2015. The colored ribbons represent the 95% confidence interval around the estimated response (solid black line) for females (orange) and males (blue). The red dashed line indicates odds ratio=1, which is interpreted as having no effect on use.

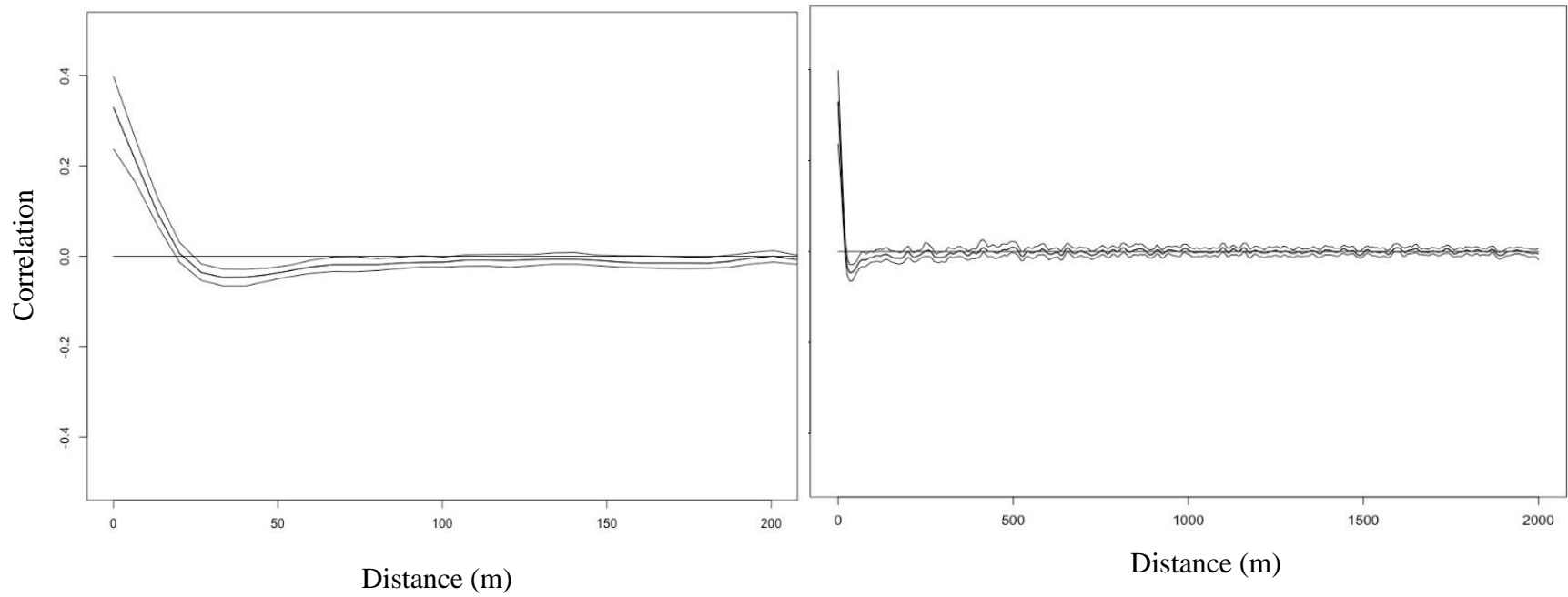


Figure 2.5. Spline correlograms of spatial correlation, with 95% bootstrap confidence intervals, of the residuals from a logistic regression model of female black bear location data and all explanatory variables.

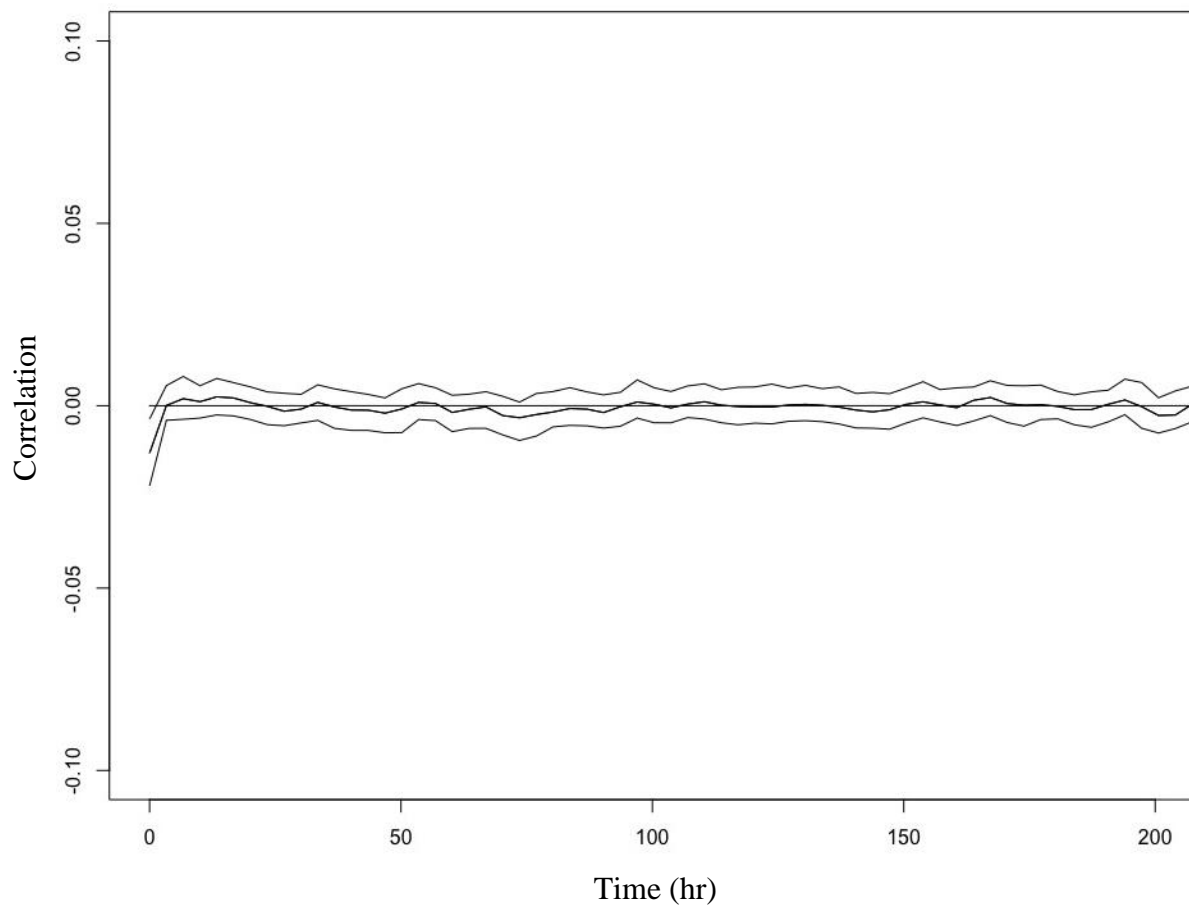


Figure 2.6. Spline correlograms of temporal correlation, with 95% bootstrap confidence intervals of the residuals, from a logistic regression model of female black bear location data and all explanatory variables.

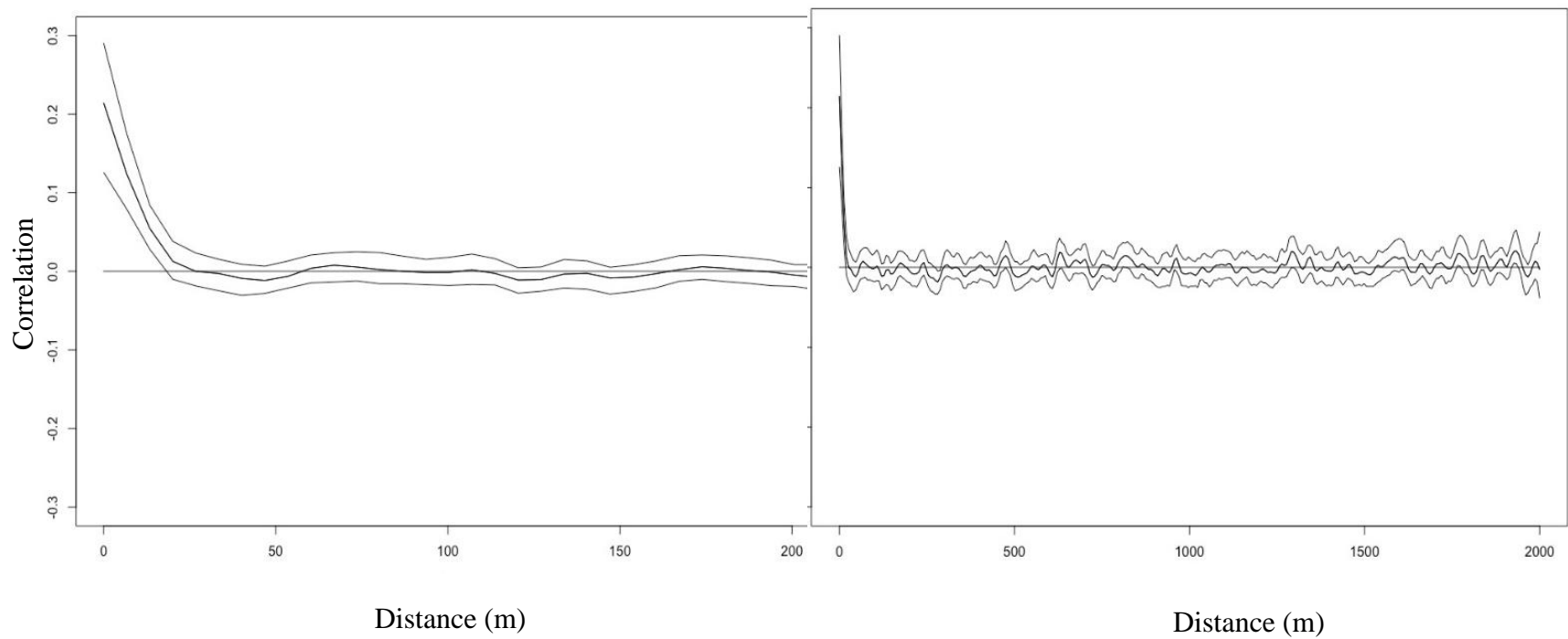


Figure 2.7. Spline correlograms of spatial correlation, with 95% bootstrap confidence intervals, of the residuals from a logistic regression model of male black bear location data and all explanatory variables.

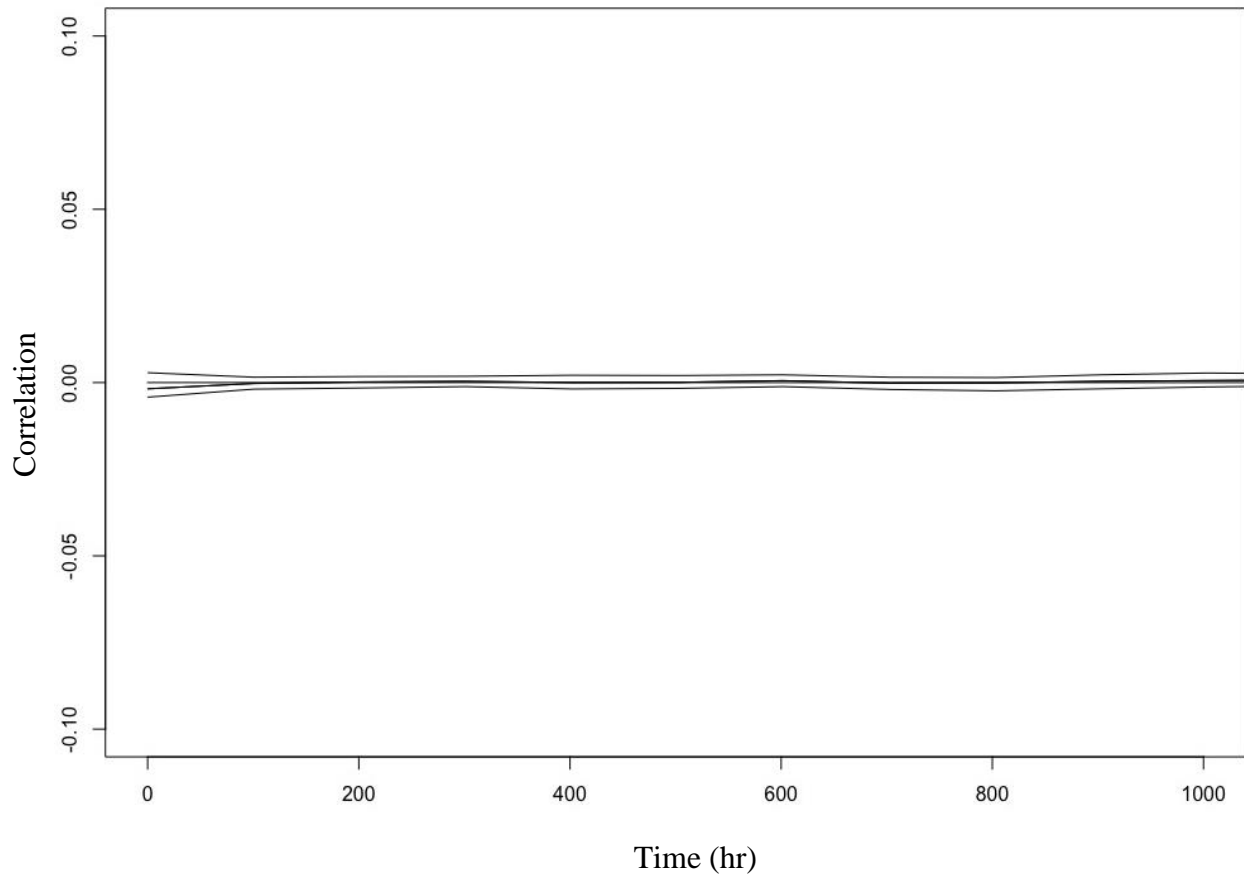


Figure 2.8. Spline correlograms of temporal correlation, with 95% bootstrap confidence intervals of the residuals, from a logistic regression model of male black bear location data and all explanatory variables.

LITERATURE CITED

LITERATURE CITED

- Albert, D. A. 1995. Regional landscape ecosystems of Michigan, Minnesota, and Wisconsin: a working map and classification. U. S. Forest Service, North Central Forest Experiment Station, St. Paul, Minnesota, USA.
- Apps, C. D., B. N. McLellan, T. A. Kinley, and J. P. Flaa. 2001. Scale-dependent habitat selection by mountain caribou, Columbia Mountains, British Columbia. *The Journal of Wildlife Management* 65:65–77.
- Austin, M. P., and K. P. Van Niel. 2011. Improving species distribution models for climate change studies: variable selection and scale. *Journal of Biogeography* 38:1–8.
- Bailey, R. G. 1995. Description of the ecoregions of the United States. US Department of Agriculture Forest Service, Washington D.C., USA.
- Barber, K. R., and F. G. Lindzey. 1986. Breeding behavior of black bears. *Bears: Their Biology and Management* 6:129–136.
- Baruch-Mordo, S., S. W. Breck, K. R. Wilson, and D. M. Theobald. 2008. Spatiotemporal distribution of black bear–human conflicts in Colorado, USA. *Journal of Wildlife Management* 72:1853–1862.
- Beckmann, J. P., and J. Berger. 2003. Using black bears to test ideal-free distribution models experimentally. *Journal of Mammalogy* 84:594–606.
- Beest, F. M. van, P. D. McLoughlin, A. Mysterud, and R. K. Brook. 2016. Functional responses in habitat selection are density dependent in a large herbivore. *Ecography* 39:515–23.
- Ben-David, M., K. Titus, and LaVern R. Beier. 2004. Consumption of salmon by Alaskan brown bears: a trade-off between nutritional requirements and the risk of infanticide? *Oecologia* 138:465–474.
- Boyce, M. S., and L. L. McDonald. 1999. Relating populations to habitats using resource selection functions. *Trends in Ecology & Evolution* 14:268–272.
- Boyce, M. S., P. R. Vernier, S. E. Nielsen, and F. K. A Schmiegelow. 2002. Evaluating resource selection functions. *Ecological Modelling* 157:281–300.
- Brody, A. J., and M. R. Pelton. 1989. Effects of roads on black bear movements in western North Carolina. *Wildlife Society Bulletin* 17:5–10.
- Burnham, K. P., and D. R. Anderson. 2004. Multimodel inference: understanding AIC and BIC in model selection. *Sociological Methods & Research* 33:261–304.

- Buskirk, S., and J. J. Millspaugh. 2006. Metrics for studies of resource selection. *Journal of Wildlife Management* 70:358-366.
- Carter, N. H., D. G. Brown, D. R. Etter, and L. G. Visser. 2010. American black bear habitat selection in Northern Lower Peninsula, Michigan, USA, using discrete-choice modeling. *Ursus* 21:57-71.
- Center for Shared Solutions and Technology Partnerships. 2014. Michigan Geographic Framework: State of Michigan v14a.
- Chetkiewicz, C-L. B., and M. S. Boyce. 2009. Use of resource selection functions to identify conservation corridors. *Journal of Applied Ecology* 46:1036-1047.
- Clark, J. D., J. S. Laufenberg, M. Davidson, and J. L. Murrow. 2015. Connectivity among subpopulations of Louisiana black bears as estimated by a step selection function. *The Journal of Wildlife Management* 79:1347-1360.
- Coulon, A., N. Morellet, M. Goulard, B. Cargnelutti, J. Angibault, and A. J. M. Hewison. 2008. Inferring the effects of landscape structure on roe deer (*Capreolus capreolus*) movements using a step selection function. *Landscape Ecology* 23:603-614.
- Ditmer, M. A. 2014. American black bears: strategies for living in a fragmented, agricultural landscape. Dissertation, University of Minnesota, Saint Paul, USA.
- Ditmer, M. A., D. L. Garshelis, K. V. Noyce, T. G. Laske, P. A. Iaizzo, T. E. Burk, J. D. Forester, and J. R. Fieberg. 2015. Behavioral and physiological responses of American black bears to landscape features within an agricultural region. *Ecosphere* 6:1-21.
- Ditmer, M. A., D. L. Garshelis, K. V. Noyce, A. W. Haveles, and J. R. Fieberg. 2016. Are American black bears in an agricultural landscape being sustained by crops? *Journal of Mammalogy* 97:54-67.
- D'eon, R. G., and D. Delparte. 2005. Effects of radio-collar position and orientation on GPS radio-collar performance, and the implications of PDOP in data screening. *Journal of Applied Ecology* 42:383-388.
- Fecske, D. M., R. E. Barry, F. L. Precht, H. B. Quigley, S. L. Bittner, and T. Webster. 2002. Habitat use by female black bears in western Maryland. *Southeastern Naturalist* 1:77-92.
- Forester, J. D., H. K. Im, and P. J. Rathouz. 2009. Accounting for animal movement in estimation of resource selection functions: sampling and data analysis. *Ecology* 90:3554-3565.

- Fortin, D., H. L. Beyer, M. S. Boyce, D. W. Smith, T. Duchesne, and J. S. Mao. 2005. Wolves influence elk movements: behavior shapes a trophic cascade in Yellowstone National Park. *Ecology* 86:1320–1330.
- Fretwell, S. D. 1972. *Populations in a seasonal environment*. Princeton University Press, Princeton, New Jersey, USA.
- Fretwell, S. D., H. L. Lucas Jr. 1970. On territorial behavior and other factors influencing habitat distribution of birds. *Acta Biotheoretica* 19:16-36.
- Garrison, E. P., J. W. McCown, and M. K. Oli. 2007. Reproductive ecology and cub survival of Florida black bears. *The Journal of Wildlife Management* 71:720–27.
- Gillies, C. S., M. Hebblewhite, S. E. Nielsen, M. A. Krawchuk, C. L. Aldridge, J. L. Frair, D. J. Saher, C. E. Stevens, and C. L. Jerde. 2006. Application of random effects to the study of resource selection by animals. *Journal of Animal Ecology* 75:887–898.
- Godvik, I. M. R., L. E. Loe, J. O. Vik, V. Veiberg, R. Langvatn, and A. Mysterud. 2009. Temporal scales, trade-offs, and functional responses in red deer habitat selection. *Ecology* 90:699–710.
- Hebblewhite, M., and E. Merrill. 2008. Modelling wildlife–human relationships for social species with mixed-effects resource selection models. *Journal of Applied Ecology* 45:834–844.
- Hess, G. 1996. Disease in metapopulation models: implications for conservation. *Ecology* 77:1617-1632
- Hiller, T. L., J. L. Belant, J. Beringer, and A. J. Tyre. 2015. Resource selection by recolonizing American black bears in a fragmented forest landscape. *Ursus* 26:116–128.
- Hristienko, H., and J. E. McDonald. 2007. Going into the 21st century: a perspective on trends and controversies in the management of the American black bear. *Ursus* 18:72–88.
- Homer, C.G., Dewitz, J.A., Yang, L., Jin, S., Danielson, P., Xian, G., Coulston, J., Herold, N.D., Wickham, J.D., and Megown, K. 2015. Completion of the 2011 National Land Cover Database for the conterminous United States-representing a decade of land cover change information. *Photogrammetric Engineering and Remote Sensing* 81 (5).
- Johnson, D. H. 1980. The comparison of usage and availability measurements for evaluating resource preference. *Ecology* 61:65–71.
- Johnson, D. S., D. L. Thomas, J. M. Ver Hoef, and A. Christ. 2008. A general framework for the analysis of animal resource selection from telemetry data. *Biometrics* 64:968–976.

- Jones, M. D., and M. R. Pelton. 2003. Female American black bear use of managed forest and agricultural lands in coastal North Carolina. *Ursus* 14:188–197.
- Kindall, J. L., and F. T. Van Manen. 2007. Identifying habitat linkages for American black bears in North Carolina, USA. *The Journal of Wildlife Management* 71:487–495.
- Latham, A. D. M., M. C. Latham, and M. S. Boyce. 2011. Habitat selection and spatial relationships of black bears (*Ursus americanus*) with woodland caribou (*Rangifer tarandus caribou*) in Northeastern Alberta. *Canadian Journal of Zoology* 89:267–277.
- Lewis, J. S., J. L. Rachlow, J. S. Horne, E. O. Garton, W. L. Wakkinen, J. Hayden, and P. Zager. 2011. Identifying habitat characteristics to predict highway crossing areas for black bears within a human-modified landscape. *Landscape and Urban Planning* 101:99–107.
- Lyons, A. L., W. L. Gaines, and C. Servheen. 2003. Black bear resource selection in the northeast Cascades, Washington. *Biological Conservation* 113:55–62.
- Lyons, A. J. 2005. Activity patterns of urban American black bears in the San Gabriel Mountains of southern California. *Ursus* 16:255–262.
- Martin, J., M. Basille, B. Van Moorter, J. Kindberg, D. Allainé, and J. E. Swenson. 2010. Coping with human disturbance: spatial and temporal tactics of the brown bear (*Ursus arctos*). *Canadian Journal of Zoology* 88:875–883.
- Manly, B. F. J., L. L. McDonald, D. L. Thomas, T. L. McDonald, and W. P. Erickson. 2002. Resource selection by animals: statistical design and analysis for field studies. Second edition. Kluwer Academic Publishers, Dordrecht, the Netherlands.
- Matthiopoulos, J., M. Hebblewhite, G. Aarts, and J. Fieberg. 2011. Generalized functional responses for species distributions. *Ecology* 92:583–589.
- Mattson, D. J. 1990. Human impacts on bear habitat use. *Bears: Their Biology and Management* 8:33–56.
- McClellan, S. A., M. A. Rumble, R. M. King, and W. L. Baker. 1998. Evaluation of resource selection methods with different definitions of availability. *The Journal of Wildlife Management* 62:793–801.
- McFadden-Hiller, J. E., D. E. Beyer Jr, and J. L. Belant. 2016. Spatial distribution of black bear incident reports in Michigan. *PLoS ONE* 11(4):e0154474.
- Morris, D. W. 1989. Density-dependent habitat selection: testing the theory with fitness data. *Evolutionary Ecology* 3:80–94.
- Mysterud, A., and R. A. Ims. 1998. Functional responses in habitat use: availability influences relative use in trade-off situations. *Ecology* 79:1435–1441.

- Nathan, R., W. M. Getz, E. Revilla, M. Holyoak, R. Kadmon, D. Saltz, and P. E. Smouse. 2008. A movement ecology paradigm for unifying organismal movement research. *Proceedings of the National Academy of Sciences* 105:19052–19059.
- Natural Resources Conservation Service. 2008. Michigan monthly precipitation by county. USDA, Washington D.C., USA.
- Nielsen, S. E., M. S. Boyce, G. B. Stenhouse, and R. H. M. Munro. 2002. Modeling grizzly bear habitats in the yellowhead ecosystem of Alberta: taking autocorrelation seriously. *Ursus* 13:45–56.
- Pearson, R. G., and T. P. Dawson. 2003. Predicting the impacts of climate change on the distribution of species: are bioclimate envelope models useful? *Global Ecology and Biogeography* 12:361–371.
- Porter, W. F., and K. E. Church. 1987. Effects of environmental pattern on habitat preference analysis. *The Journal of Wildlife Management* 51:681–685.
- Powell, R. A., J. W. Zimmerman, D. E. Seaman. 1997. Ecology and behavior of North American black bears: home ranges, habitat, and social organization. Chapman & Hall, London, United Kingdom.
- Prokopenko, C. M., M. S. Boyce, and T. Avgar. 2017. Characterizing wildlife behavioural responses to roads using integrated step selection analysis. *Journal of Applied Ecology* 54:470–79.
- Rosenzweig, M. L. 1981. A theory of habitat selection. *Ecology* 62:327–35.
- Sadeghpour, M. H., and T. F. Ginnett. 2011. Habitat selection by female American black bears in northern Wisconsin. *Ursus* 22:159–166.
- Sawyer, H., R. M. Nielson, F. Lindzey, and L. L. McDonald. 2006. Winter habitat selection of mule deer before and during development of a natural gas field. *The Journal of Wildlife Management* 70:396–403.
- Støen, Ol-G., A. Ordiz, A. L. Evans, T. G. Laske, J. Kindberg, O. Frøbert, J. E. Swenson, and J. M. Arnemo. 2015. Physiological evidence for a human-induced landscape of fear in brown bears (*Ursus arctos*). *Physiology & Behavior* 152:244–248.
- Tilman, D. 1994. Competition and biodiversity in spatially structured habitat. *Ecology* 75:2-16
- Tri, A. N., J. W. Edwards, M. P. Strager, J. T. Petty, C. W. Ryan, C. P. Carpenter, M. A. Ternent, and P. C. Carr. 2016. Habitat use by American black bears in the urban–wildland interface of the mid-Atlantic, USA. *Ursus* 27:45–56.

Wooding, J. B., and T. S. Hardisky. 1994. Home range, habitat use, and mortality of black bears in north-central Florida. *Bears: Their Biology and Management* 9:349–356.

Zuur, A.F., E. N. Ieno, N. J. Walker, A. A. Saveliev, and G. M. 2009. *Mixed effects models and extensions in ecology with R*. Springer, New York, New York, USA.